Copyright

by

Abhishek Kumar

2010

The Thesis Committee for Abhishek Kumar
Certifies that this is the approved version of the following thesis:

Quantitative Geometric Model of Connected Carbonaceous Material in Mudrocks

APPROVED BY
SUPERVISING COMMITTEE:

Supervisor:

Steven L. Bryant

Jon T. Holder

Quantitative Geometric Model of Connected Carbonaceous Material in Mudrocks

by

Abhishek Kumar, B.Tech.

Thesis

Presented to the Faculty of the Graduate School of

The University of Texas at Austin

in Partial Fulfillment

of the Requirements

for the Degree of

Master of Science in Engineering

The University of Texas at Austin

December 2010

Dedication

This thesis is dedicated to my mentors, parents and friends.

Acknowledgements

I would like to thank my supervisor Dr. Steven L. Bryant for his support, patience and encouragement throughout this research. Thanks to geoscientists of Bureau of Economic Geology for providing useful comments in my thesis. I am thankful to Dr. Jon T. Holder for reading this thesis and adding valuable comments.

I express my gratitude to the faculty and staff of the Petroleum and Geosystems Engineering Department. And last, but not the least, I would like to thank my friends and fellow graduate students at The University of at Texas who made my time at Austin even more enjoyable.

I acknowledge the financial support of ExxonMobil for this research.

December 3rd, 2010

Abstract

Quantitative Geometric Model of Connected Carbonaceous Material in Mudrocks

Abhishek Kumar, M.S.E

The University of Texas at Austin, 2010

Supervisor: Steven L. Bryant

Unconventional gas resources have become important as an environment-friendly source of fuel. It is important to understand the pore level geometries of grains and voids in mudrocks in order to understand the flow potential of gas from these rocks.

Recent observations of nanopores within carbonaceous material in mudrocks have led to the hypothesis that such material provides conduits for gas migration within the mudrock matrix. This hypothesis requires that the carbonaceous material exist not as isolated grains but as connected clusters of grains within the mudrock. To examine this hypothesis, we develop an algorithm for the grain-scale modeling of the spatial distribution of grains of carbonaceous matter in a matrix of non-carbonaceous material (silt, clay). The algorithm produces a grain-scale model of the sediment which is

precursor to a mudrock, then a sequence of models of the grain arrangement as burial compacts the sediment into mudrock.

The carbonaceous material is approximated by the simplest possible geometric model of spherical grains. These grains are distributed randomly within a population of other spheres that represent silt and clay grains. A cooperative rearrangement algorithm is used to generate a disordered packing of the grain mixture having a prescribed initial porosity. This model represents the sediment precursor of the shale in its original depositional setting. Periodic boundary conditions are imposed on the packing to eliminate wall-induced artifacts in the grain arrangement; in effect the packing extends infinitely in all three coordinate directions. We simulate compaction of the model sediment by incrementally rescaling the vertical coordinate axis, repeating the cooperative rearrangement calculation with periodic boundaries after each increment.

We determine the size distribution of clusters of touching carbonaceous grains, focusing particularly upon the approach toward percolation (when a cluster spans the entire packing). The model allows estimation of threshold fraction of carbonaceous material for significantly connected clusters to form. Beyond a threshold degree of compaction, connected clusters become much more prevalent. Other factors affecting the threshold fraction such as ductility of the carbonaceous material is also evaluated. Ductility is modeled by taking a grain consisting inner rigid core covered by the outer soft shell which can be penetrated and deformed during geometrical transformation.

The emergence of large numbers of clusters, or of a few large clusters, increases the probability that nanoporous conduits within the clusters would intersect a fracture in

the mudrock. This should correlate with greater producibility of gas from the mudrock. Thus the dependence of the statistics of the clusters upon other parameters, such as the fraction of carbonaceous material, porosity, degree of compaction, etc., could be useful for estimating resource quality. For example, it is observed that the threshold concentration of carbonaceous material in the initial sediments for "significant clustering" enough to approach percolation is about 20 percent of the volume fraction. The degree of compaction needed to get "significant clustering" is 50%.

Table of Contents

List of Tables

List of Figures

Chapter 1: Overview

This Chapter gives an overview of the topics discussed in the thesis. The research is focused on grain-scale modeling of the unconventional reservoirs in mudrocks.

1.1 Problem statement

Shale gas is one of the most important unconventional gas resources. It is increasingly becoming one of the most important energy sources for the world. Most of the shale gas reservoirs are explored in the United States and are exploited to meet the ever increasing demand of energy. It is important to understand the pore level geometries of grains and voids of the mudrocks which play an important role in the transport of hydrocarbons through them. The present work consists of making mechanistic models of certain aspects of the evolution of mudrocks. The models focus on the effect of mechanical compaction on the connectivity of carbonaceous material at the grain scale. The hypothesis is that the extent to which particles of organic matter touch each other determines the extent to which nanopores, which subsequently evolve within these particles, could be connected within the mudrock. Greater connectivity of nanopores should correlate with greater producibility once the mudrock has been stimulated.

1.2 Pore System and Transport Mechanism in Mudrocks

The pore systems in mudrocks are generally composed of two types of pores:-

a) Intergranular Pores

b) Intragranular Pores

The former type of pores is not common in mudrocks, and the intragranular pore system is assumed to be the main network for storage and transport of the hydrocarbon throughout this study. Nanopores in carbonaceous material in gas-producing mudrocks, Figure 1.1, are attributed to thermal maturation and conversion of solid carbonaceous matter into a fluid hydrocarbon phase. Thermal cooking of this solid carbonaceous material results in increase of pressure within this material, resulting in the formation of nanopores. This leads to the hypothesis that carbonaceous material particles are the preferred conduits of hydrocarbon in mudrocks. The greater the extent to which carbonaceous particles are connected, Figure 1.2, the greater the conductivity of these conduits. The pore networks present in other lithofacies are generally small and isolated. As a limiting case, we assume that these other networks do not contribute to the flow of hydrocarbon in these types of unconventional reservoirs.

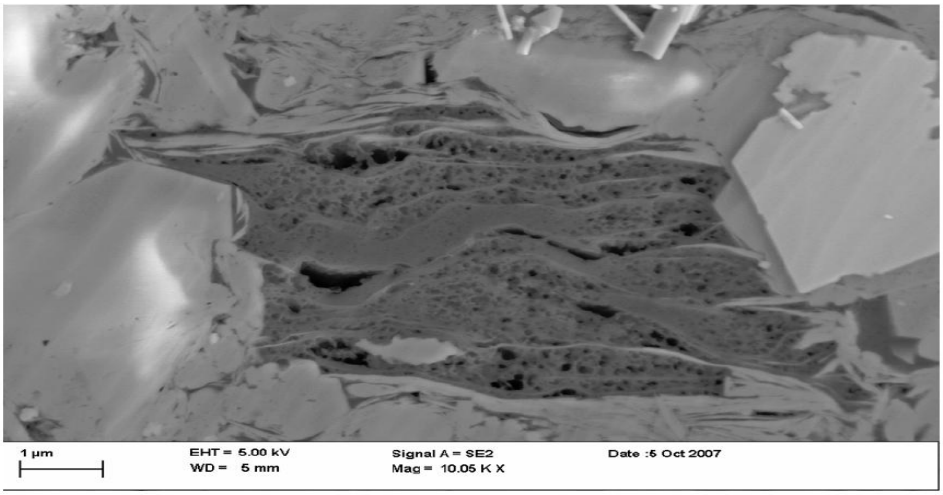

Figure 1.1: Scanning electron micro-image of Ar-ion-beam milled surface showing pores in organic matter (Wang and Reed, 2009)

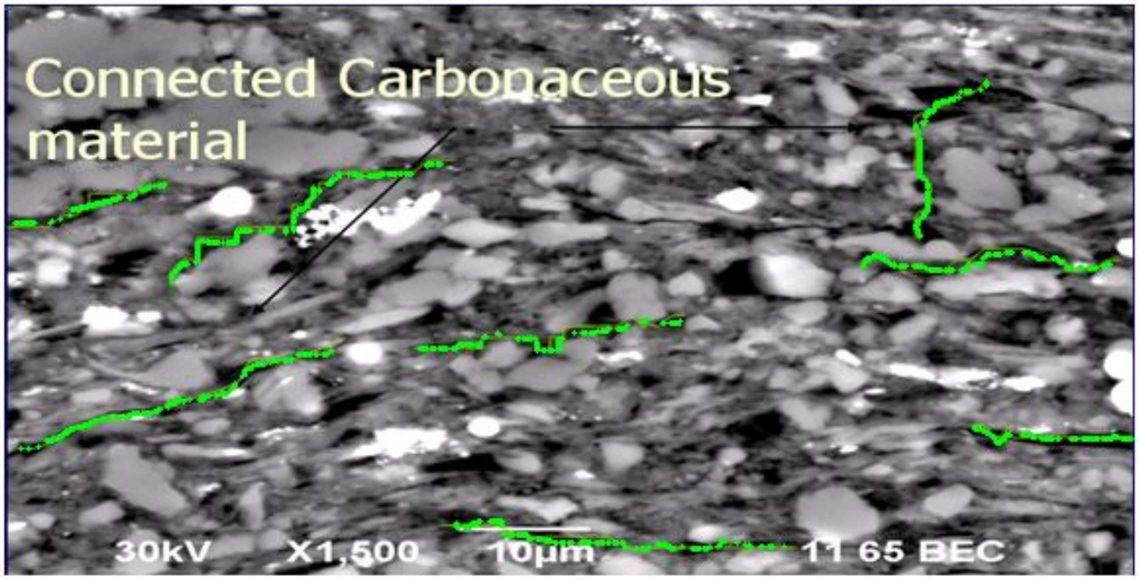

Figure 1.2: Connected carbonaceous material in typical SEM image of shale gas sample (Barnett shale). The connections are interpreted to have formed as smaller, separate pieces of material come into contact during burial and compaction. (Courtesy Dr. K Milliken, University of Texas Bureau of Economic Geology)

1.3 Previous Work on Modeling Gas Transport in Shale

Javadpour (2009) observed that the gas production from mudrocks was greater than that anticipated from their Darcy permeability. Using images of nanopores obtained by Atomic Force Microscopy, he concluded that the gas flow in nanopores cannot be described simply by Darcy's equation. Taking into account of Knudsen diffusion and slip flow he introduced an apparent permeability concept which is significant for the pore sizes smaller than 100 nm.

The mass balance equation can be written as follows :-

$$\frac{\delta c}{\delta t} + U.\nabla c - D:\nabla^2 c - \kappa c = 0 \quad \ldots\ldots\ldots\ldots\ldots\ldots\ldots\ldots\ldots\ldots \text{(1)}$$

The first term in Equation 1 is the accumulation term, the second one is advection, the third one is Knudsen diffusion and the last term is for desorption of fluid from the surface of carbonaceous material. The parameter κ is the desorption constant, D is the Knudsen diffusion and U is the advective velocity. Knudsen diffusion is an important gas transport process in nanopores which are present in the carbonaceous material of the mudrock system and thus relevant to the hypothesis of this study.

Roy et al. (2003) proposed a model to predict the flow characteristics for reasonably high Knudsen number flow regimes through micro channels and nanopores. The Knudsen number (Kn) is defined as the ratio of the fluid mean-free path (λ) to the macroscopic length scale of the physical system (Λ) :-

$$Kn = \frac{\lambda}{\Lambda} \quad \text{..... (2)}$$

where $\lambda = 16\mu / 5\rho\sqrt{2\pi RT}$; μ = viscosity; T = temperature; $\Lambda = \rho / \frac{\partial \rho}{\partial x}$ and ρ is fluid density ; R is the universal gas constant and x is the direction of the pressure gradient. They developed a two dimensional microscale flow model to predict the overall flow characteristics for reasonably high Knudsen number flow in microchannels and nanopores. If connected paths of nanopores exist within the organic material in a mudrock, then this model could be applied to those paths to predict the macroscopic flow behavior in the mudrock.

Reed et al. (2009) identified four types of porous media in productive gas shale systems (shown in Figure 1.3):-

a) Non organic matrix

b) Organic matrix

c) Natural fractures

d) Hydraulic fractures

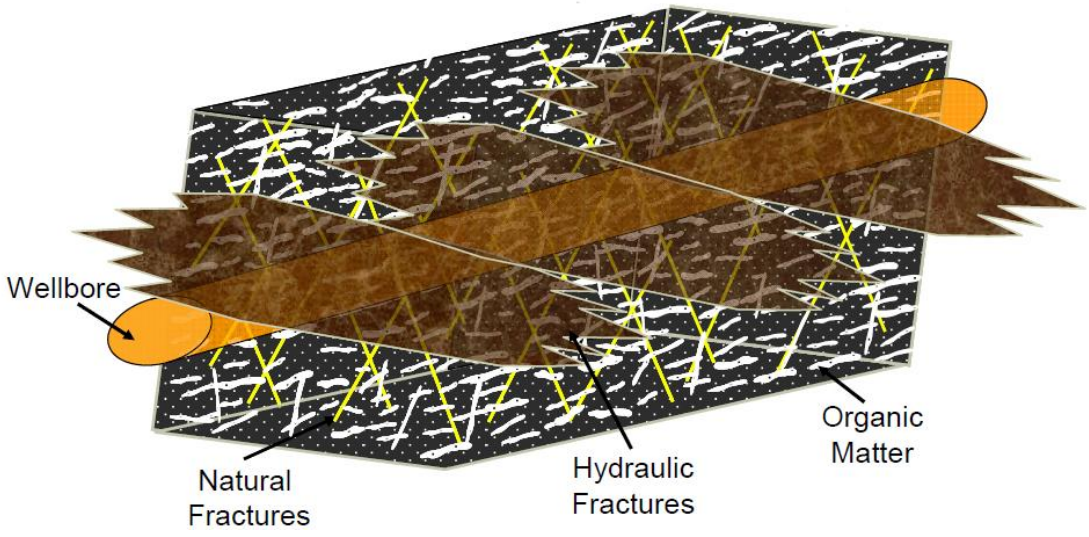

Figure 1.3: Schematic diagram showing high- permeability elements in gas shale: organic matter, natural fractures, and hydraulic fractures. (Reed et al. 2009)

They stated that organic matter pores, ranging from 5 to 1,000 nm have the ability to adsorb and store free gases. They noted that porosity in organic matter can be as high as five times that in material in a non organic matrix. As organic matter is oil wet, flow of gas in organic matter is predominantly single phase. All these factors tend to enhance gas permeability in gas shale. The pore network in organic matter could be the pathways to high gas production in gas shale when connected to natural and hydraulic fractures.

The hypothesis of this thesis is that the organic material provides the preferred conduits for gas flow in mudrocks. This organic material is a small volume fraction of the mudrock, so it can be expected that particles are distributed as isolated grains. However, to form conduits they must be present in clusters of touching particles within the mudrock. The results of simulations of compaction in the sediment model shows that the

grains of organic material come in contact and form clusters which are the representation of actual connected organic material in mudrocks.

1.4 ORGANIZATION OF THESIS

The thesis has been divided into five distinct chapters. The current chapter summarizes the background, hypothesis and research work done in the current study. Chapter 2 describes the cooperative rearrangement algorithm which is used for creating the grain packing. The chapter explains the two methodologies used for representing compaction in sediments: the unconserved volume approach and the conserved volume approach. Both rigid and ductile grains are defined. It analyzes the tolerance value used for defining a contact and the effect of the tolerance value on the cluster size distribution.

Chapter 3 describes the effect of the volume fraction of carbonaceous material on the number of clusters in the model sediment. It investigates the relationship of the maximum cluster size with the volume fraction of carbonaceous material and defines the threshold value of the volume fraction of carbonaceous material resulting in percolation. Cluster length and aspect ratios in model sediment are also studied in this chapter.

Chapter 4 explains the effect of compaction on clustering of carbonaceous material. It considers the significance of compaction in forming clusters in model sediment, and the threshold value of compaction resulting in “significant clustering” by studying the ductility of the carbonaceous material and silt/clay grains. Chapter 5 presents the conclusions and the future aspects of the current study.

A listing of codes for compaction with cooperative rearrangement and other analysis done in this study is given in the Appendix.

Chapter 2: Methods for modeling the sediments

2.1 INTRODUCTION

Sphere packings have been widely used to simulate sediments and soil and to examine any other process in which particles are packed in space (Rodriguez 2006, Thane 2005). Here we use a grain packing algorithm based on a cooperative rearrangement method. In this treatment touching of two or more grains leads to cluster formation. Cluster size distribution analysis is carried out to study the connectivity of the spheres which represent carbonaceous material. This chapter discusses the cluster formation, its size and frequency formed by the sphere packing algorithm.

A random loose packing with a user- defined solid fraction within a periodic cell is used to model sediments. The process of random packing models the arrangement of carbonaceous material in mudrock, and the main variable controlling cluster formation is the volume fraction of carbonaceous material. Burial compacts the model sediments into model mudrock.

2.2 COOPERATIVE REARRANGEMENT ALGORITHM

The cooperative rearrangement algorithm developed by Thane (2005) was used for this study. Her algorithm creates a dense disordered packing of grains in a defined space with periodic boundaries, referred to here as a "unit cell" or a "periodic cell". Periodic boundaries eliminate artifacts in the packing due to rigid boundaries. The algorithm consists of three steps-:

1) Initial point generation – The points are randomly selected in a given 3D volume.

2) Growth of spheres – The points are allowed to grow into spheres incrementally in a concentric manner like an onion peel.

3) Removal of Overlaps- The growing of spheres may cause overlaps which are removed by moving the overlapped spheres away from each other in the direction of the line joining their centers.

Steps 2 and 3 are iterated until the packing reaches a user-specified density fraction, or alternatively, the densest possible arrangement. Thane's original code produced the latter arrangement; for equal spheres such packings have porosity of 36%. The code was revised in this work to allow for stopping at an arbitrary solid volume fraction within the periodic cell.

Figure 2.1 shows an illustration of periodicity. The spheres in the unit cell are shown in the projected *y*-*z* plane in the center of the diagram; four copies of the unit cell are placed around the center cell. The red spheres represent the real spheres in the unit cell and green spheres are their images. A sphere coming out of one face will have one image in the opposite face. A sphere coming out of a edge will have three images, and a sphere coming out from a corner will have seven images. The encircled regions in Figure 2.1 show the exact fitting of real spheres with their images (red spheres touching green spheres without overlap). The regions also show image spheres which fit with other image spheres (green spheres fitting with green ones).

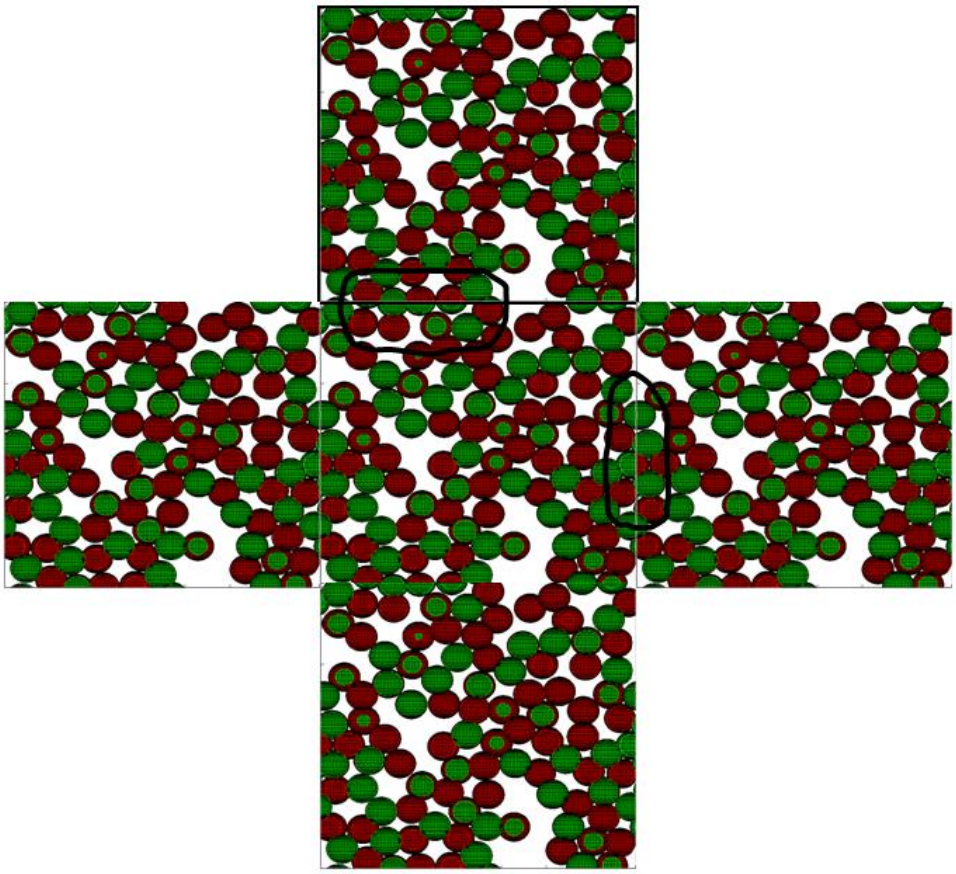

Figure 2.1: Concept of periodicity as implemented in the sphere packing code. The spheres in the unit cell are shown in the projected *y*-*z* plane in the center of the diagram; four copies of the unit cell are placed around the center cell. Red spheres are real spheres and green spheres are their images. A sphere at or near one face of unit cell can thus be in virtual contact with a sphere at or near the opposite face. Such contacts are accounted for during the cooperative rearrangement steps.

2.3 ALGORITHM FOR SIMULATING COMPACTION

Sphere packings created with the cooperative rearrangement algorithm above represent sediments in the original depositional environment. These model sediments are subjected to geometric transformation intended to model the process of compaction. The effect of compaction on connectivity of carbonaceous material is studied at multiple stages. The compaction is modeled by compacting the sediments uniaxially. This is achieved by decreasing a compaction factor c ($c < 1.0$) in increments while maintaining periodic boundaries. The factor c scales the vertical dimension of the assembly of packed spheres relative to its initial value as shown in Figure 2.2. The z coordinate of the spheres is rescaled by the same factor. Thus the value c=1 does not change the sphere locations or unit cell volume. As c decreases, the amount of compaction increases.

The approach accounts for the relative motion of spheres within the unit cell and the shape of spheres is not distorted during compaction. This motion is representative of the motion of grains in nature and in uniaxial compaction experiments of sediments at the macroscopic level. A single compaction factor is applied to the unit cell. However, in layered natural sediments the compaction of each layer may be different and depends mainly on the mechanical property of each layer.

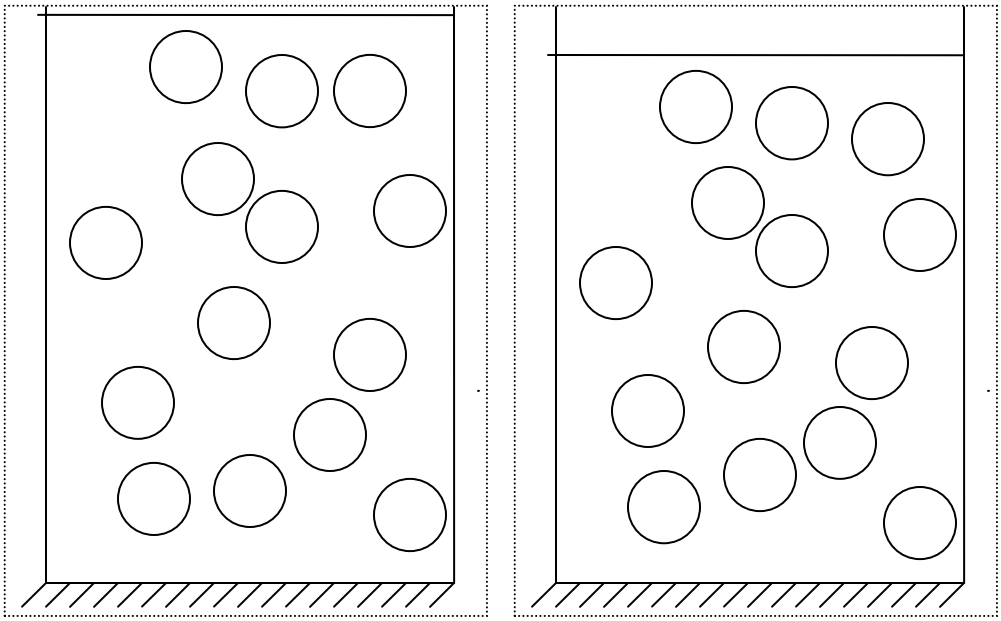

Figure 2.2: Schematic showing various stages of compaction. Original model sediment is uncompacted (*c*=1).The final state corresponds to mudrock.

It is useful to compare the relative motion of spheres in the compacted unit cell with grains in a sediment during burial or in a bench-scale resedimentation experiment. As depicted in Figure 2.3, let Z^0_{top} and Z^0_{bottom} be the distance from the datum of top and bottom of a layer of sediment undergoing compaction. Let Z^f_{top} and Z^f_{bottom} be the layer final position, and let d_{top} and d_{bottom} be the distance traversed by the top and bottom of the layer during compaction. During compaction the thickness H of the layer of grains decreases representing consolidation of sediments in that layer. The extent of translation of grains in the direction of compaction also decreases with depth. The deformation can be described by

$H^0 = Z^0_{bottom} - Z^0_{top}$ (Initial thickness of layer of grains)
$H^f = Z^f_{bottom} - Z^f_{top}$ (Final thickness of layer of grains)

$$H^0 / H^f = (Z^0_{bottom} - Z^0_{top}) / (Z^f_{bottom} - Z^f_{top}) = 1/c$$

$$H^0 - H^f = d_{top} - d_{bottom}$$
$$(H^0 - H^f) / H^0 = (d_{top} - d_{bottom}) / H^0 = c$$

Relative motion of grains as well as translation of the layer's bottom (from Z^0_{bottom} to Z^f_{bottom}) happens in nature. In the model, the top of the periodic cell moves downward, but the bottom of the cell remains stationary. The grains are forced to move relative to each other as the rescaling of grain center locations cause overlaps that are removed by cooperative rearrangement. However, the grains in the model have the same experience as in nature when the value of c of the compaction model corresponds to the overall compaction c in nature. Rescaling the grains in compaction model is representative of overall compaction of a sediment layer in nature.

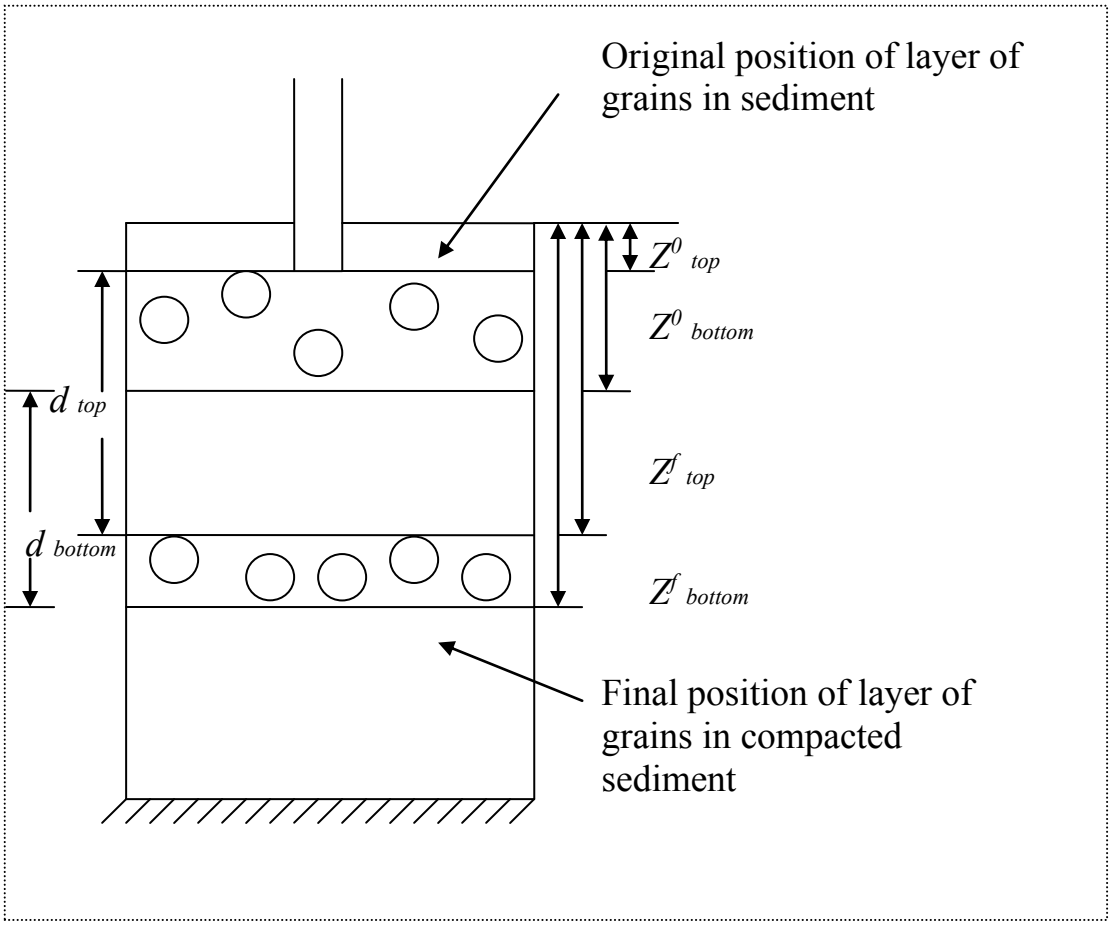

Figure 2.3: Schematic showing the relative motion of spheres within a box in mechanical compaction

2.4 RESCALING IN THE DIRECTION OF COMPACTION

Using this procedure connectivity of carbonaceous material is simulated for 5 and 10 percent of carbonaceous material as a function of compaction stages (values of *c*). The percentage refers to the total bulk volume of the model sediment which undergoes compaction. Connectivity is studied in two scenarios:

a) Rescaling in the direction of compaction without cooperative rearrangement (Unconserved volume approach). Some solid volume is lost in rescaling due to non removal of overlaps and hence the grain volume is not conserved.

b) Rescaling in the direction of compaction with cooperative rearrangement (Conserved volume approach). The overlap created by rescaling is removed by moving the spheres apart in the line joining their centres to conserve the grain volume.

2.5 RESCALING IN THE DIRECTION OF COMPACTION WITHOUT COOPERATIVE REARRANGEMENT

In this scenario, the effect of mechanical compaction is studied by rescaling the grain packing in the direction of compaction without cooperative rearrangement. The mechanical compaction is assumed to be uniaxial. It is imposed geometrically by incrementally rescaling the z-coordinate of the spheres and the box containing the packing.

$$Z^f = Z^0 c$$

where Z^f is the final z- coordinate and Z^0 is the initial z-coordinate. This procedure is repeated for a series of values of c. This process results in an overlap of spheres. The overlap of the spheres is not removed in any of the compaction stages. Thus this method does not conserve mass or volume. A more rigorous approach is defined next.

2.6 RESCALING IN THE DIRECTION OF COMPACTION WITH COOPERATIVE REARRANGEMENT

In this simulation the effect of mechanical compaction is also studied by rescaling the grain packing in the direction of compaction, and then allowing cooperative rearrangement after each increment. The overlaps created by rescaling are removed by moving the spheres apart in the line joining their centre. Overlap is removed in an iterative manner while keeping all the boundaries periodic. The algorithm stops when more compaction would cause unremovable overlaps for rigid grains or greater than

allowable overlap for the ductile grains. The compaction is done in stages with a constant decrement of 0.02 in the value of *c* starting from 1.00.

This approach is used to study connectivity of both rigid and ductile grains. Following Thane (2005), the rigid grain is represented by a hard sphere whereas a ductile grain is represented by a hard core with soft shell around it as shown in Figure 2.4. Ductility of a grain is defined in terms of the ratio of the rigid radius to the initial sphere radius. For example, a sphere of 0.9 rigid radius means that the hard core comprises 0.9 times the radius of the sphere with an outer shell of thickness 0.1*R*. The ductility of the grains is simulated for rigid radius ratios of 0.9, 0.8 and 0.7.

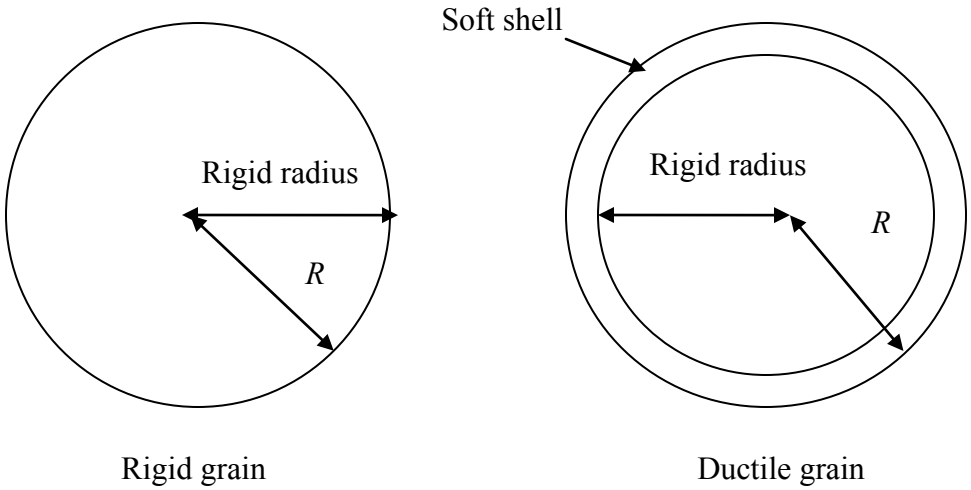

Figure 2.4: Illustration of rigid and ductile grains. For rigid grain, the rigid radius equals grain radius *R*. For ductile grains, the rigid radius is less than the grain radius *R*.

2.7 CLUSTER FORMATION

In this work, a code was developed for studying the connectivity of the grains created by the cooperative rearrangement algorithm. Initially all the spheres of the packing are assigned a null cluster ID. All spheres are then tested for connectivity. Two spheres are said to be connected if the distance between their centers is equal to the sum of the radius of the spheres within some tolerance value. If the gap between the spheres (D) is more than the tolerance value the spheres are not considered to be connected as shown in Figure 2.5. A tolerance value (D) of 0.001 R was chosen in all the simulations. Rodriguez (2006) studied the gap size distribution in packings of equal spheres created with Thane's code and found that a tolerance of $|10^{-3}|\ R$ gives the experimentally observed average number of neighbors in a dense packing of porosity ~36%. Connected spheres form clusters and a distinct cluster ID assigned to these arrays of spheres. The cluster algorithm accounts for the periodic boundaries of the packing, That is, a sphere at or near one face of the cubic space (unit cell) can be in contact with a sphere at or near the opposite face.

Standard outputs of the simulation code consist of the size and frequency of the various cluster IDs. The size of a cluster is defined by the number of spheres in that cluster and its frequency gives the number of such clusters formed. The plot of cluster size versus cluster frequency gives the cluster size distribution of a sphere packing.

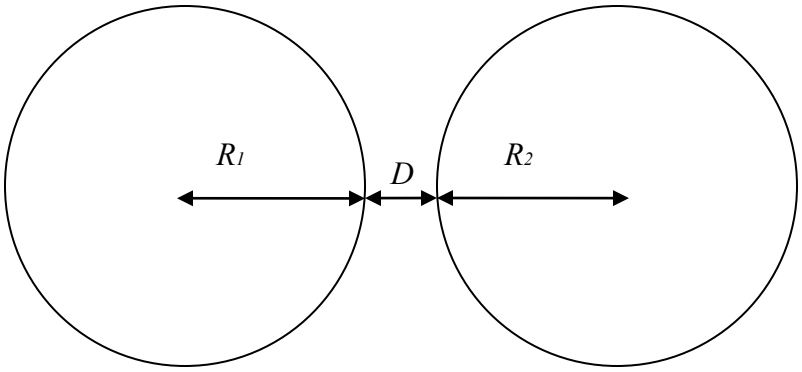

Figure 2.5: The criterion for touching spheres is whether the gap D between the spheres is less than a user-specified tolerance.

The sensitivity of cluster numbers to the tolerance D on a sphere packing of 100 spheres with a solid volume fraction of 0.05 is illustrated in Figures 2.6-2.11. The maximum cluster size is very large at a tolerance of $1.0R$ which is expected since tolerance and radius of sphere are of the same order. The maximum cluster size decreases as the tolerance value is decreased from $0.1R$ to $0.00001R$. The cluster distribution remains qualitatively similar from a tolerance value of $0.1R$ to $0.00001R$. In this work we use D=$0.001R$ to define touching spheres.

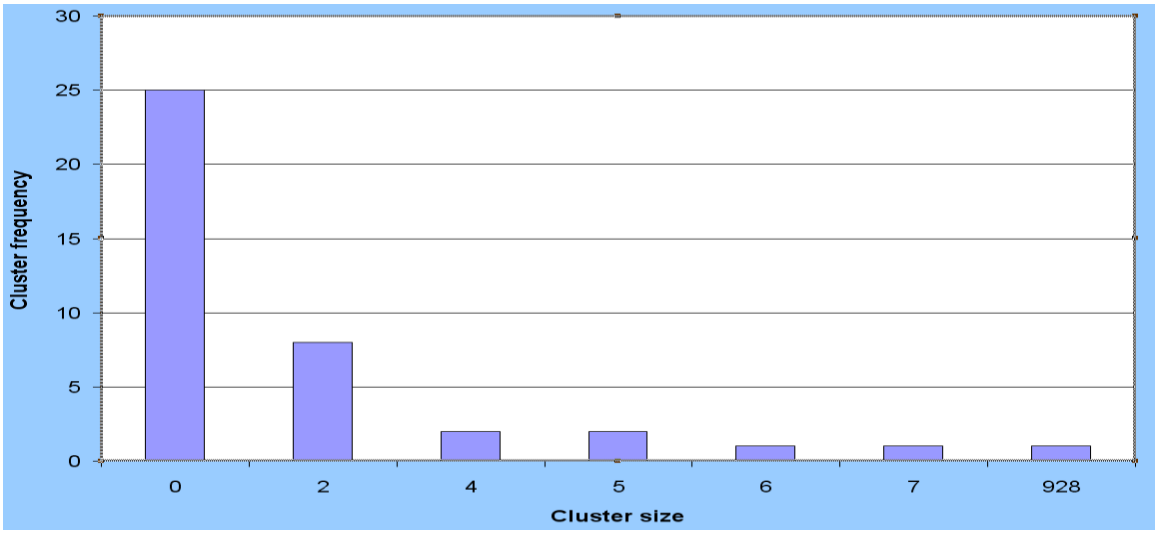

Figure 2.6: Cluster size distribution for 100 spheres for one component sphere packing for tolerance value $D = 1.0\ R$

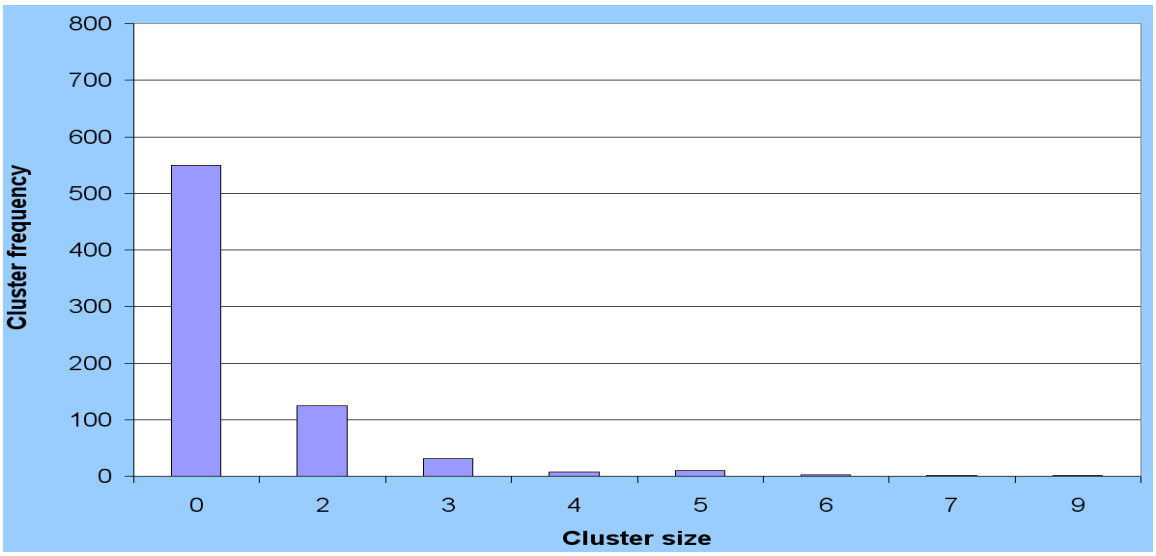

Figure 2.7: Cluster size distribution for 100 spheres for one component sphere packing for tolerance value $D = 0.1\ R$

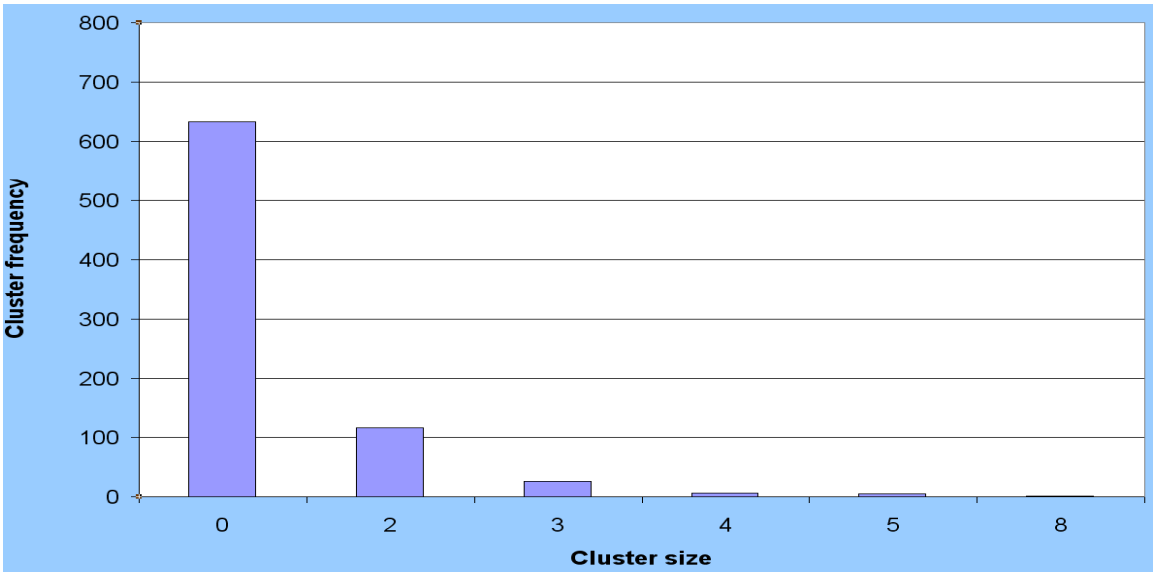

Figure 2.8: Cluster size distribution for 100 spheres for one component sphere packing for tolerance value $D = 0.01\ R$

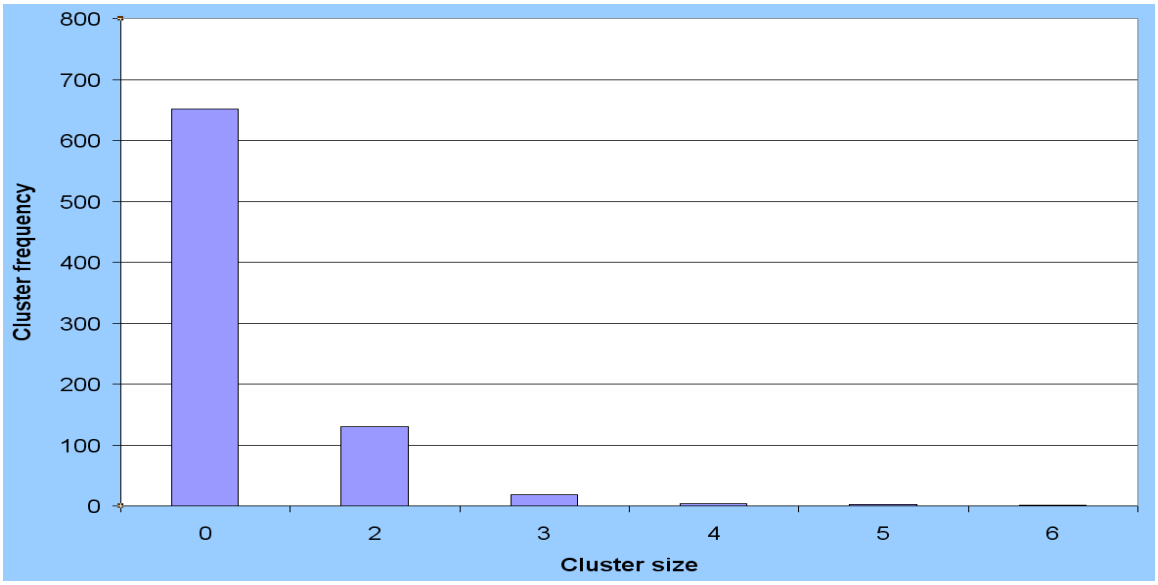

Figure 2.9: Cluster size distribution for 100 spheres for one component sphere packing for tolerance value $D = 0.001\ R$

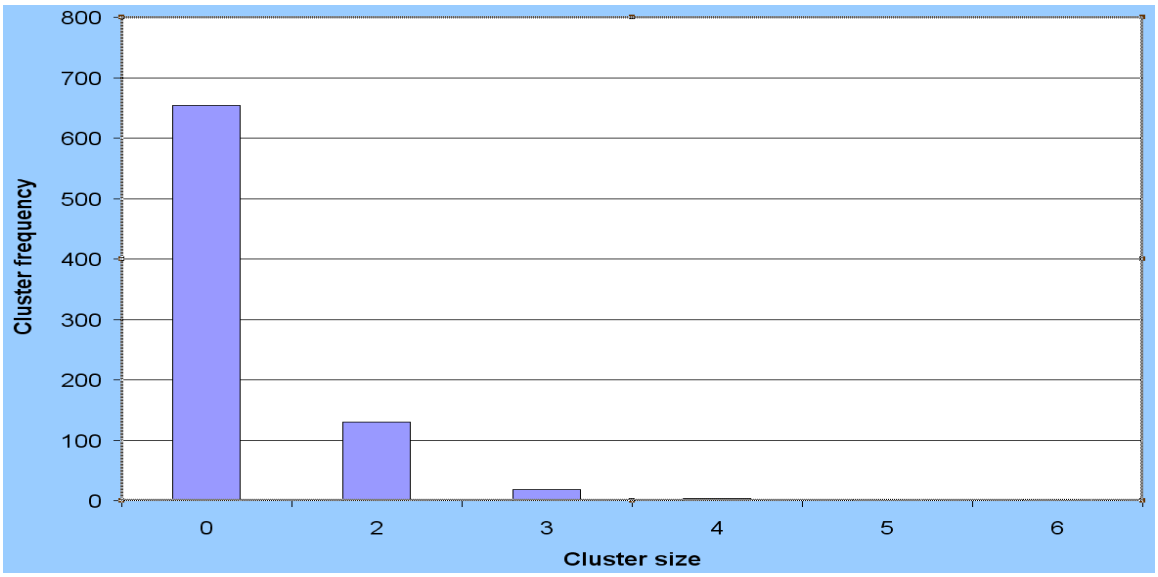

Figure 2.10: Cluster size distribution for 100 spheres for one component sphere packing tolerance value $D = 0.0001\ R$

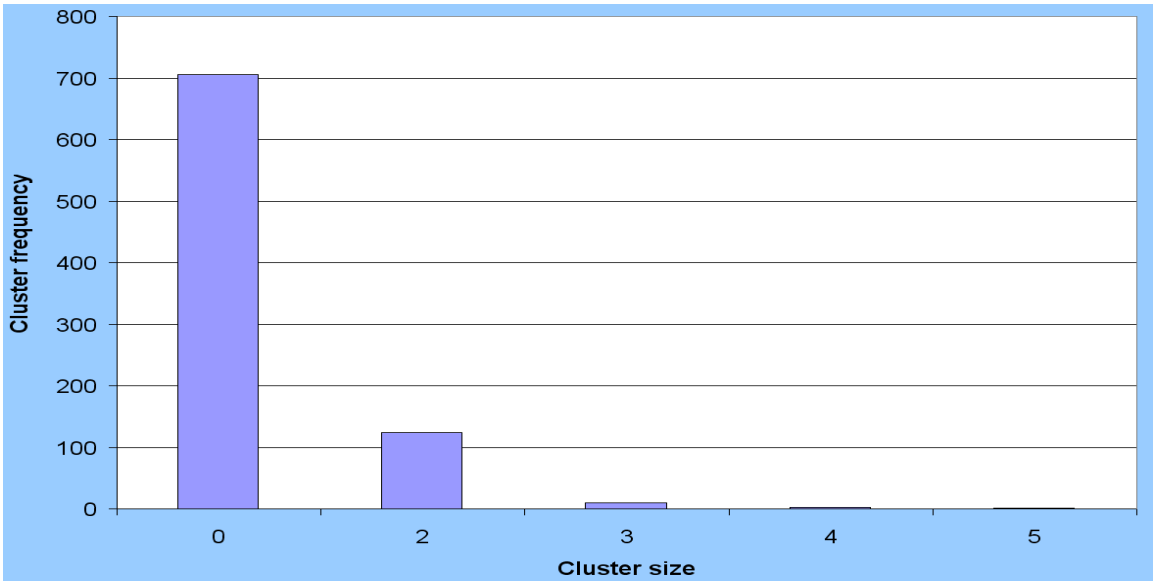

Figure 2.11: Cluster size distribution for 100 spheres for one component sphere packing for tolerance value $D = 0.00001$

Chapter 3: Effect of volume fraction of carbonaceous material on number of clusters in model sediments

3.1 ALGORITHM FOR CREATING PACKINGS WITH PRESCRIBED VOLUME FRACTION OF GRAINS

As discussed in Chapter 2, the cooperative rearrangement algorithm developed by Thane (2005) was revised in this study to allow stopping at an arbitrary solid volume fraction within the periodic cell with a user- defined number of spheres. The variable of density fraction (equivalent to user-defined density fraction in the original code) was used to perform the above analysis. The number of spheres and the desired solid volume as a percentage of total cell volume are the inputs. Figure 3.1 and 3.2 show a periodic packing of 5 % and 10% of the cell volume occupied by solid for 100 and 1000 spheres, respectively.

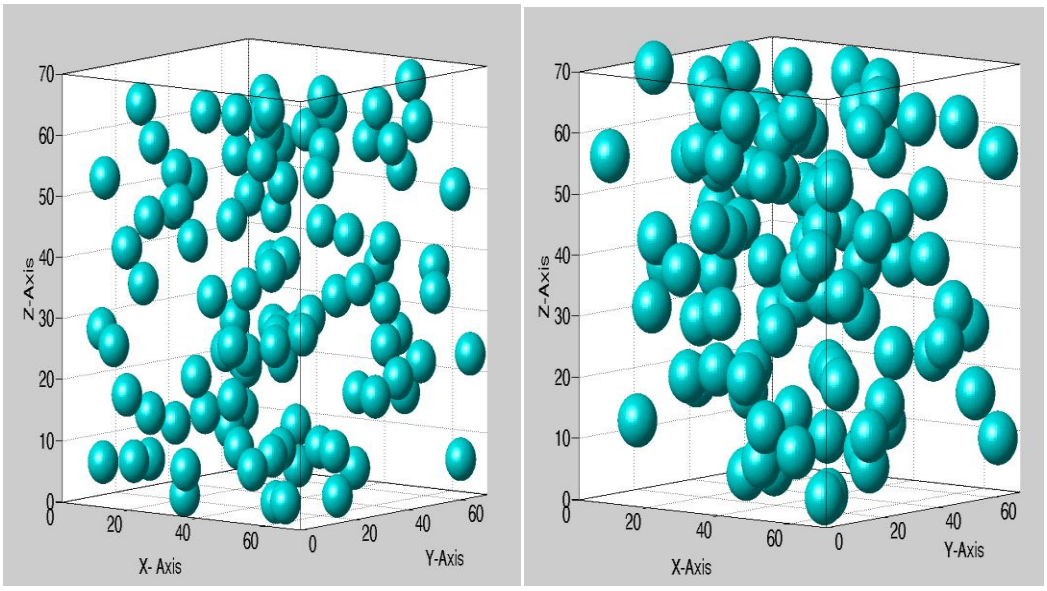

Figure 3.1: Periodic packing of 100 spheres showing 5% (left) and 10% (right) of cell volume occupied by solid

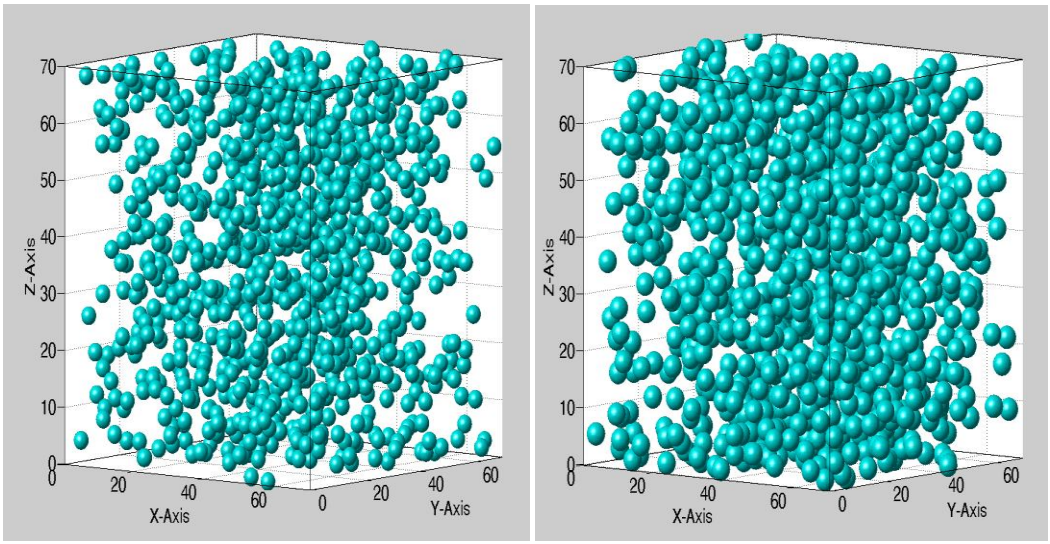

Figure 3.2: Periodic packing of 1000 spheres showing 5% (left) and 10% (right) of cell volume occupied by solid

The simplest model assumes that the other material in the sediment (silt, clay, etc.) does not influence the ability of carbonaceous grains to come into contact. In this case we need not model the other material explicitly. This case can be simulated by creating "one component sphere packings", Figure 3.3, whose solid volume fraction corresponds to the volume fraction of organic material in sediments. All the grains in these model sediments represent carbonaceous material, hence the term "one component". The number of spheres is varied from 100 to 5000 to check that the statistics are representative. This scenario involves a single independent parameter, the initial volume fraction of organic material.

The idea behind this approach is to study the connectivity of particles grown in an unrestricted growth environment assuming that the growth of carbonaceous material is not affected by other material around it, Figure 3.3. This decoupling may not accurately

reflect what happens in nature. Thus, a more realistic model explicitly includes grains that represent other constituents of the sediment. This case is simulated with two component sphere packings representing carbonaceous and silt grains mixed together with varying fraction of carbonaceous material.

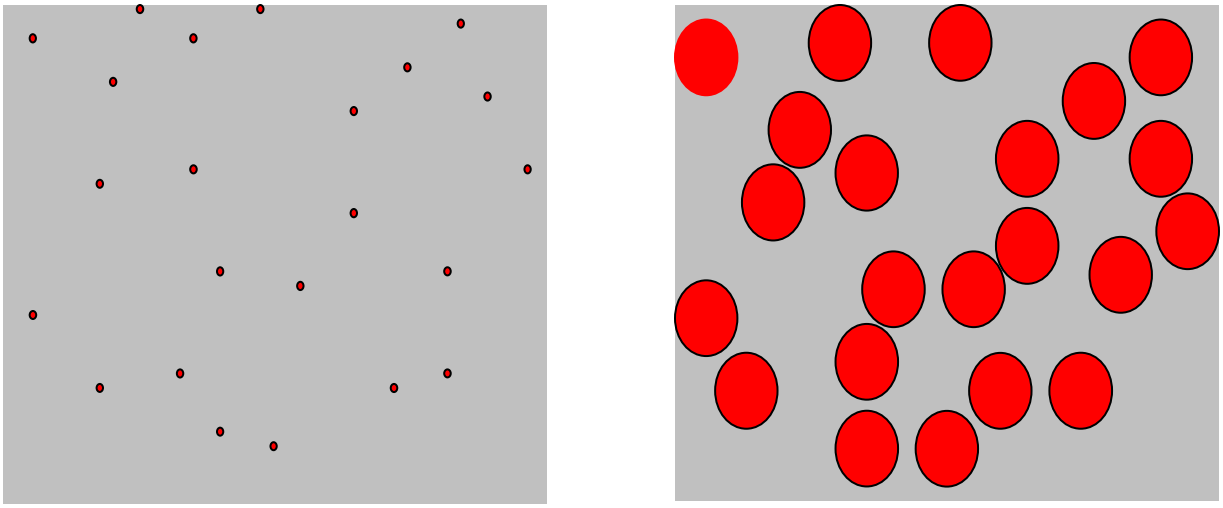

Figure 3.3: Initial point generation (Left) and particle growth (Right) in one component sphere packing representing only carbonaceous material in the original sediment

In Figure 3.4, only a prescribed fraction of grains in the packing represent carbonaceous material. The idea of this approach is to model the interference of other grains on the clustering material as the sediment precursor is compacted into mudrock. This scenario involves two parameters, the initial volume fraction of organic material and the prescribed porosity of the initial model sediment

To create a two component model, the same grain packing code described in Chapter 2 is used to generate a packing of spheres of two slightly different sizes. The size difference is a simple way to identify a subset of the grains and assign them the attribute of being carbonaceous. The ratio of the sphere sizes is kept close to one (1.01) so that the

effect of the relative size of the grains on grain rearrangement and connectivity is negligible. In these models both sizes of sphere are grown simultaneously. The number fraction of larger spheres is chosen to give the desired volume fraction of organic material. Target sediment porosities of 50%, 60% and 70% are considered in this scenario which is assumed to be representative of the sediment precursor to mudrock.

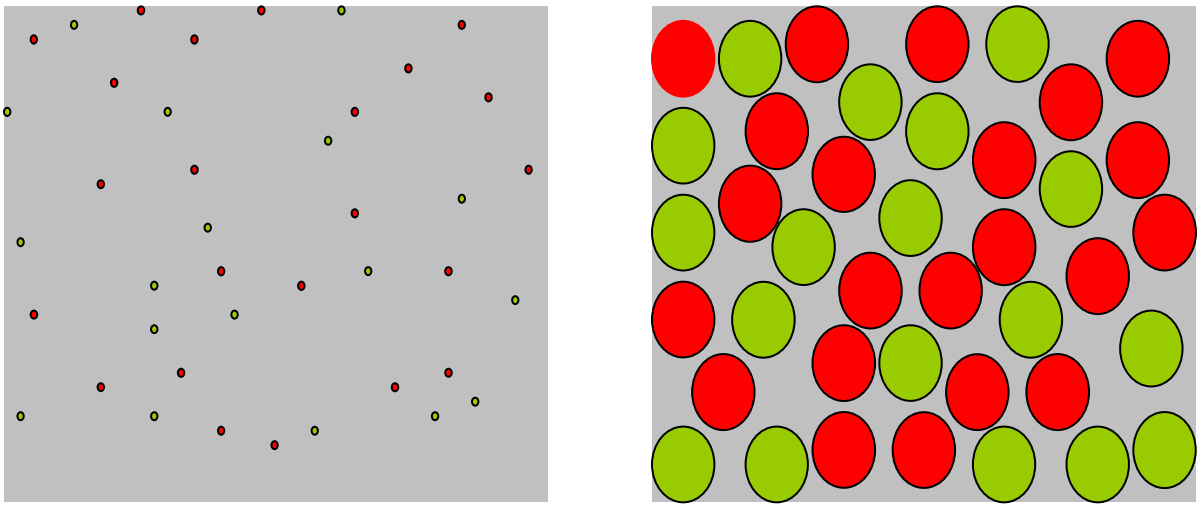

Figure 3.4: Initial point generation (Left) and particle growth (Right) in two component sphere packing, red colored spheres representing carbonaceous material and green colored spheres representing silt/clay

3.2 CARBONACEOUS MATERIAL ONLY (ONE COMPONENT SPHERE PACKING)

The grain packing code described above was used to make numerous one component sphere packings. Packings of 500, 1000, 2500, 3000, 3500 and 5000 spheres were created with prescribed solid volume fraction ranging from 0.05 to 0.30 in step size of 0.05 (Table 3.1). As it is one component sphere packing all the solid volume corresponds to carbonaceous material.

Plots of cluster size and cluster frequency were made to characterize the span of clusters in 3D. The volume fraction of the solids representing carbonaceous matter was varied and maximum cluster size with varying density fraction was simulated. Normalized maximum cluster size (maximum cluster size/ total number of spheres in the packing) was tabulated (Tables 3.2-3.8) and plotted against volume fraction of carbonaceous material (Figure 3.5).

Table: 3.1 One component sphere packing representing carbonaceous material used for analysis with prescribed solid volume representing carbonaceous material

Packing Number	**Prescribed volume fraction of carbonaceous material**
1	0.05
2	0.10
3	0.15
4	0.20
5	0.25
6	0.30

Table: 3.2 Normalized maximum cluster size for various volume fraction of carbonaceous material for 100 spheres for D=0.001R

Volume fraction of carbonaceous material	**Maximum Cluster size**	**Normalized cluster size**
0.05	5	0.05
0.10	7	0.07
0.15	16	0.16
0.20	48	0.48
0.25	73	0.73
0.30	87	0.87

Table: 3.3 Normalized maximum cluster size for various volume fraction of carbonaceous material for 500 spheres for D=0.001R

Volume fraction of carbonaceous material	**Maximum Cluster size**	**Normalized cluster size**
0.05	4	0.008
0.10	12	0.024
0.15	31	0.062
0.20	70	0.140
0.25	340	0.680
0.30	420	0.840

Table: 3.4 Normalized maximum cluster size for various volume fraction of carbonaceous material for 1000 spheres for D=0.001R

Volume fraction of carbonaceous material	**Maximum Cluster size**	**Normalized cluster size**
0.05	6	0.006
0.10	13	0.013
0.15	34	0.034
0.20	88	0.088
0.25	667	0.667
0.30	879	0.879

Table: 3.5 Normalized maximum cluster size for various volume fraction of carbonaceous material for 2500 spheres for D=0.001R

Volume fraction of carbonaceous material	Maximum Cluster size	Normalized cluster size
0.05	7	0.002
0.10	12	0.004
0.15	42	0.016
0.20	203	0.081
0.25	1328	0.531
0.30	2146	0.858

Table: 3.6 Normalized maximum cluster size for various volume fraction of carbonaceous material for 3000 spheres for D=0.001R

Volume fraction of carbonaceous material	Maximum Cluster size	Normalized cluster size
0.05	10	0.003
0.10	21	0.007
0.15	38	0.012
0.20	137	0.045
0.25	1894	0.631
0.30	2643	0.881

Table: 3.7 Normalized maximum cluster size for various volume fraction of carbonaceous material for 3500 spheres for D=0.001R

Volume fraction of carbonaceous material	Maximum Cluster size	Normalized cluster size
0.05	13	0.003
0.10	22	0.005
0.15	59	0.012
0.20	491	0.067
0.25	2896	0.545
0.30	3321	0.867

Table: 3.8 Normalized maximum cluster size for various volume fraction of carbonaceous material for 5000 spheres for D=0.001R

Volume fraction of carbonaceous material	Maximum Cluster size	Normalized cluster size
0.05	8	0.001
0.10	15	0.003
0.15	62	0.012
0.20	229	0.045
0.25	2999	0.599
0.30	4324	0.864

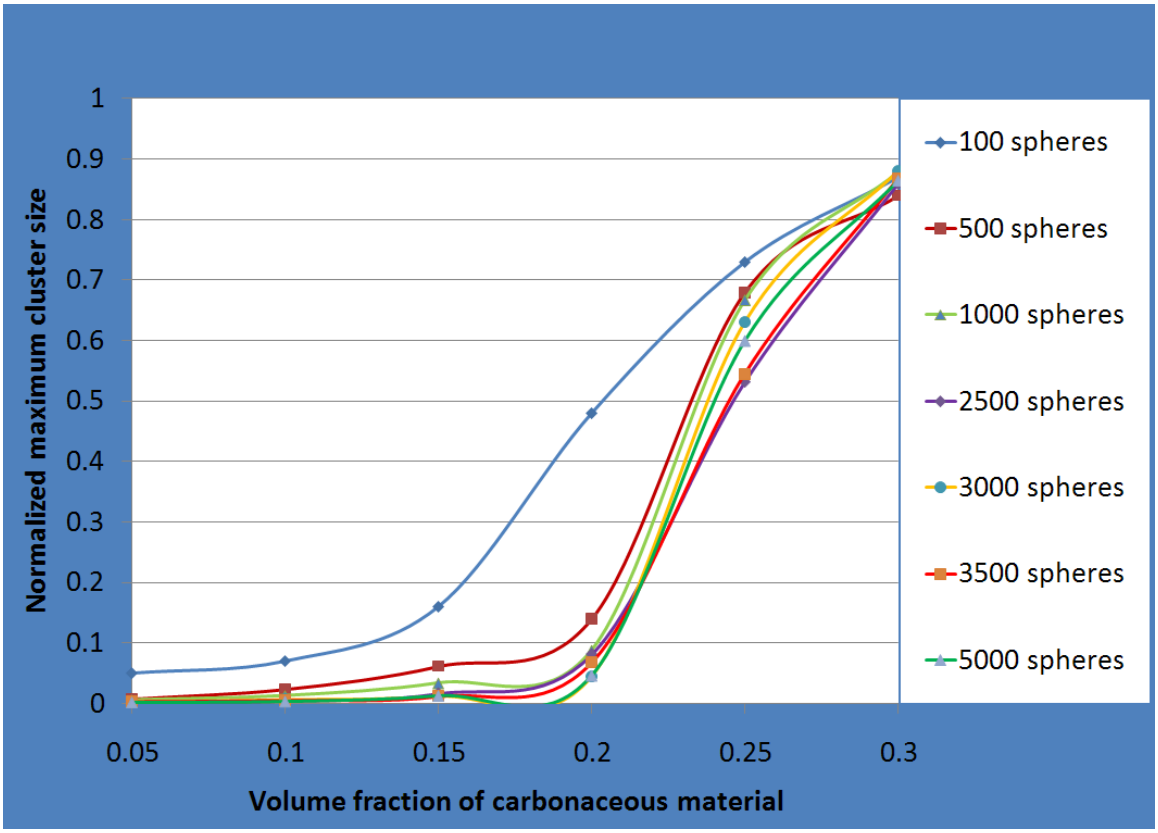

Figure 3.5: Normalized maximum cluster size for D = 0.001R vs. volume fraction of carbonaceous material for one component sphere packing

As shown in Figure 3.5, model sediments that assume carbonaceous material arrangement unaffected by other grains have a characteristic trend of maximum cluster size. The normalized maximum cluster size starts increasing with the volume fraction of carbonaceous material and makes a 'S' shaped profile. A rapid increase in normalized maximum cluster size is observed at 0.2 volume fraction of carbonaceous material for tolerance value $D = 0.001R$. This is the point at which smaller different sized clusters mingle to form a big cluster which may result in percolation.

These results suggest that, if mudrocks have a volume fraction of carbonaceous material from 0.20 to 0.25, we can expect a pore network of connected carbonaceous material leading to percolation. Such rocks should have significantly larger permeability to gas than rocks with carbonaceous material volume fraction less than 0.20. However, it is observed that cooperative rearrangement leads to clustering (section 3.7), as there is enough void space to accommodate all the spheres without any formation of clusters. Thus these results predict more clustering that may occur in nature.

3.3 CARBONACEOUS MATERIAL WITH MATRIX (TWO COMPONENT SPHERE PACKING)

The same grain packing code was used to make numerous two component sphere packing by using slightly different size of spheres to distinguish their chemical identity (carbonaceous material or silt/clay).

Packings of 100, 500, 1000 and 2000 spheres of carbonaceous material were created. The volume fraction of carbonaceous material ranged from 0.05 to 0.30 in step size of 0.05. Target porosities of 50%, 60% and 70% were used to represent a range of

sediments. In this scenario, porosities represent the void volume in the mixtures of carbonaceous material and silt/clay which are sediment precursor to mudrock.

Each set of packings with a given amount of carbonaceous grains had a range of numbers of silt grains. The values were chosen to yield different porosities and volume fractions of carbonaceous material. This results in a "probability factor", the fraction of the total number of spheres that are carbonaceous material. The cooperative rearrangement code allows specifying this fraction to be carbonaceous, so the resulting packing does not have exactly the desired number of carbonaceous spheres. The fraction and the total number of spheres for packings containing 1000 spheres (desired number) representing carbonaceous material are tabulated in the tables 3.9 to 3.11. Similar tables can be constructed for packings in which 100, 500 or 2000 spheres are carbonaceous and others non carbonaceous. The plots are shown in Figure 3.6-3.8.

Table: 3.9 Composition of two component packings: Carbonaceous material with other grains for target porosity of 70%; the desired number of carbonaceous material spheres is 1000. Volume fraction refers sediment bulk volume

Volume fraction of carbonaceous material	**Probability factor for carbonaceous material**	**Total number of spheres in packing**
0.05	0.1666	6000
0.10	0.3333	3000
0.15	0.5000	2000
0.20	0.6666	1500
0.25	0.8333	1200
0.30	1.0000	1000

Table: 3.10 Composition of two component packings: Carbonaceous material with other grains for target porosity of 60%; the desired number of carbonaceous material spheres is 1000. Volume fraction refers sediment bulk volume

Volume fraction of carbonaceous material	Probability factor for carbonaceous material	Total number of spheres in packing
0.05	0.1250	8000
0.10	0.2500	4000
0.15	0.3750	2667
0.20	0.5000	2000
0.25	0.6250	1600
0.30	0.7500	1334

Table: 3.11 Composition of two component packings: Carbonaceous material with other grains for target porosity of 50%; the desired number of carbonaceous material spheres is 1000. Volume fraction refers sediment bulk volume

Volume fraction of carbonaceous material	Probability factor for carbonaceous material	Total number of spheres in packing
0.05	0.1	10000
0.10	0.2	5000
0.15	0.3	3334
0.20	0.4	2500
0.25	0.5	2000
0.30	0.6	1667

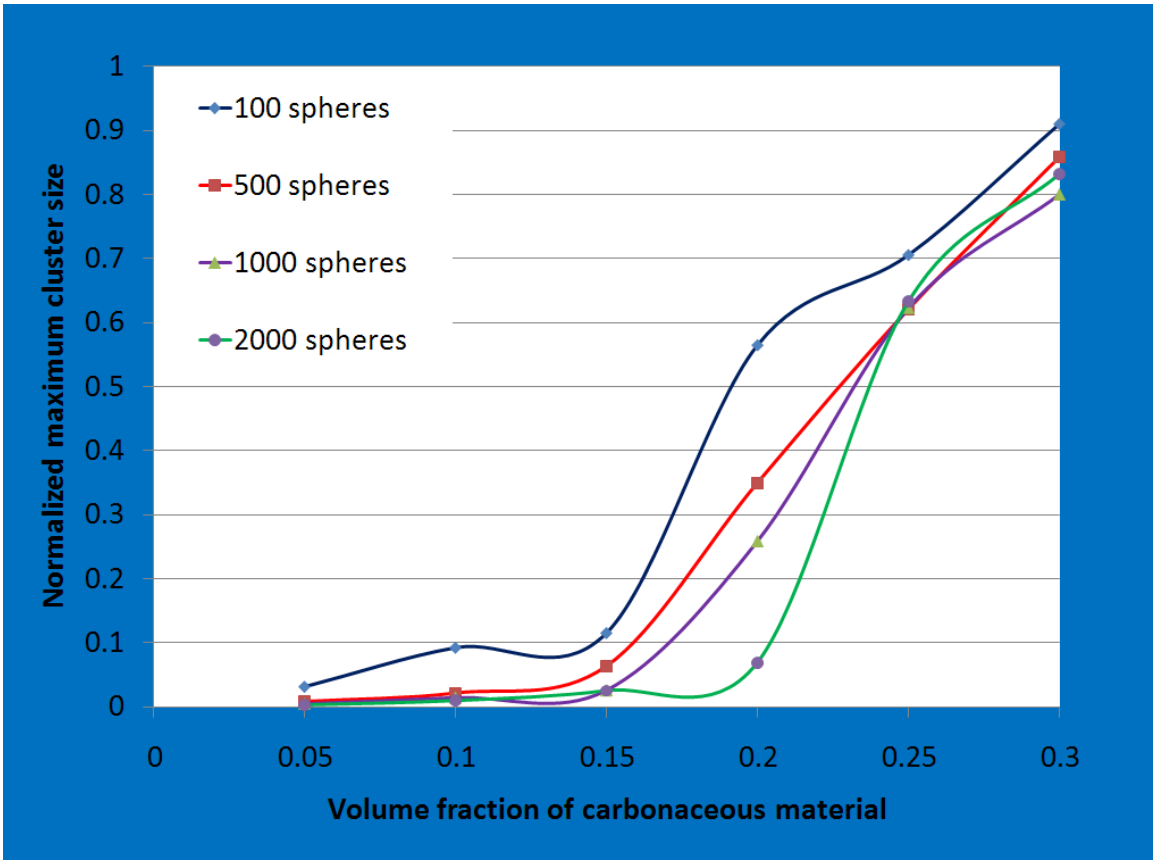

Figure 3.6: Normalized maximum cluster size for $D = 0.001R$ vs. volume fraction of carbonaceous material in sediment for packing of carbonaceous material with matrix. Sediment porosity is 70 percent. Curves refer to sets of packings in which number of carbonaceous material grains is constant

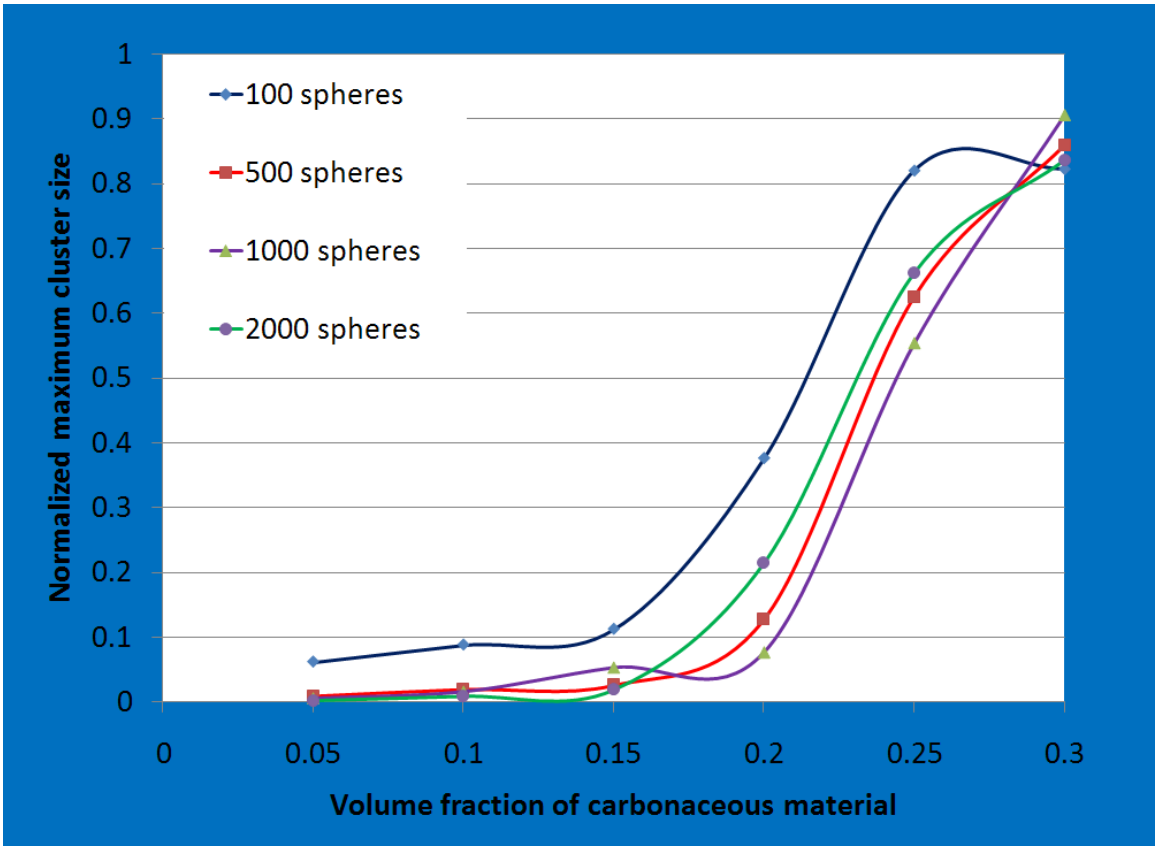

Figure 3.7: Normalized maximum cluster size for $D = 0.001R$ vs. volume fraction of carbonaceous material in sediment for packing of carbonaceous material with matrix. Sediment porosity is 60 percent. Curves refer to sets of packings in which number of carbonaceous material grains is constant

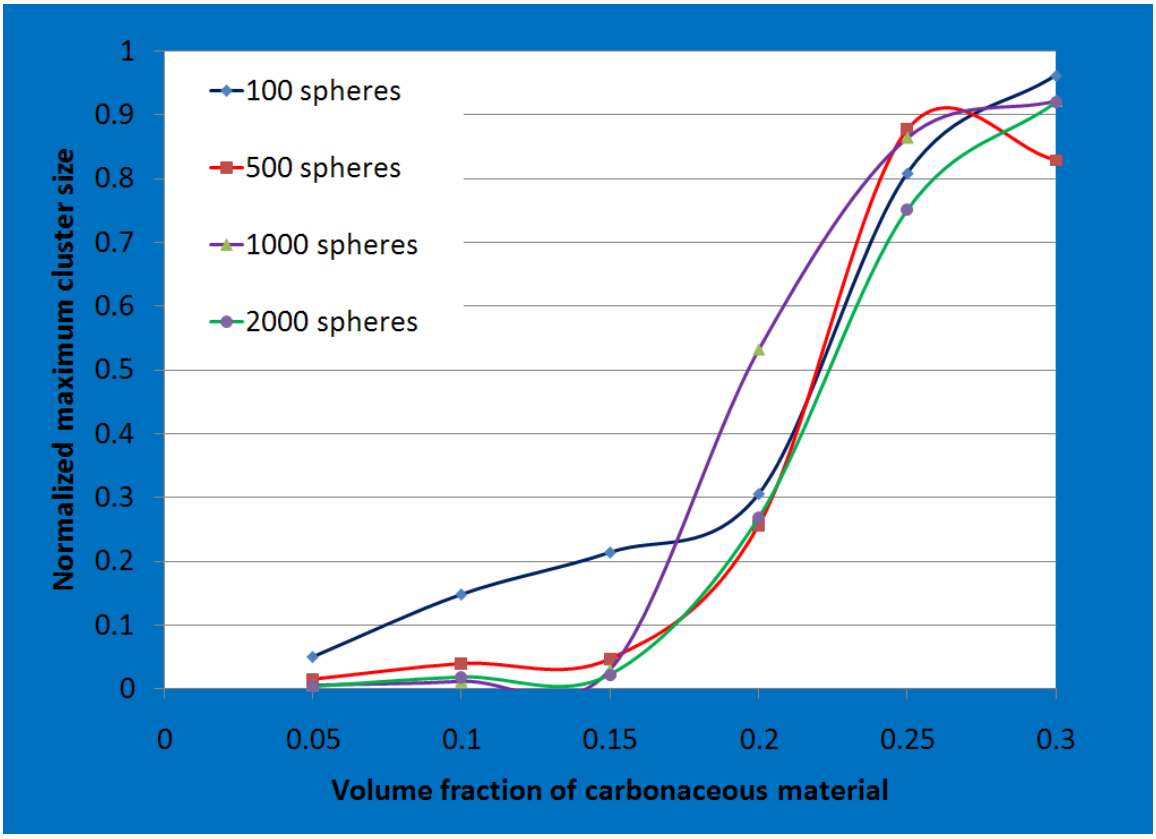

Figure 3.8: Normalized maximum cluster size for $D = 0.001R$ vs. volume fraction of carbonaceous material in sediment for packing of carbonaceous material with matrix. Sediment porosity is 50 percent. Curves refer to sets of packings in which number of carbonaceous material grains is constant

Similar to the one component packing Figure 3.5, packing of carbonaceous material with other grains also yields a 'S' shaped curve in the plot of normalized maximum cluster size vs. volume fraction of carbonaceous material. The maximum cluster size starts increasing when the volume fraction of carbonaceous material reaches about 0.15. Rapid changes in normalized maximum cluster sizes are again observed at 0.2 volume fraction of carbonaceous material for a tolerance value (D) of $0.001R$.

Similar to the results of one component packing discussed in the section 3.2, even in the presence of other component like silt/clay we can expect a pore network of connected carbonaceous material leading to percolation for a mudrock having 0.2-0.25 volume fraction of carbonaceous material.

3.4 CLUSTER LENGTH ANALYSIS

The clusters formed from the sphere packing in the previous section were subjected to cluster length analysis to study their span in 3D, based on the presumption that connected carbonaceous materials are the preferred conduits of gas migration in mudrocks. The length distribution of each cluster in *x*, *y*, and *z* directions was calculated and with the help of suitable geometric transformation its extent was studied in 3D. The 3D envelope made by the geometrical transformation gives an idea of the ranges of lateral extent of the clusters observed in slices cut through any plane for SEM (Scanning Electron Microscope) analysis. For example in Figure 3.9, length in the *X* direction is calculated as :

Length in *X* direction $(LX) = X_{max} - X_{min} + R_1 + R_2$

where X_{max} and X_{min} are the maximum and minimum *x* coordinates of spheres in a particular cluster ID and R_1 and R_2 are the radii of them. Similarly length in *Y* and *Z* directions *LY* and *LZ* were also calculated and the length distribution was studied. The results, Figure 3.10, showed that the distribution of the length in *x y* and *z* directions were quite uniform; i.e. no preferred direction which should be the case as the spheres in the packing were randomly generated.

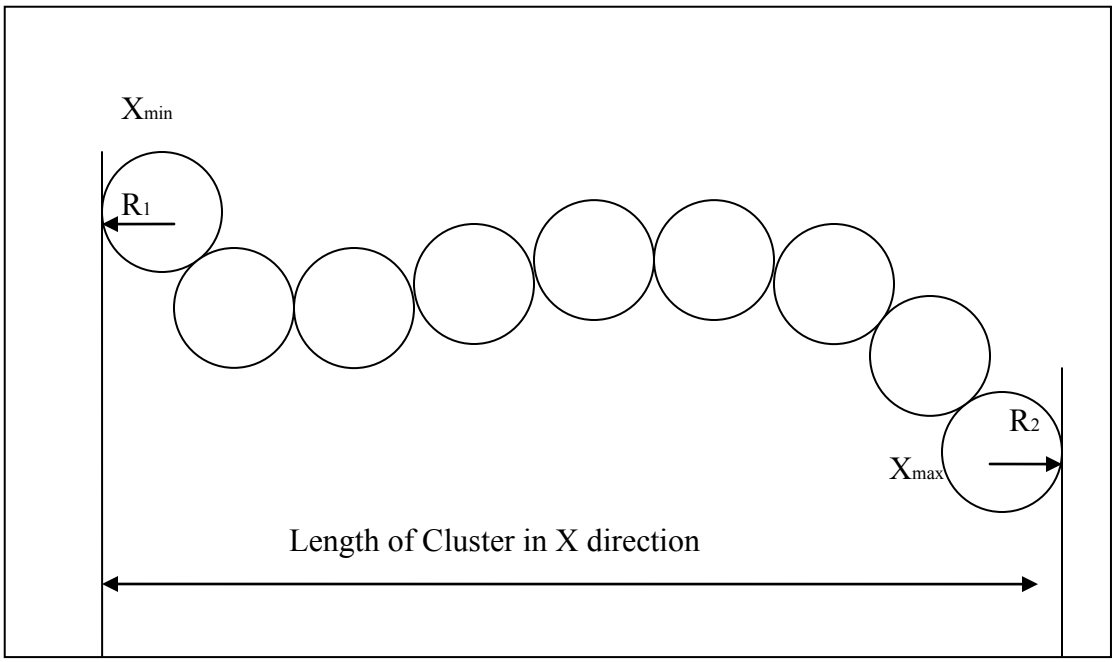

Figure 3.9: Cluster Length calculation in X direction

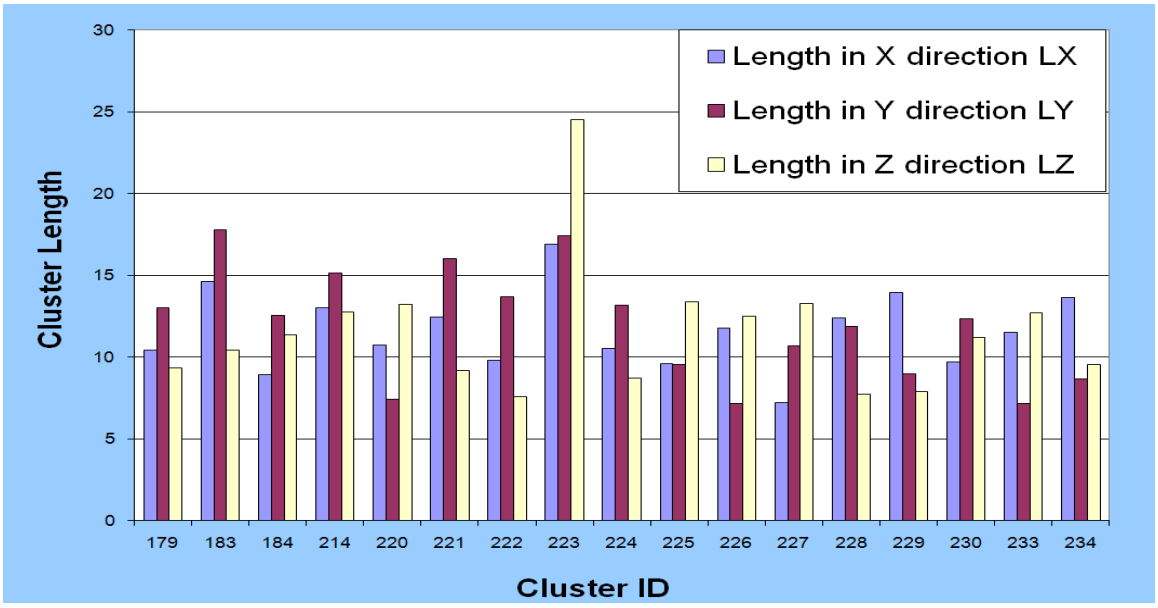

Figure 3.10: Selected cluster length analysis for 5 percent carbonaceous material for one component sphere packing of 100 spheres representing carbonaceous material with radius = 3.56 units

As an example shown in Figure 3.10, it is observed that the cluster ID 223 corresponds to biggest cluster (size =5) for one component sphere packing of 100 spheres with radius 3.56 units.

3.5 GEOMETRICAL TRANSFORMATION

A geometrical transformation was carried out in order to study the 3D envelope of clusters formed. It gives a better idea about the span of cluster with the coordinate axes. The geometrical transformation includes the translation as well as the rotation of the coordinate axes. The spheres nearest and farthest from the origin are identified. The origin of the coordinate system is shifted to the centre of the sphere which is nearest to the old origin with the help of translation. Then the coordinate axes are rotated in such a manner that the z axis of the new coordinate system coincides with the line joining the centre of the spheres identified above(as shown in Figure 3.11). The whole cluster is rotated about this new z axis at steps of 10 degrees from 0 to 180 degrees and its length in the x and a y direction is reported. It is observed that the variation in length of the cluster with angle of rotation is sinusoidal shown in Figure 3.12. The maximum value of cluster length in the x direction is at the minimum value of cluster length in the y direction indicating a constant phase shift of 90 degrees between the two length values.

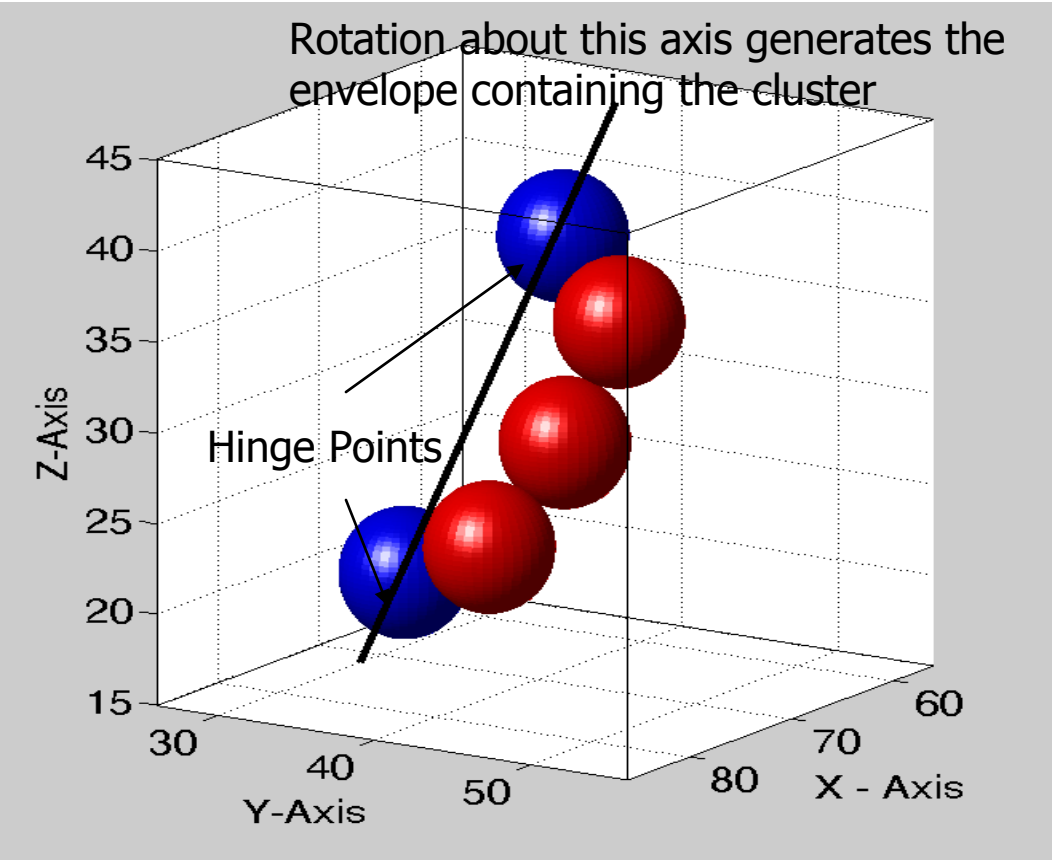

Figure 3.11: Geometrical transformation for the biggest cluster from one component sphere packing of 100 spheres representing carbonaceous material with radius = 3.56 units

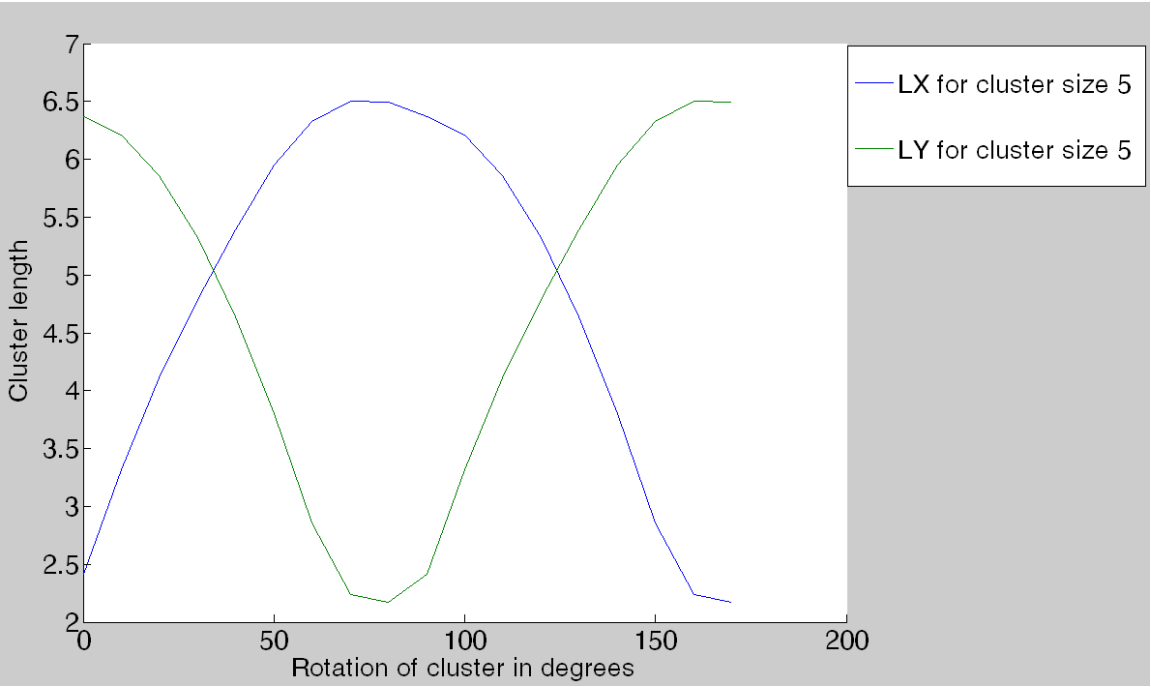

Figure 3.12: Variation of LX and LY in new coordinate system showing a phase difference of 90 degrees between them for the biggest cluster from one component sphere packing of 100 spheres with radius = 3.56 units

3.6 ASPECT RATIO

The aspect ratio of a cluster is defined as the ratio of the maximum cluster length to the minimum cluster length in coordinate directions. The aspect ratios of the clusters were also calculated and reported for different volume fractions of the carbonaceous material. The aspect ratio gives an idea about the appearance of a cluster in 3D for a particular volume fraction of the carbonaceous material. The geometrical transformation with aspect ratios tabulated below in Tables 3.12-3.18.

Table 3.12: Cluster length and cluster aspect ratios for D=0.001R and 5 percent carbonaceous material of bulk volume and 100 spheres with radius = 3.56 units for one component sphere packing after the geometrical transformation

Cluster number	**length_ xmax**	**length_x min**	**length_ ymax**	**length_ ymin**	**length_z max**	**length_z min**	**Aspect ratio**	**Number of spheres in cluster**
1	7.12	7.12	7.12	7.12	14.24	14.24	2.00	2
2	9.54	7.15	9.54	7.15	20.52	20.52	2.87	3
3	7.12	7.12	7.12	7.12	14.24	14.24	2.00	2
4	11.96	7.31	11.96	7.31	17.56	17.56	2.40	3
5	7.12	7.12	7.12	7.12	14.24	14.24	2.00	2
6	12.65	7.38	12.65	7.38	16.09	16.09	2.18	3
7	7.12	7.12	7.12	7.12	14.24	14.24	2.00	2
8	13.63	9.29	13.63	9.29	26.94	26.94	2.90	5
9	7.12	7.12	7.12	7.12	14.24	14.24	2.00	2
10	7.12	7.12	7.12	7.12	14.24	14.24	2.00	2
11	7.12	7.12	7.12	7.12	14.24	14.24	2.00	2
12	7.12	7.12	7.12	7.12	14.24	14.24	2.00	2
13	7.12	7.12	7.12	7.12	14.24	14.24	2.00	2
14	7.12	7.12	7.12	7.12	14.24	14.24	2.00	2
15	7.12	7.12	7.12	7.12	14.24	14.24	2.00	2
16	7.12	7.12	7.12	7.12	14.24	14.24	2.00	2
17	7.12	7.12	7.12	7.12	14.24	14.24	2.00	2

Table 3.13: Cluster length and cluster aspect ratios for D=0.001R and 10 percent carbonaceous material of bulk volume and 100 spheres with radius = 4.42 units for one component sphere packing after the geometrical transformation

Cluster number	length_x max	length_x min	length_ ymax	length_ ymin	length_z max	length_z min	Aspect ratio	Number of spheres in cluster
1	9.84	9.18	9.84	9.18	22.85	22.85	2.49	3
2	10.84	8.88	10.84	8.88	25.98	25.98	2.92	3
3	11.84	8.94	11.84	8.94	23.64	23.64	2.64	3
4	12.84	8.84	12.84	8.84	17.68	17.68	2.00	2
5	13.84	8.84	13.84	8.84	17.68	17.68	2.00	2
6	14.84	8.84	14.84	8.84	17.68	17.68	2.00	2
7	15.84	8.96	15.84	8.96	23.62	23.62	2.64	3
8	16.84	9.04	16.84	9.04	21.30	21.30	2.35	3
9	17.84	8.84	17.84	8.84	17.68	17.68	2.02	2
10	18.84	8.84	18.84	8.84	17.68	17.68	2.13	2
11	19.84	8.84	19.84	8.84	17.68	17.68	2.24	2
12	20.84	8.84	20.84	8.84	17.68	17.68	2.36	2
13	21.84	8.84	21.84	8.84	17.68	17.68	2.47	2
14	22.84	9.18	22.84	9.18	24.30	24.30	2.65	3
15	23.84	9.11	23.84	9.11	25.10	25.10	2.75	3
16	24.84	8.84	24.84	8.84	17.68	17.68	2.81	2
17	25.84	8.84	25.84	8.84	17.68	17.68	2.92	2
18	26.84	9.33	26.84	9.33	21.49	21.49	2.88	3
19	27.84	8.84	27.84	8.84	17.68	17.68	3.15	2
20	28.84	15.73	28.84	15.73	35.94	35.94	2.29	7
21	29.84	8.84	8.84	8.84	17.68	17.68	3.38	2
22	30.84	8.84	8.84	8.84	17.68	17.68	3.49	2

Table 3.14: Cluster length and cluster aspect ratios for D=0.001R and 15 percent carbonaceous material of bulk volume and 100 spheres with radius = 5.03 units for one component sphere packing after the geometrical transformation

Cluster number	**length_x max**	**length_x min**	**length_y max**	**length_y min**	**length_z max**	**length_z min**	**Aspect ratio**	**Number of spheres in cluster**
1	49.95	38.40	49.95	38.40	78.96	78.96	2.06	16
2	10.91	10.11	10.91	10.11	30.13	30.13	2.98	3
3	16.39	10.94	16.39	10.94	36.00	36.00	3.29	5
4	28.38	20.38	28.38	20.38	31.79	31.79	1.56	4
5	29.05	16.38	29.05	16.38	39.76	39.76	2.43	7
6	10.06	10.06	10.06	10.06	20.13	20.13	2.00	2
7	13.43	10.12	13.43	10.12	29.04	29.04	2.87	3
8	27.20	22.92	27.20	22.92	37.96	37.96	1.66	6
9	10.06	10.06	10.06	10.06	20.13	20.13	2.00	2
10	10.06	10.06	10.06	10.06	20.13	20.13	2.00	2
11	10.06	10.06	10.06	10.06	20.13	20.13	2.00	2
12	10.06	10.06	10.06	10.06	20.13	20.13	2.00	2
13	30.53	18.80	30.53	18.80	64.41	64.41	3.43	11
14	16.86	10.47	16.86	10.47	24.88	24.88	2.38	3
15	10.06	10.06	10.06	10.06	20.13	20.13	2.00	2

Table 3.15: Cluster length and cluster aspect ratios for D=0.001R and 20 percent carbonaceous material of bulk volume and 100 spheres with radius = 5.52 units for one component sphere packing after the geometrical transformation

Cluster number	length_x max	length_x min	length_y max	length_y min	length_z max	length_z min	Aspect ratio	Number of spheres in cluster
1	28.25	14.56	28.25	14.56	39.94	39.94	2.74	5
2	85.02	69.05	85.02	69.05	88.61	88.61	1.28	48
3	17.98	11.56	17.98	11.56	28.22	28.22	2.44	3
4	11.04	11.04	11.04	11.04	22.09	22.09	2.00	2
5	11.04	11.04	11.04	11.04	22.09	22.09	2.00	2
6	11.04	11.04	11.04	11.04	22.09	22.09	2.00	2
7	11.04	11.04	11.04	11.04	22.09	22.09	2.00	2
8	29.90	18.57	29.90	18.57	40.00	40.00	2.15	7
9	11.04	11.04	11.04	11.04	22.09	22.09	2.00	2
10	20.52	16.07	20.52	16.07	34.15	34.15	2.13	4
11	11.04	11.04	11.04	11.04	22.09	22.09	2.00	2

Table 3.16: Cluster length and cluster aspect ratios for D=0.001R and 25 percent carbonaceous material of bulk volume and 100 spheres with radius = 5.89 units for one component sphere packing after the geometrical transformation

Cluster number	length_x max	length_x min	length_y max	length_y min	length_z max	length_z min	Aspect ratio	Number of spheres in cluster
1	17.37	12.27	17.37	12.27	32.51	32.51	2.65	3
2	11.78	11.78	11.78	11.78	23.57	23.57	2.00	2
3	11.78	11.78	11.78	11.78	23.57	23.57	2.00	2
4	11.78	11.78	11.78	11.78	23.57	23.57	2.00	2
5	94.19	77.59	94.19	77.59	125.06	125.06	1.61	73

Table 3.17: Cluster length and cluster aspect ratios for D=0.001R and 30 percent carbonaceous material of bulk volume and 100 spheres with radius = 6.83 units for one component sphere packing after the geometrical transformation

Cluster number	length_x max	length_x min	length_y max	length_y min	length_z max	length_z min	Aspect ratio	Number of spheres in cluster
1	22.32	12.77	22.32	12.77	29.71	29.71	2.33	3
2	101.54	85.02	101.54	85.02	114.08	114.08	1.34	87

The maximum aspect ratio increases with the volume fraction of the carbonaceous material. It reaches a maximum value near percolation and then starts decreasing gradually as shown in Figure 3.13.

The aspect ratio of the large clusters increases with volume fraction of carbonaceous material reaches a maximum value (2.06 for cluster size of 16 for 15 percent of carbonaceous material packing) and then starts decreasing with increase in volume fraction of carbonaceous material (1.34 for cluster size of 87 for 30 percent of carbonaceous material packing).

Table 3.18: Maximum, minimum and average aspect ratios for one component sphere packing of 100 spheres for D=0.001R

Volume fraction of carbonaceous material	Max Aspect ratio	Min Aspect ratio	Avg Aspect ratio
0.05	2.90	2.00	2.14
0.10	3.49	2.00	2.57
0.15	3.43	1.56	2.31
0.20	2.74	1.28	2.07
0.25	2.65	1.61	2.05
0.30	2.33	1.34	1.83

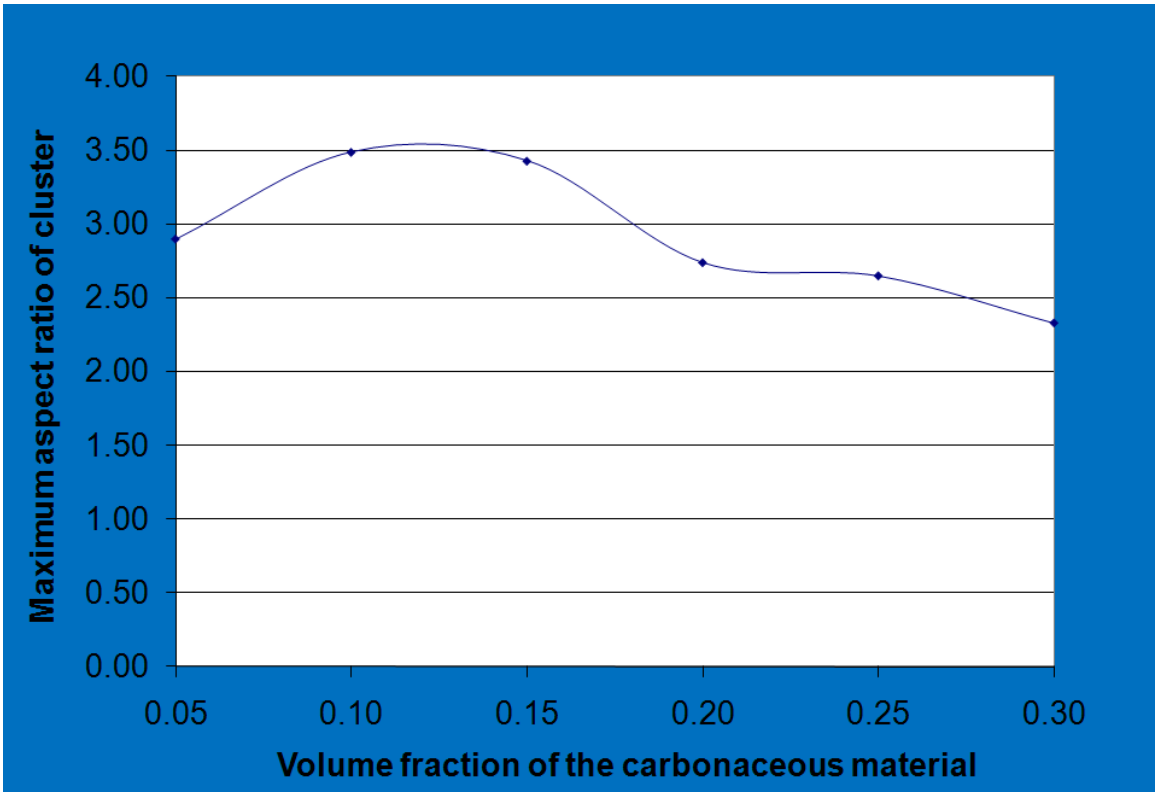

Figure 3.13: Maximum aspect ratio of clusters vs. volume fraction of carbonaceous material for one component sphere packing of 100 spheres for D=0.001R

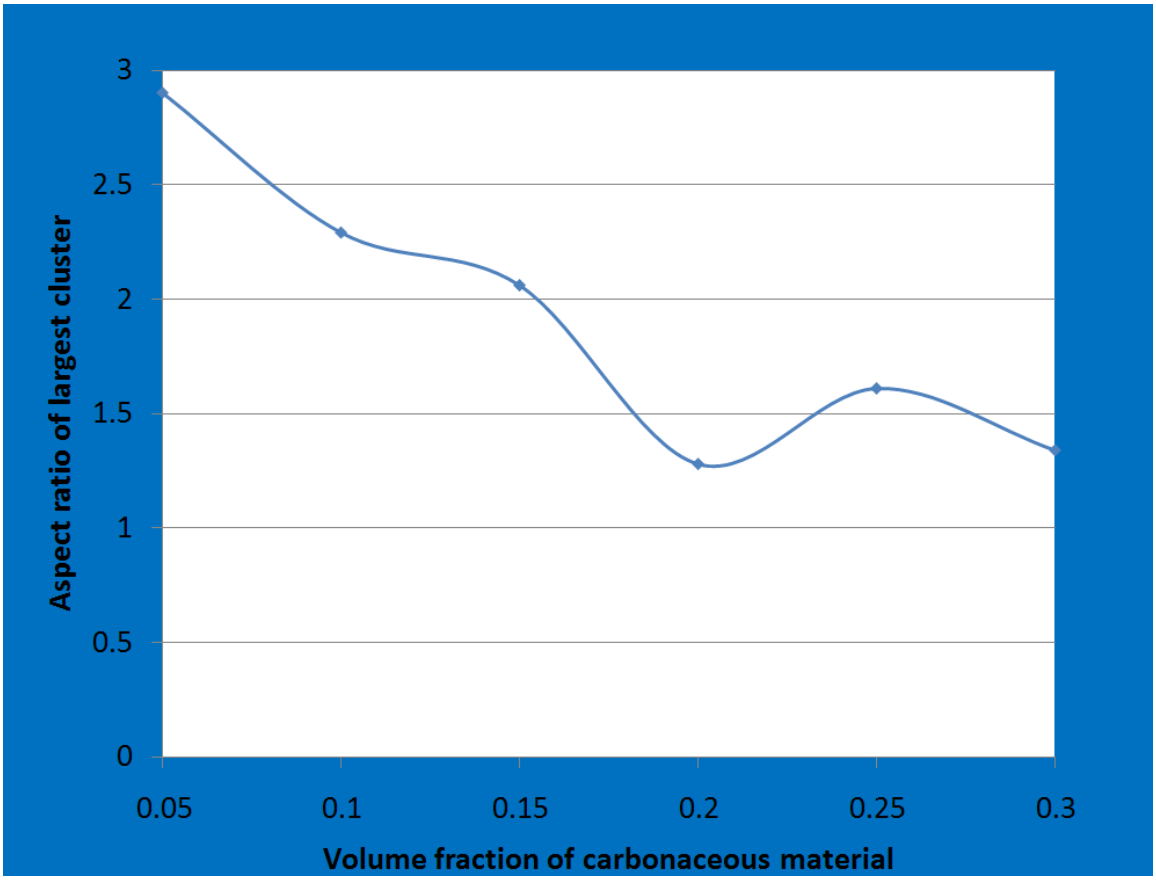

Figure 3.13: Aspect ratio of largest cluster vs. volume fraction of carbonaceous material for one component sphere packing of 100 spheres for D=0.001R

3.7 INHERENT CLUSTERING OF SPHERES INDUCED BY COOPERATIVE REARRANGEMENT ALGORITHM

The algorithm for rescaling the grains with and without cooperative rearrangement was also assessed for inducing clustering of spheres. The cooperative rearrangement algorithm by its nature is conducive to creating clusters, because overlapping spheres are moved until they just touch. Packings in which the grains occupy small volume fractions, e.g. 15%, can easily be arranged to have no grains touching at all.

Thus it is of interest to quantify how much clustering is inherent in the method used to create model sediments.

A one component packing of 0.25 solid volume fraction was considered for analysis. The radius of all the spheres in the packing was reduced so that the packing had a 0.05 solid volume fraction. This method ensured that no sphere was touching with another in the initial sediment precursor. In fact it ensures that the distance between spheres was at least 1.42 sphere radii. The packing was then rescaled in the direction of compaction without cooperative rearrangement. The statistics of cluster frequency and number of spheres associated with particular cluster size class were generated and shown in Figure 3.14-3.15 (bar labeled with suffix-2). They are compared with the statistics of the packing having a 0.05 solid fraction created by Thane's code (Figure 3.14-3.15). That is, two packing have same initial solid fraction (0.05), one containing contacts inherent to the cooperative rearrangement algorithm, the other having all spheres separated, are subjected to the same compaction simulation.

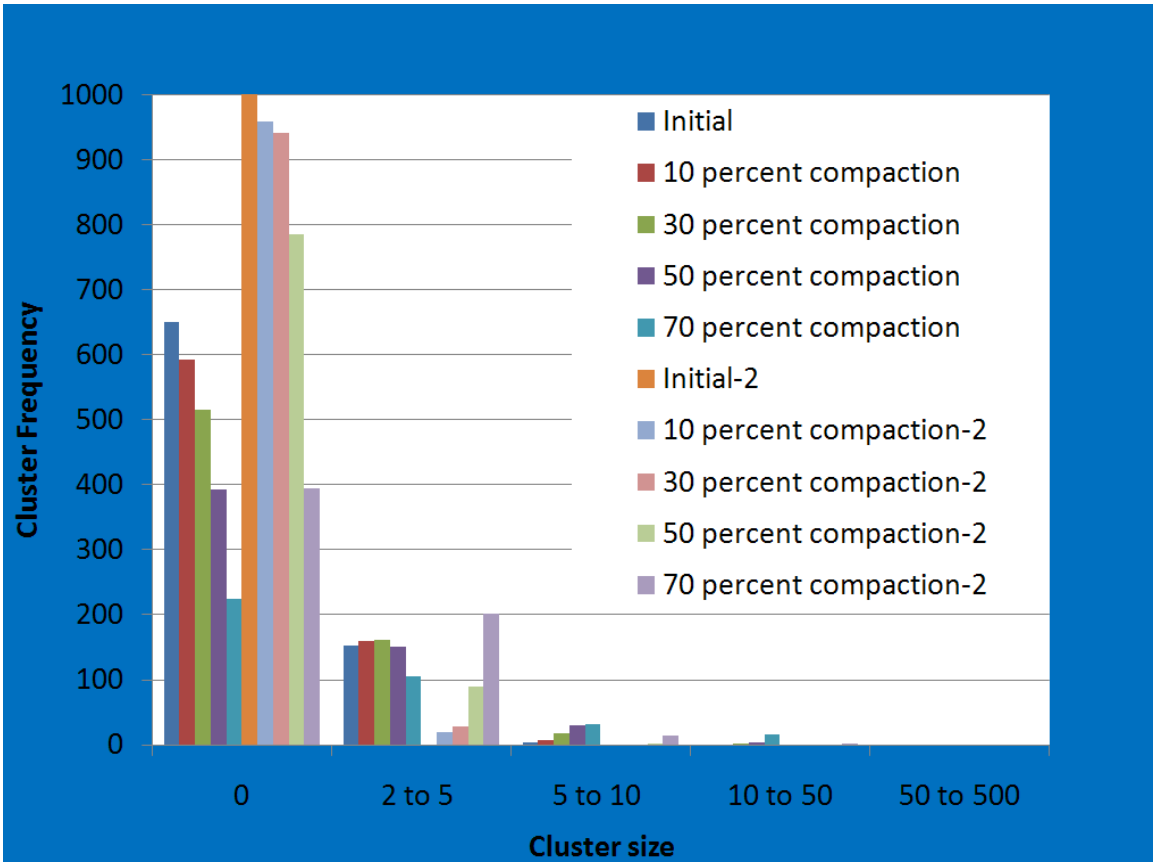

Figure 3.14: Comparison of cluster frequency vs. cluster size for D=0.001R of the compaction stages of one component packing created by Thane's code and dispersed spheres represented by suffix-2 (1000 rigid spheres of carbonaceous material)

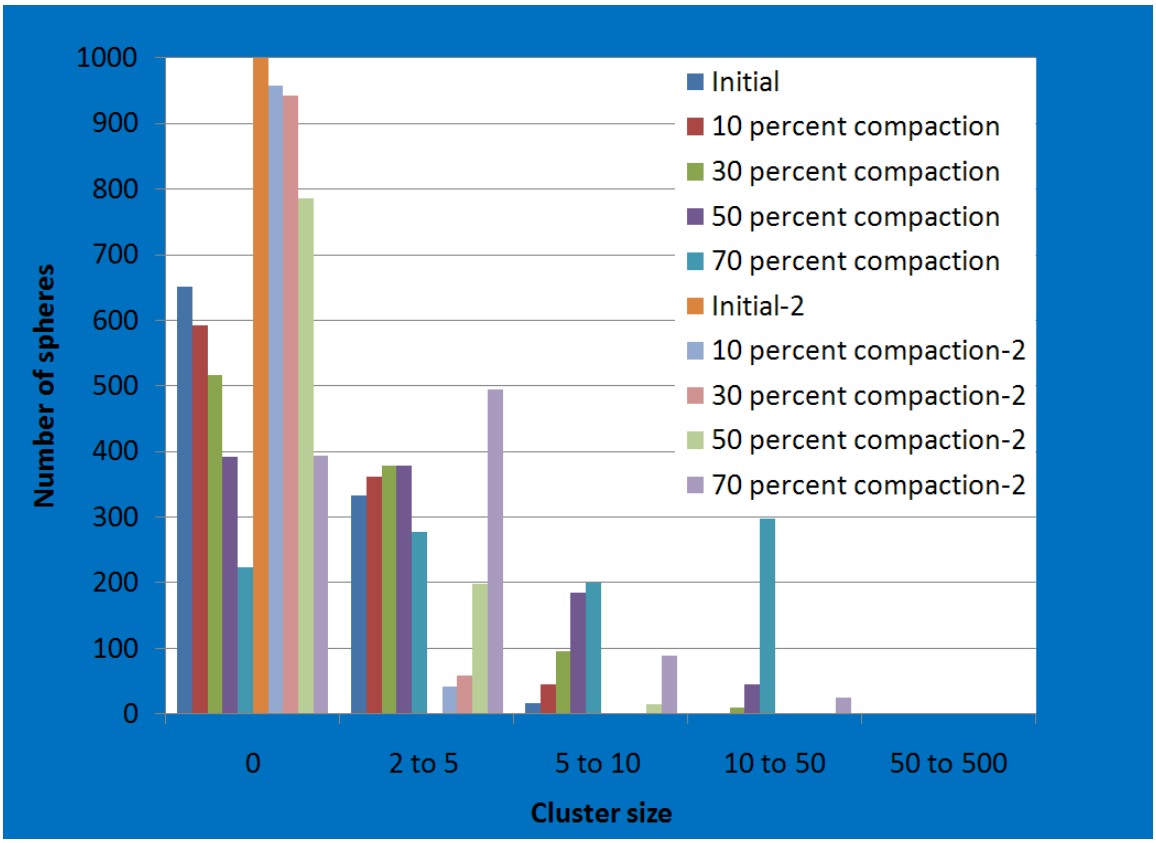

Figure 3.15: Comparison of number of spheres vs. cluster size for D=0.001R of the compaction stages of one component packing created by Thane`s code and dispersed spheres represented by suffix-2 (1000 rigid spheres of carbonaceous material)

The cluster frequency and the number of spheres associated with a particular cluster size class were significantly different in the two model sediments. The one with no initially touching spheres yielded fewer large clusters during compaction. The clustering of spheres in this scenario, however, depended on the initial position of spheres as there was no rearrangement of spheres at any compaction stage.

To test the same effect for the algorithm of rescaling in the direction of compaction with cooperative rearrangement, two component packing of target porosity

50% having 5 percent carbonaceous material by bulk volume having rigid spheres was taken into consideration. The above packing was changed to 70 % porosity by reducing the radius of all the spheres by the same ratio ensuring that no spheres touch each other at the initial stage. The distance between spheres was at least 0.09 sphere radii. The packing was subjected to compaction with cooperative rearrangement. Meanwhile another two-component sphere packing of 70% initial porosity was created with the modified Thane's code that uses cooperative rearrangement. It was subjected to the same process of compaction with cooperative rearrangement. The results are shown in Figure 3.16-3.17.

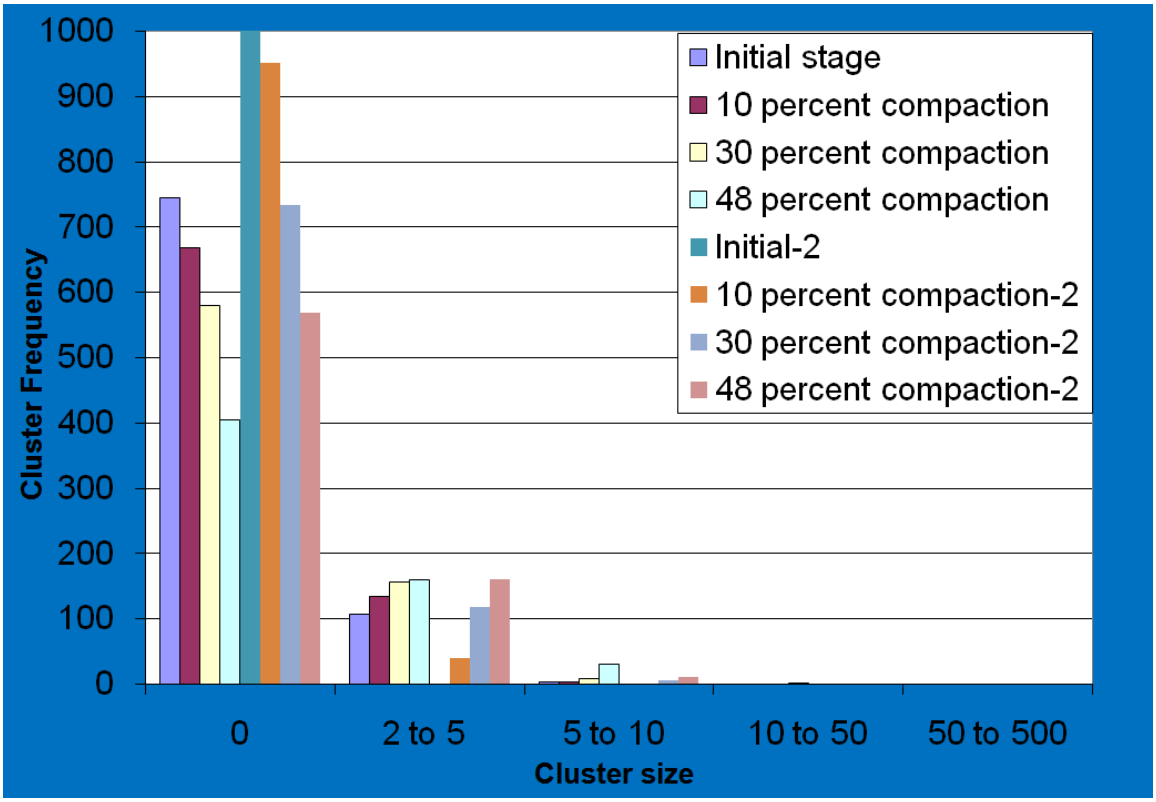

Figure 3.16: Comparison of cluster frequency vs. cluster size for D=0.001R of the compaction stages of two component packing created by Thane`s code and dispersed spheres represented by suffix-2 (1000 rigid spheres of carbonaceous material and 70 % target porosity)

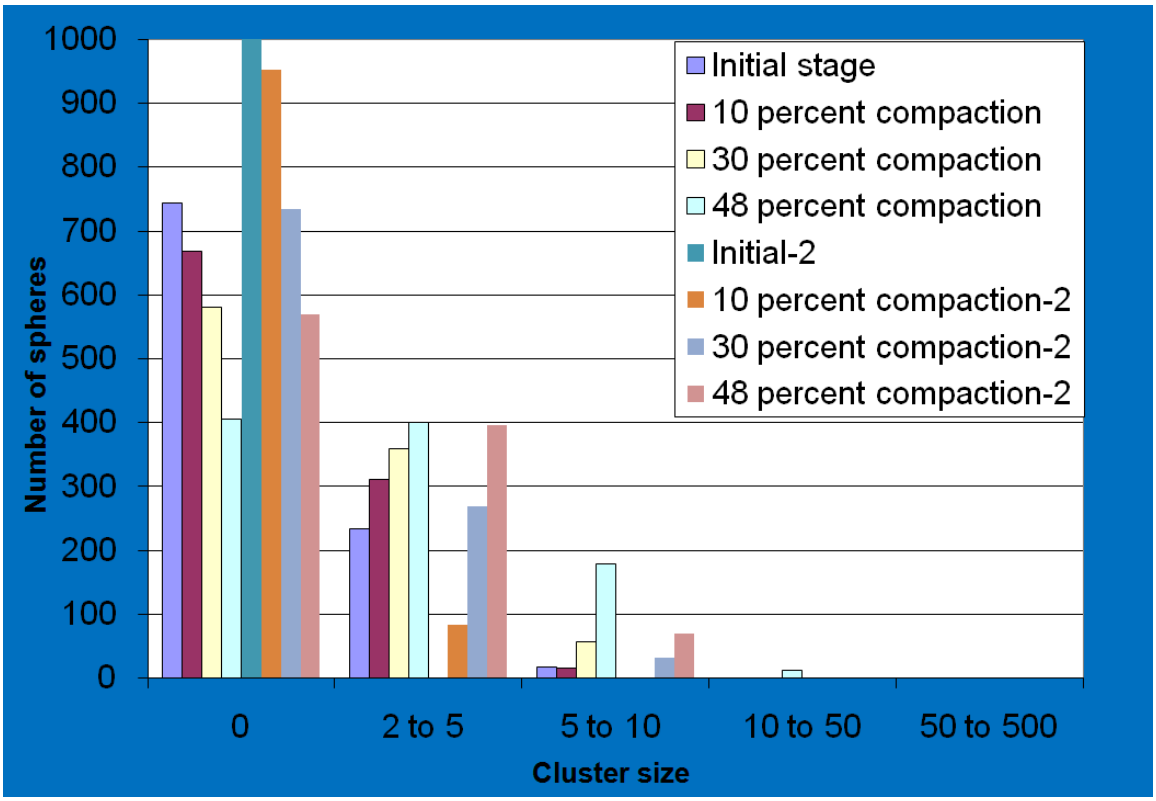

Figure 3.17: Comparison of number of spheres vs. cluster size for D=0.001R of the compaction stages of two component packing created by Thane`s code and dispersed spheres represented by suffix-2 (1000 rigid spheres of carbonaceous material and 70 % target porosity)

The cluster frequency and the number of spheres associated with a particular cluster size class were quite different for the above compared scenarios. The isolated spheres were more in case of dispersed sediments in which spheres were not touching each other at every stage of compaction. Even compaction with cooperative rearrangement for the dispersed sediments did not give enough big clusters of cluster size 5 to 10 and no cluster of size 10 to 50 at 48 percent compaction when compared to

compaction of the sphere packing created by Thane's code. The results showed some biasing of cluster formation in the sphere packing created from Thane`s code. This suggests that the cluster statistics reported in this chapter and the next are biased toward cluster formation. This could represent behavior in nature if carbonaceous particles have some affinity for each other. If this were the case, small clusters of particles could form during deposition, and then the models described above, in which the initial grains are forced to be separated, would be more representative. Further research is needed to evaluate which model is applicable.

Chapter 4: Effect of compaction on clustering of carbonaceous material

In this section the sphere packing of Chapter 3, created from the cooperative rearrangement algorithm in Chapter 2, was subjected to mechanical compaction using algorithms of Chapter 2. The resulting change in connectivity of the carbonaceous material was investigated at the grain scale (Figure 4.1). Compaction of carbonaceous material only (one component sphere packing) and carbonaceous material with matrix (two component sphere packing) were considered. For each class of model sediments, plots of cluster frequency and number of spheres in cluster size ranges were analyzed as a function of cluster size for rescaling in the direction of compaction with and without cooperative rearrangement. The former plot gives the number of clusters present in each cluster size class while the latter gives the number of spheres associated with that cluster size class.

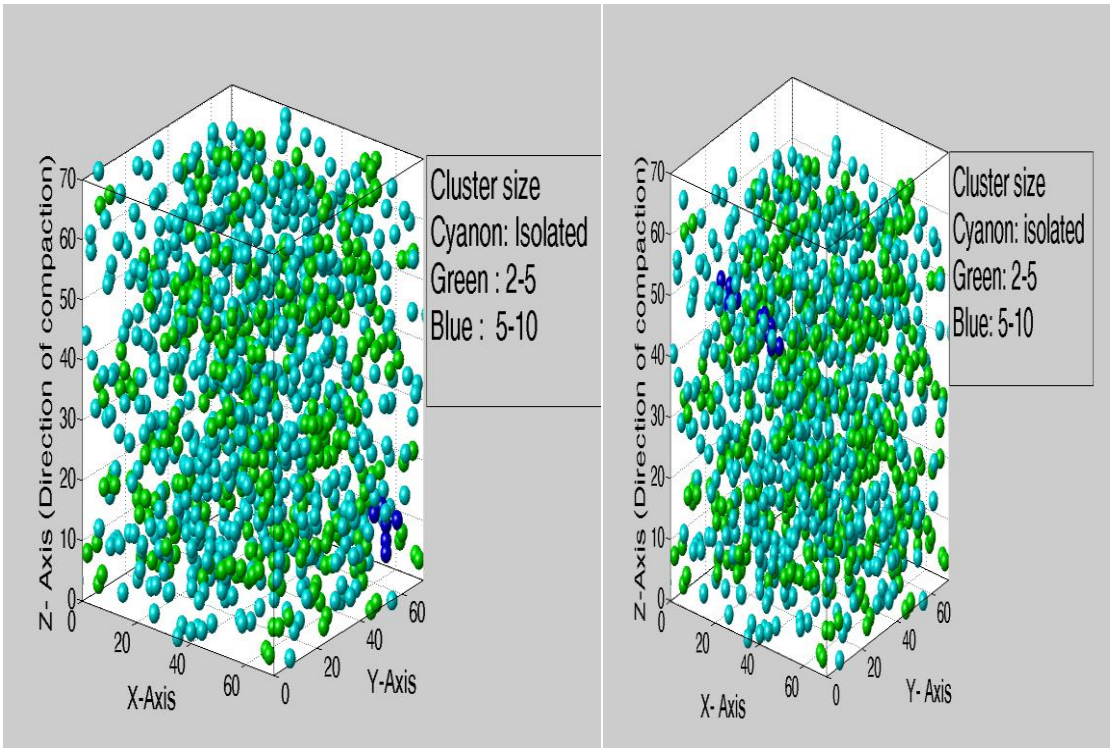

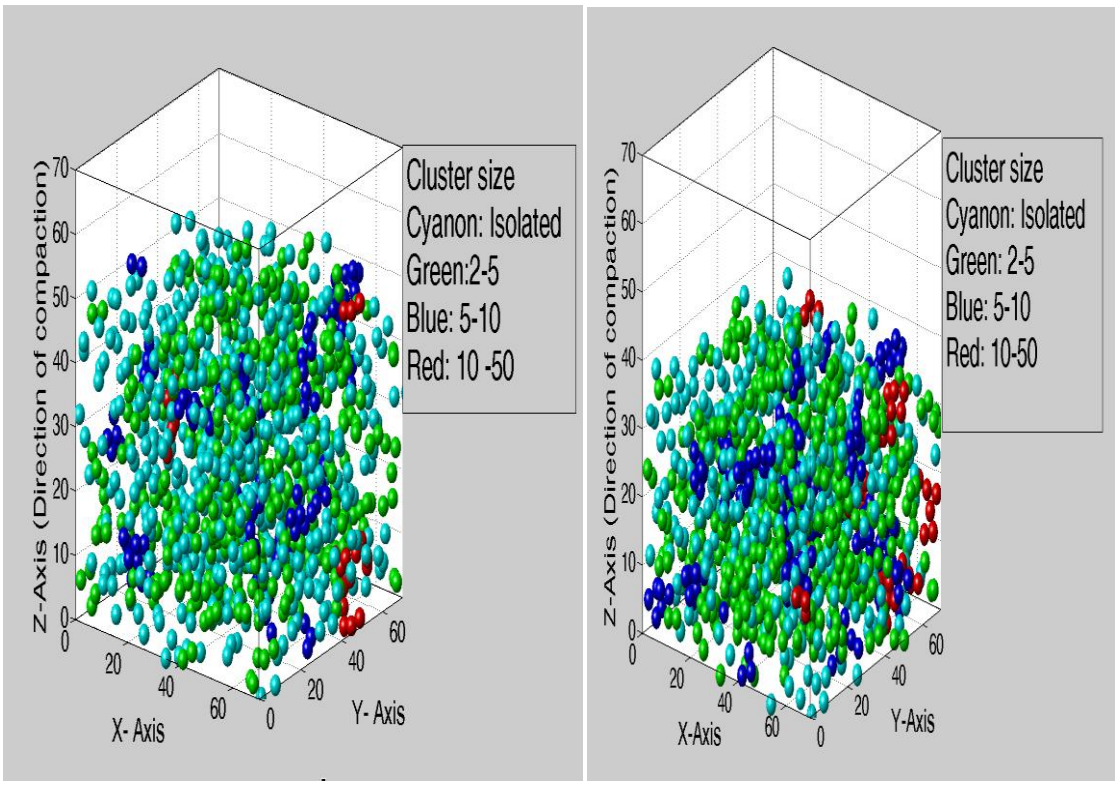

Figure 4.1: Grain packing showing the effect of compaction

4.1 RESCALING IN THE DIRECTION OF COMPACTION WITHOUT COOPERATIVE REARRANGEMENT: APPLICATION TO ONE COMPONENT PACKINGS

One component sphere packing representing only carbonaceous material is carried out by rescaling the grain packing in the direction of compaction without cooperative rearrangement. Packings of 0.05 and 0.10 volume fraction of carbonaceous material were compacted to various reductions of the initial bulk volume 10%, 30%, 50% and 70%.Plots of cluster frequency vs. cluster size are shown in Figure 4.2-4.5.

The stages of volume reduction are related to the compaction factor of Chapter 2 (*c*) by:

Compaction factor (*c*) = Volume of cell at compacted stage/ Initial volume of the cell

As shown in Figures 4.2-4.3, the compaction resulted in increase in cluster size and in numbers of spheres associated with larger cluster sizes. The effect of compaction on connectivity is greater for the case of 0.10 volume fraction than in 0.05 volume fraction of carbonaceous material for these model sediments. Because this model of compaction does not conserve the volume of solid grains, the results are not applicable to mudrocks. However, they are useful for establishing the range of behavior that might be observed in more realistic compaction models, discussed in Section 4.3.

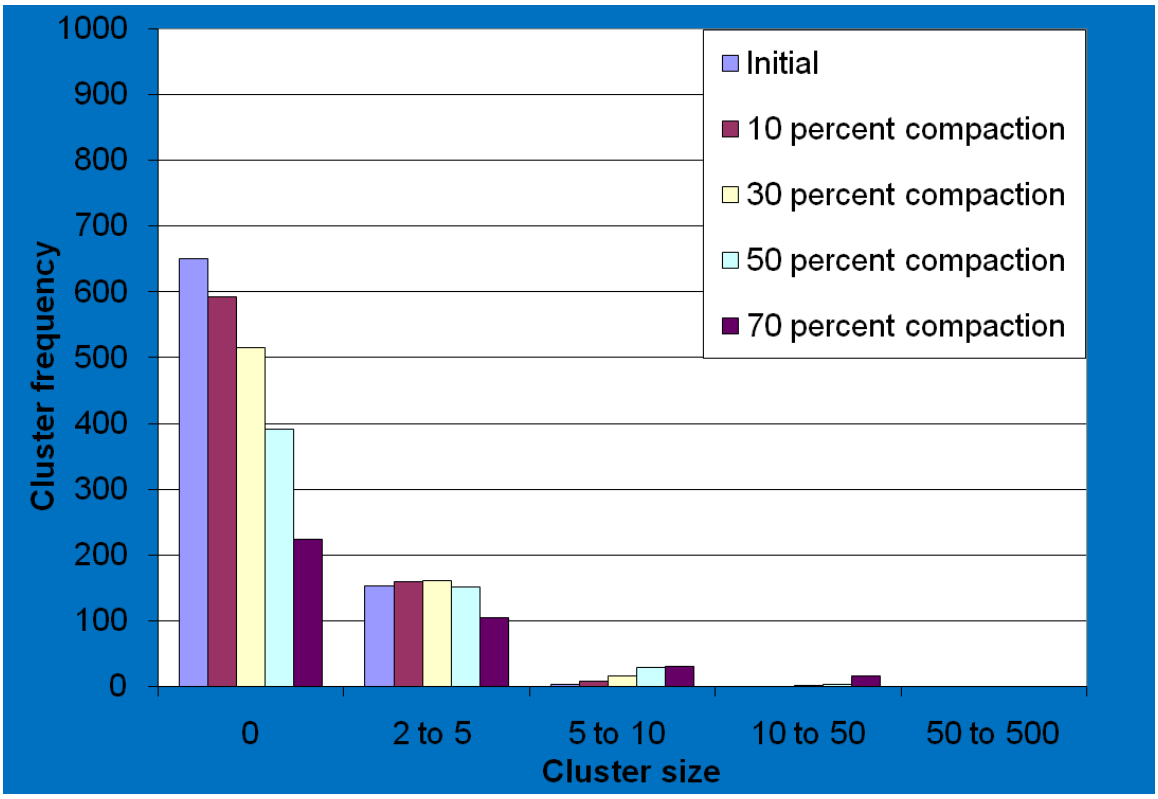

Figure 4.2: Cluster frequency vs. cluster size for $D = 0.001R$ as a function of compaction without cooperative rearrangement with 5 percent of carbonaceous material in the initial bulk volume for one component sphere packing (1000 spheres of carbonaceous material)

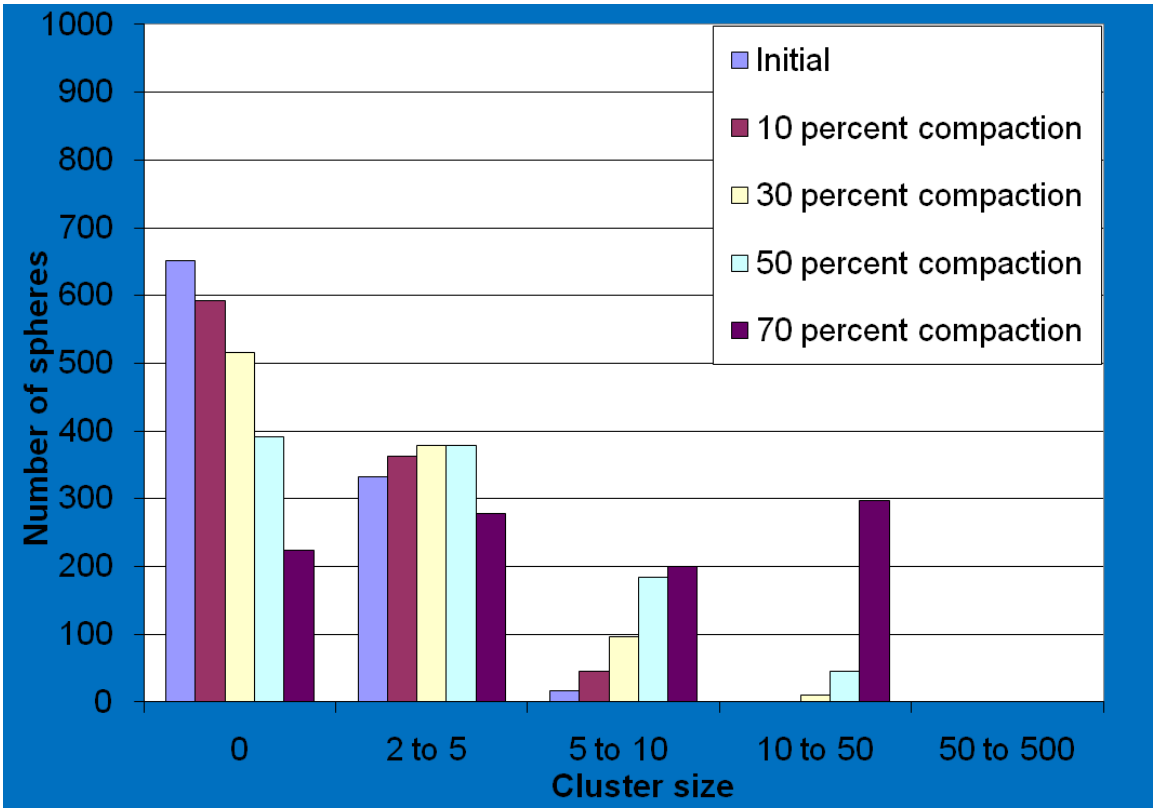

Figure 4.3: Number of spheres in cluster size vs. cluster size for D=0.001R as a function of compaction without cooperative rearrangement with 5 percent of carbonaceous material in the initial bulk volume for one component sphere packing (1000 spheres of carbonaceous material)

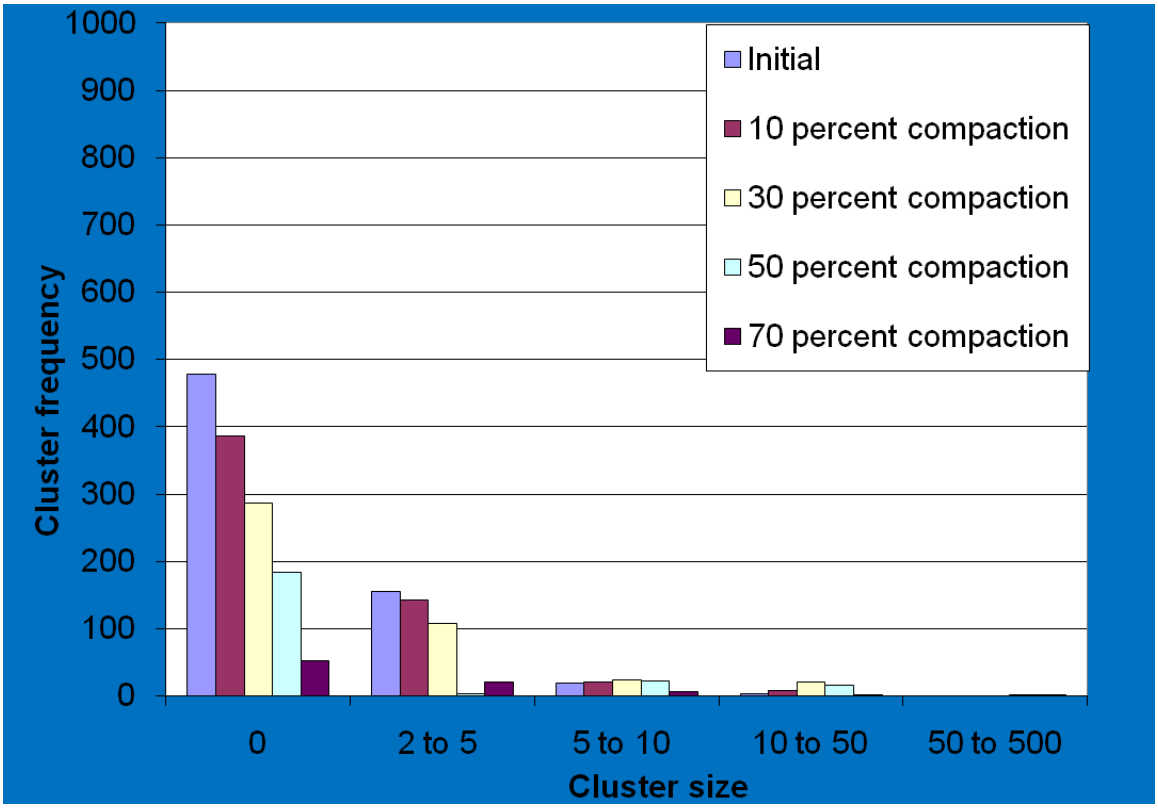

Figure 4.4: Cluster frequency vs. cluster size for D=0.001R as a function of compaction without cooperative rearrangement with10 percent of carbonaceous material in the initial bulk volume for one component sphere packing (1000 spheres of carbonaceous material)

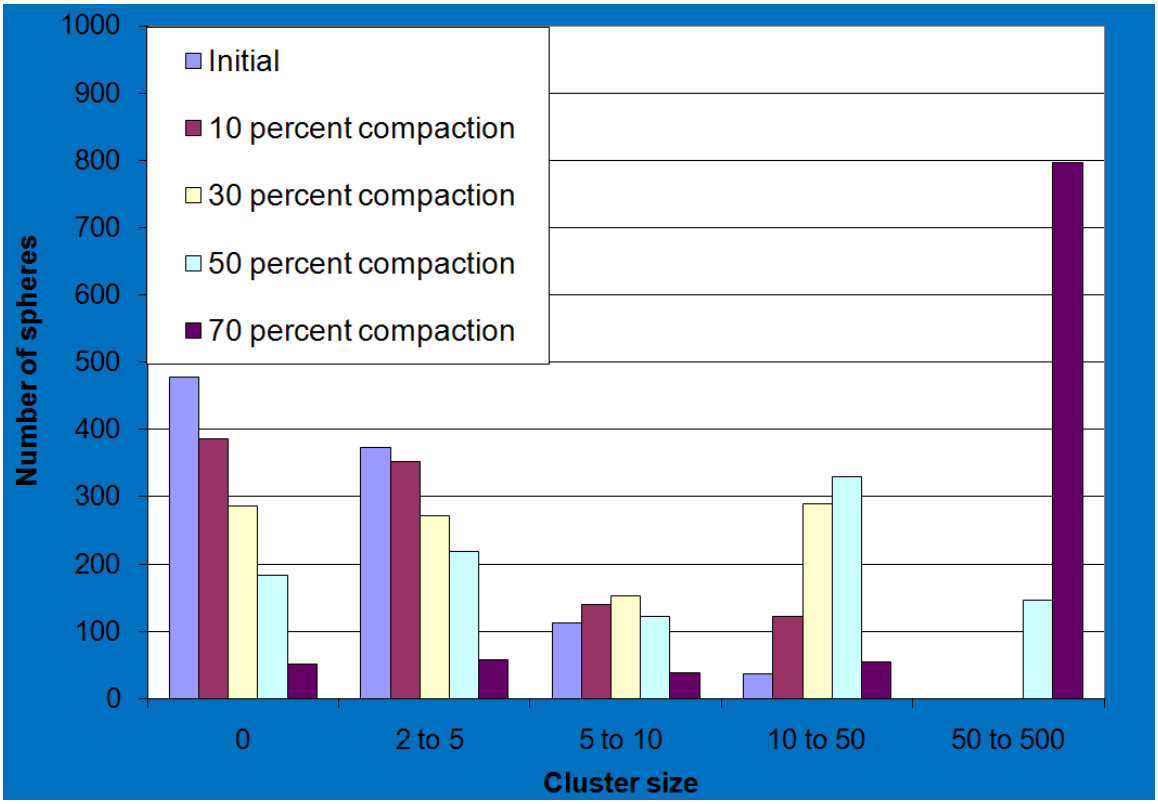

Figure 4.5: Number of spheres in cluster size vs. cluster size for D=0.001R as a function of compaction without cooperative rearrangement with 10 percent of carbonaceous material in the initial bulk volume for one component sphere packing (1000 spheres of carbonaceous material)

4.2 RESCALING IN THE DIRECTION OF COMPACTION WITHOUT COOPERATIVE REARRANGEMENT : APPLICATION TO TWO COMPONENT PACKINGS

Two component sphere packing in which the carbonaceous material and clay/silt were combined, was compacted by rescaling the grain packing in the direction of compaction without cooperative rearrangement and studied in the similar way as one component sphere packing in the preceding section. The compaction stages of 10%, 30%, 50% and 70% were carried out for the 0.05 and 0.10 volume fraction of the carbonaceous material.

The result of compaction on the cluster size distribution was found to be (Figure 4.6 to Figure 4.9) similar to that of one component sphere packing (Figure 4.2 to Figure 4.5) representing only carbonaceous material. There is no significant effect of the presence of clay/silt grains on connectivity of carbonaceous material grains at various compaction stages. This may be due to the simplicity of the compaction simulation, which does allow arbitrary degrees of sphere overlap and does not conserve solid volume.

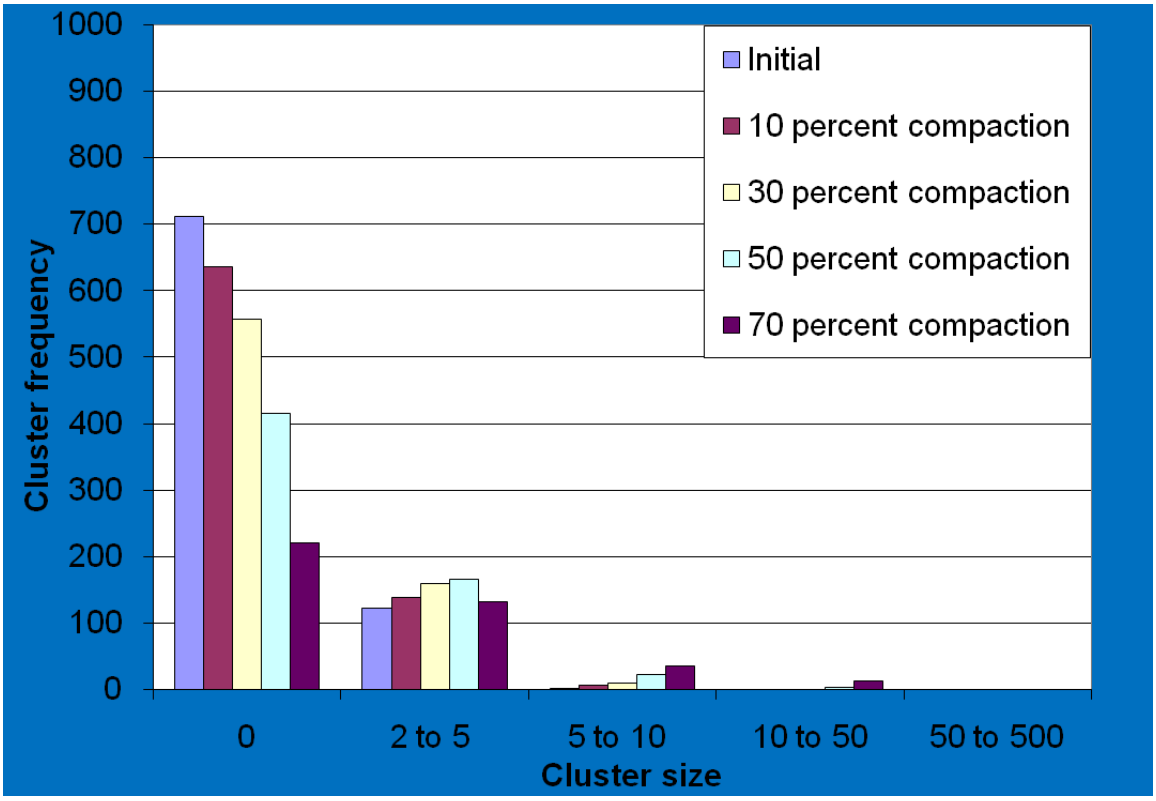

Figure 4.6: Cluster frequency vs. cluster size for D=0.001R as a function of compaction without cooperative rearrangement with 5 percent of carbonaceous material in the initial bulk volume for two component sphere packing (1000 spheres of carbonaceous material)

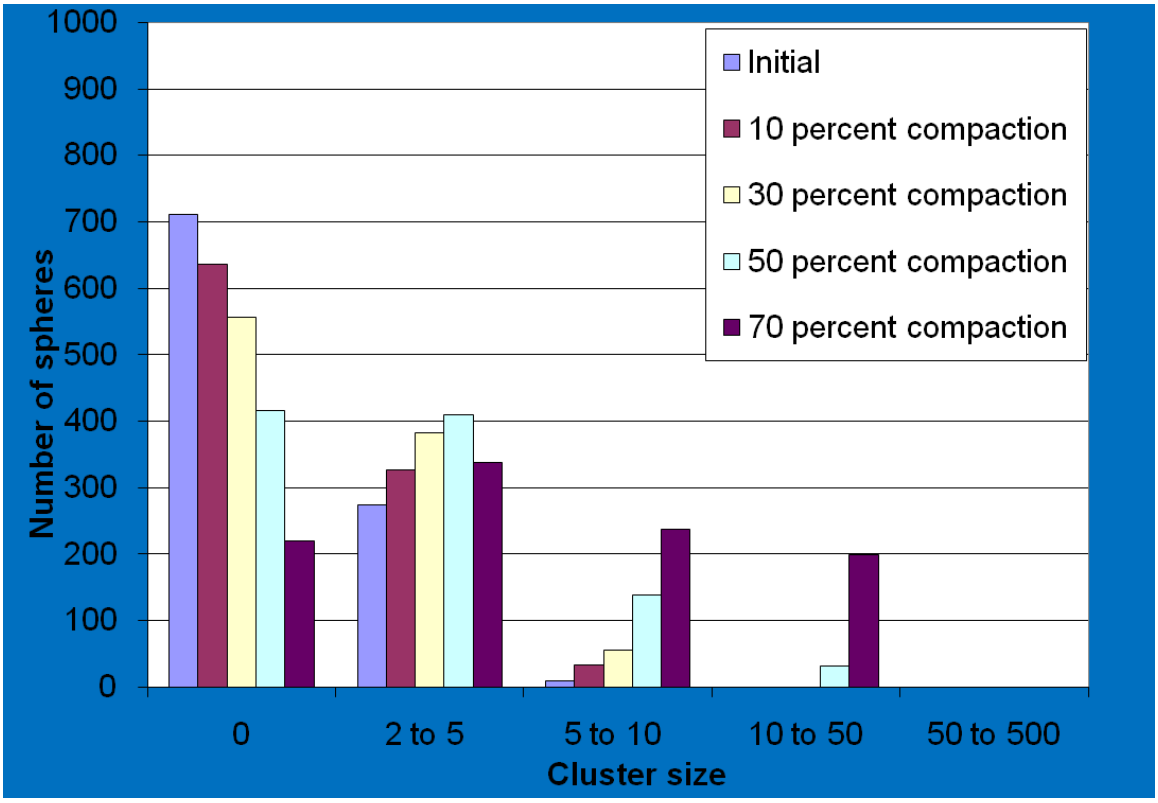

Figure 4.7: Number of spheres in cluster size vs. cluster size for D=0.001R as a function of compaction without cooperative rearrangement with 5 percent of carbonaceous material in the initial bulk volume for two component sphere packing (1000 spheres of carbonaceous material)

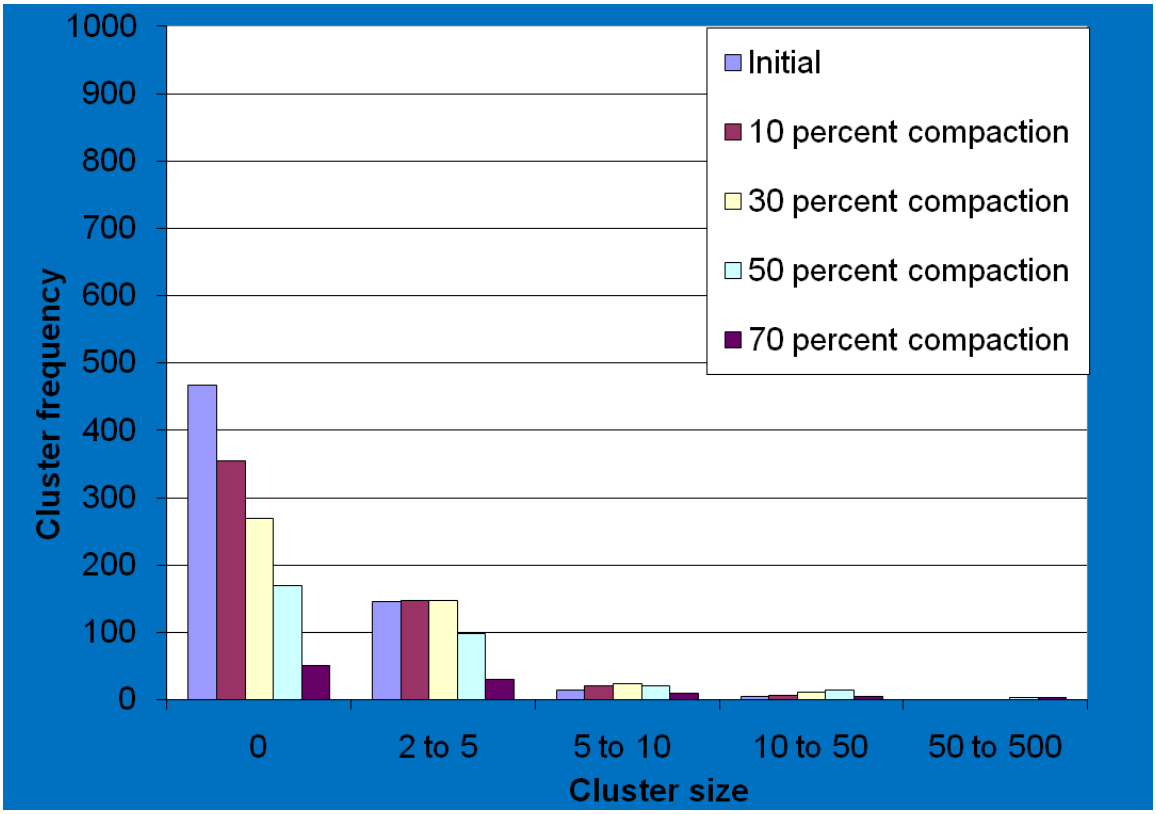

Figure 4.8: Cluster frequency vs. cluster size for D=0.001R as a function of compaction without cooperative rearrangement with 10 percent of carbonaceous material in the initial bulk volume for two component sphere packing (1000 spheres of carbonaceous material)

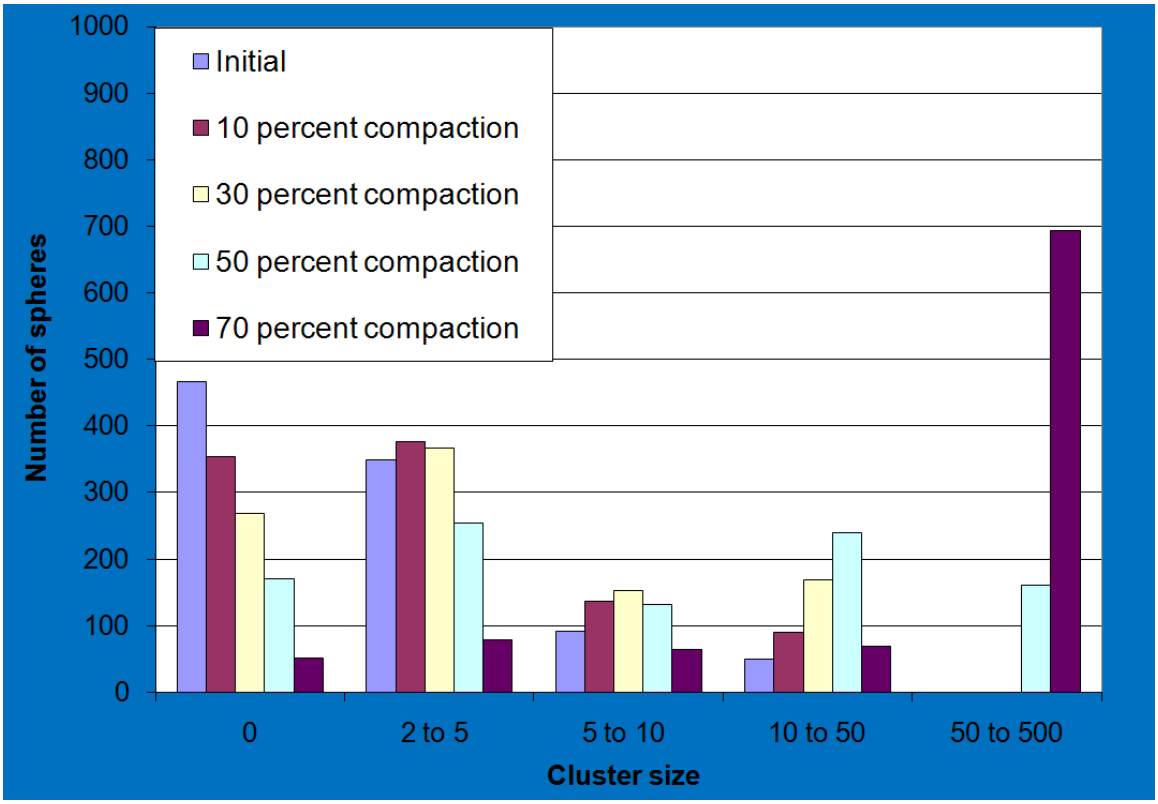

Figure 4.9: Number of spheres in cluster size vs. cluster size for D=0.001R as a function of compaction without cooperative rearrangement with 10 percent of carbonaceous material in the initial bulk volume for two component sphere packing (1000 spheres of carbonaceous material)

4.3 RESCALING IN THE DIRECTION OF COMPACTION WITH COOPERATIVE REARRANGEMENT: APPLICATION TO TWO COMPONENT PACKINGS

Three scenarios for sediments were investigated by using this approach.

1) Rigid carbonaceous material and silt/clay grains
2) Both carbonaceous and silt/clay grains are ductile
3) Carbonaceous grains are ductile and silt/clay grains are rigid

Grain packings of prescribed porosity 70 %, having 0.05 and 0.10 volume fraction of carbonaceous material were used as a base case for this study. Compaction with

cooperative rearrangement was used to remove overlaps, thereby conserving solid volume, and periodic boundaries to allow unconfined grain motion. Thus these packings have a more realistic representation of the compaction process in nature.

4.3.1 RIGID CARBONACEOUS MATERIAL AND SILT/CLAY GRAINS

Under this scenario, both carbonaceous material and silt/clay grains are assumed to be rigid. Results for grain packing subjected to compaction and both cluster frequency vs. cluster size and numbers of spheres vs. cluster size are shown in Figure 4.10-4.13 and summarized in Table 4.1-4.4. We observe that the grain packing of prescribed porosity 70% is compacted to 48% (c= 0.52) giving a final porosity of approximately 42%. The final volume fraction of carbonaceous material for initial 5% and 10% volume fraction of carbonaceous material is 9.6% and 19.2% respectively. As the compaction increases, the number of larger clusters increases. At 52 percent compaction, for 5 percent carbonaceous material by bulk volume 1 cluster with associated 12 spheres is formed in cluster size class of 10 to 50 and for 10 percent carbonaceous material by bulk volume 2 clusters with associated 242 spheres in the class of 50-500 are formed.

Table 4.1: Cluster frequency distribution for D=0.001R at different levels of compaction for two component packing with 5 percent of carbonaceous material in the initial bulk volume. Cooperative rearrangement, 1000 spheres of carbonaceous material, carbonaceous material and silt/clay both rigid grains.

Compaction stage	**Porosity**	**Max cluster size**	**Normalized max cluster size**	**Frequency of clusters by size**				
				0	**2 to 5**	**5 to 10**	**10 to 50**	**50 to 500**
Initial	0.7030	7	0.007035	744	107	3	0	0
0.9	0.6700	5	0.005025	669	135	3	0	0
0.7	0.5757	9	0.009045	580	157	9	0	0
0.52	0.4288	12	0.012060	405	160	30	1	0

Table 4.2: Number of spheres distribution for D=0.001R at different levels of compaction for two component packing with 5 percent of carbonaceous material in the initial bulk volume. Cooperative rearrangement, 1000 spheres of carbonaceous material, carbonaceous material and silt/clay both rigid grains.

Compaction stage	**Porosity**	**Max cluster size**	**Normalized max cluster size**	**Total number of spheres in clusters of different size ranges**				
				0	**2 to 5**	**5 to 10**	**10 to 50**	**50 to 500**
Initial	0.7030	7	0.007035	744	233	18	0	0
0.9	0.6700	5	0.005025	669	311	15	0	0
0.7	0.5757	9	0.009045	580	359	56	0	0
0.52	0.4288	12	0.012060	405	400	178	12	0

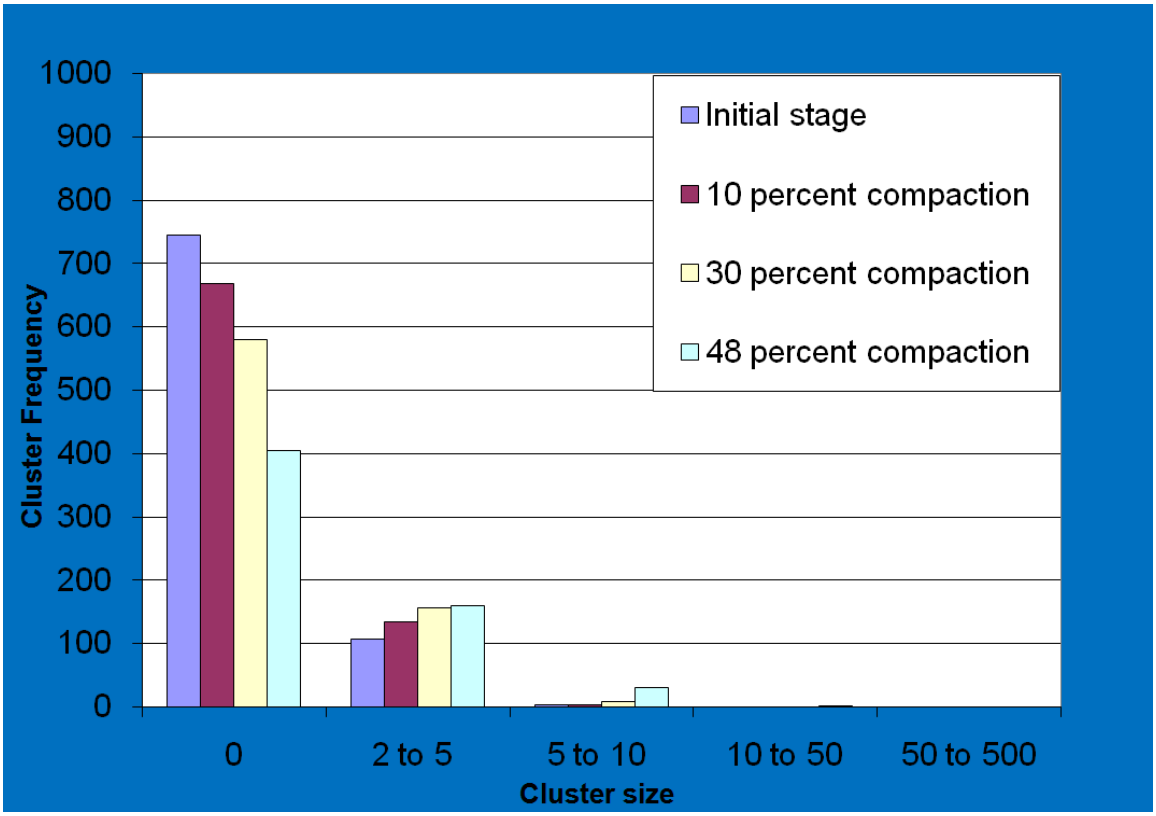

Figure 4.10: Cluster frequency distribution for D=0.001R at different levels of compaction for two component packing with 5 percent of carbonaceous material in the initial bulk volume. Cooperative rearrangement, 1000 spheres of carbonaceous material, carbonaceous material and silt/clay both rigid grains

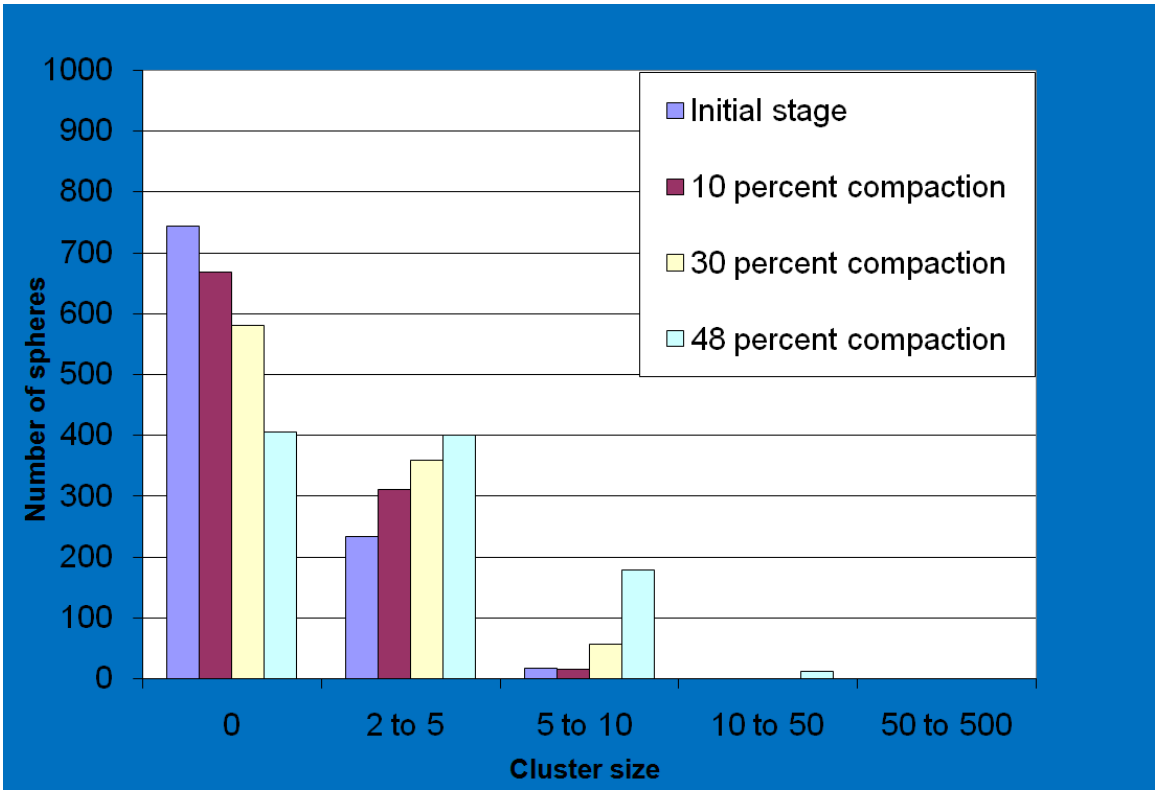

Figure 4.11: Number of spheres distribution for D=0.001R at different levels of compaction for two component packing with 5 percent of carbonaceous material in the initial bulk volume. Cooperative rearrangement, 1000 spheres of carbonaceous material, carbonaceous material and silt/clay both rigid grains.

Table 4.3: Cluster frequency distribution for D=0.001R at different levels of compaction of two component packing with 10 percent of carbonaceous material in the initial bulk volume. Cooperative rearrangement, 1000 spheres of carbonaceous material, carbonaceous material and silt/clay both rigid grains.

Compaction stage	**Porosity**	**Max cluster size**	**Normalized max cluster size**	**Frequency of clusters by size**				
				0	**2 to 5**	**5 to 10**	**10 to 50**	**50 to 500**
Initial	0.6973	17	0.017782	461	143	15	3	0
0.9	0.6637	17	0.017782	420	145	23	3	0
0.7	0.5676	32	0.033473	339	147	24	6	0
0.52	0.4179	135	0.141213	170	70	24	13	2

Table 4.4: Number of spheres distribution for D=0.001R at different levels of compaction of two component packing with 10 percent of carbonaceous material in the initial bulk volume. Cooperative rearrangement, 1000 spheres of carbonaceous material, carbonaceous material and silt/clay both rigid grains.

Compaction stage	**Porosity**	**Max cluster size**	**Normalized max cluster size**	**Total number of spheres in clusters of different size ranges**				
				0	**2 to 5**	**5 to 10**	**10 to 50**	**50 to 500**
Initial	0.6973	17	0.017782	461	351	99	45	0
0.9	0.6637	17	0.017782	420	348	143	45	0
0.7	0.5676	32	0.033473	339	374	150	93	0
0.52	0.4179	135	0.141213	170	185	155	204	242

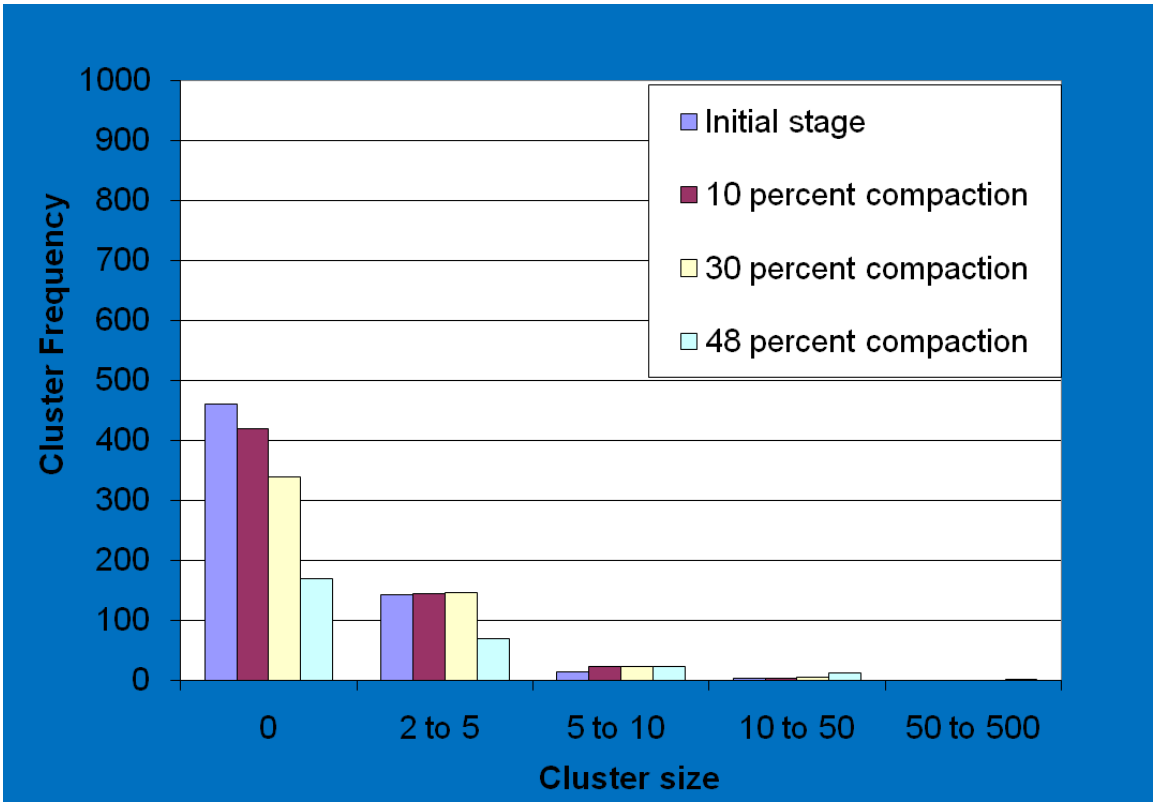

Figure 4.12: Cluster frequency distribution for D=0.001R at different levels of compaction of two component packing with 10 percent of carbonaceous material in the initial bulk volume. Cooperative rearrangement, 1000 spheres of carbonaceous material, carbonaceous material and silt/clay both rigid grains.

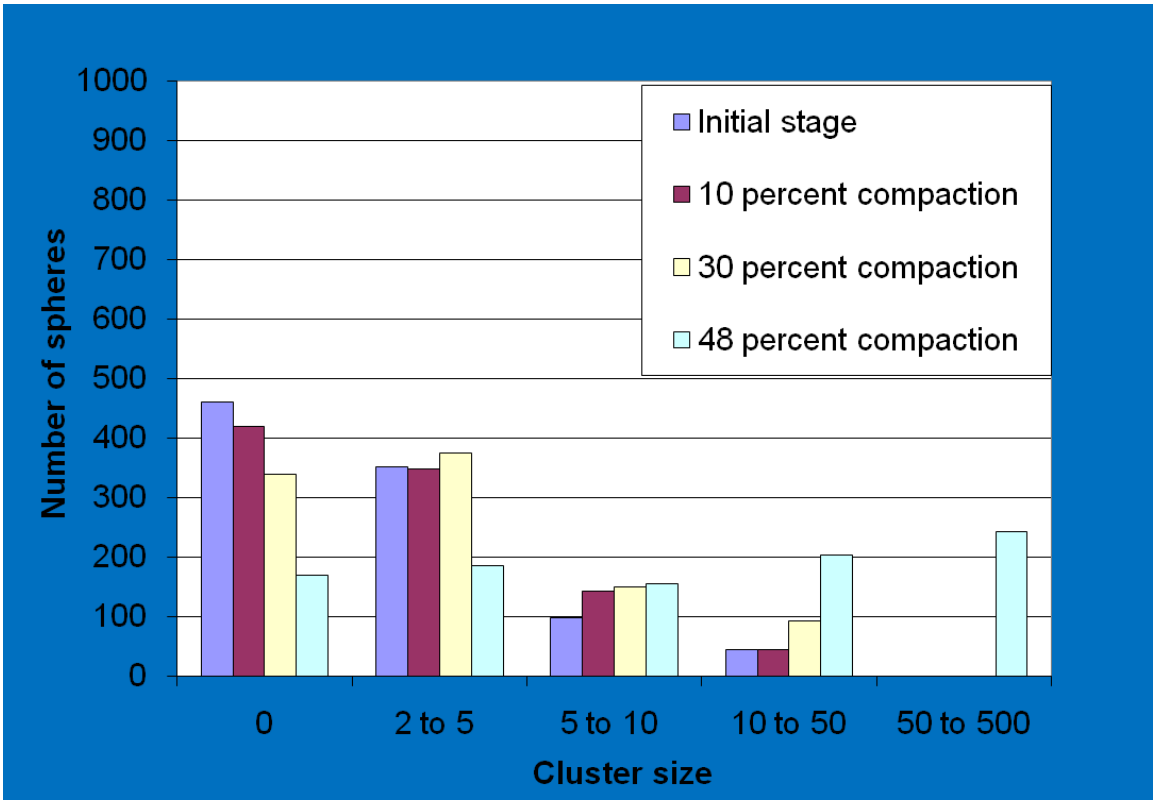

Figure 4.13: Number of spheres distribution for D=0.001R at different levels of compaction of two component packing with 10 percent of carbonaceous material in the initial bulk volume. Cooperative rearrangement, 1000 spheres of carbonaceous material, carbonaceous material and silt/clay both rigid grains.

4.3.2 BOTH CARBONACEOUS AND SILT/CLAY GRAINS ARE DUCTILE

Under this scenario, both carbonaceous material and silt/clay grains are assumed ductile. Grain packing is subjected to compaction, and both cluster frequency and number of spheres vs. cluster size are plotted in Figure 4.14-4.17 and summarized in Table 4.5-4.8. The grain packing of prescribed porosity 70% is compacted to 56% (c= 0.44) for 0.9 rigid radius, 62% (c= 0.38) for 0.8 rigid radius and 68% (c= 0.32) for 0.7 rigid radius giving final residual porosity ~42%, ~23% and ~13% respectively.

The final volume fraction of carbonaceous material for initial volume fractions of 5% and 10% of carbonaceous material is 11.3% and 22.7% for 0.9 rigid radius, 13.1% and 26.3% for 0.8 rigid radius and 15.6% and 31.2% for 0.7 rigid radius respectively(Table 4.5-4.16 and Figure 4.14-4.25).

It is observed that as the compaction increases, the number of large clusters increases but the effect of compaction on connectivity of carbonaceous material is more pronounced as the grains are ductile in this scenario.

Table 4.5: Cluster frequency distribution for D=0.001R at different levels of compaction of two component packing with 5 percent of carbonaceous material in the initial bulk volume. Cooperative rearrangement, 1000 spheres of carbonaceous material, carbonaceous material and silt/clay both ductile grains with rigid ratio =0.9R

Compaction stage	**Porosity**	**Max cluster size**	**Normalized max cluster size**	**Frequency of clusters by size**				
				0	2 to 5	5 to 10	10 to 50	50 to 500
Initial	0.7003	8	0.0079	586	165	5	0	0
0.9	0.6639	8	0.0079	546	173	9	0	0
0.7	0.5717	11	0.0108	472	169	20	1	0
0.5	0.3948	17	0.0167	354	155	34	4	0
0.44	0.3178	29	0.0285	304	140	29	12	0

Table 4.6: Number of spheres distribution for D=0.001R at different levels of compaction of two component packing with 5 percent of carbonaceous material in the initial bulk volume. Cooperative rearrangement, 1000 spheres of carbonaceous material, carbonaceous material and silt/clay both ductile grains with rigid ratio =0.9R

Compaction stage	**Porosity**	**Max cluster size**	**Normalized max cluster size**	**Total number of spheres in clusters of different size ranges**				
				0	2 to 5	5 to 10	10 to 50	50 to 500
Initial	0.7003	8	0.0079	586	402	29	0	0
0.9	0.6639	8	0.0079	546	421	50	0	0
0.7	0.5717	11	0.0108	472	410	124	11	0
0.52	0.3948	17	0.0167	354	400	214	49	0
0.44	0.3178	29	0.0285	352	352	184	177	0

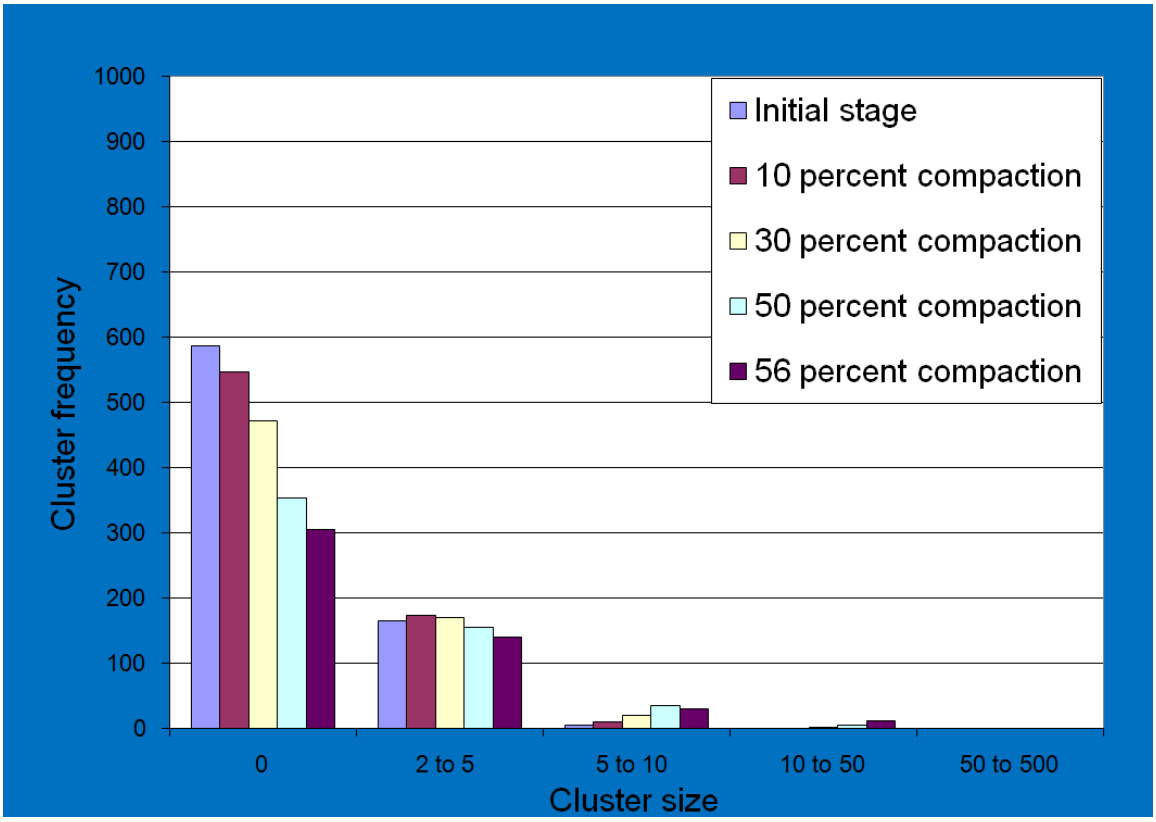

Figure 4.14: Cluster frequency distribution for D=0.001R at different levels of compaction of two component packing with 5 percent of carbonaceous material in the initial bulk volume. Cooperative rearrangement, 1000 spheres of carbonaceous material, carbonaceous material and silt/clay both ductile grains with rigid radius ratio =0.9R

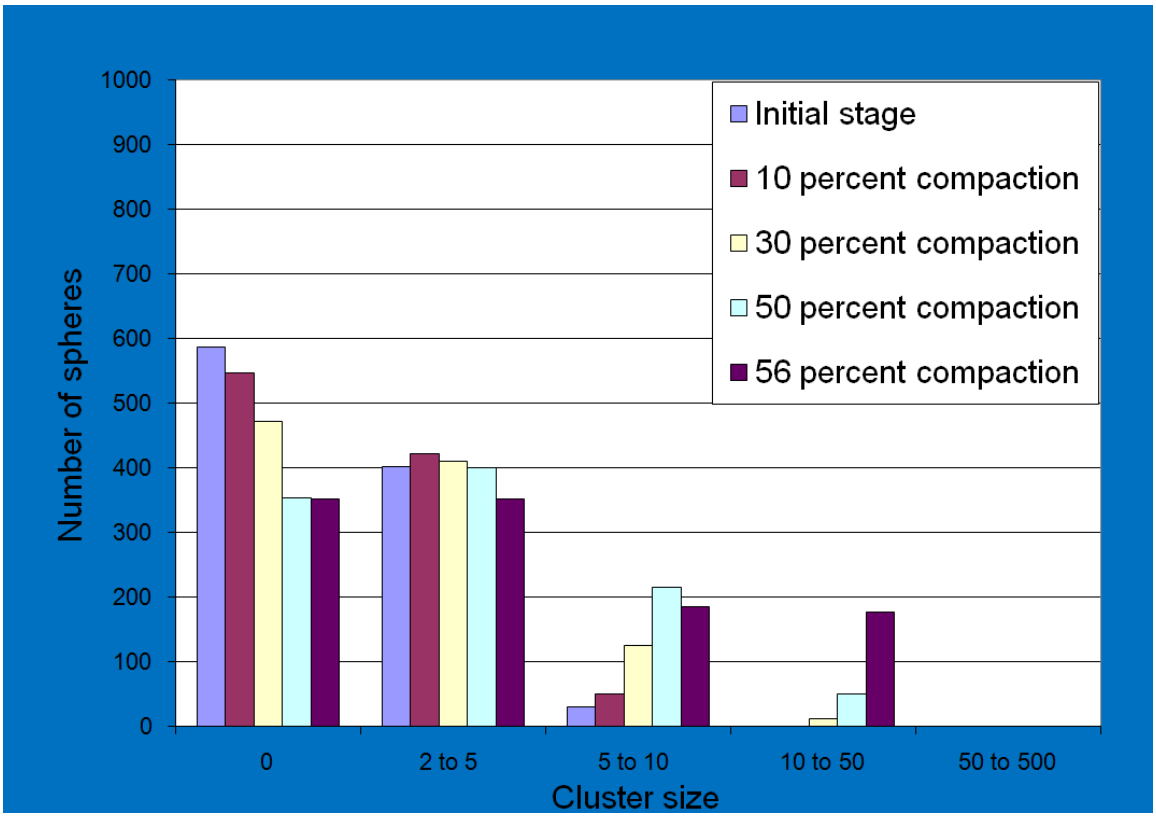

Figure 4.15: Number of spheres distribution for D=0.001R at different levels of compaction of two component packing with 5 percent of carbonaceous material in the initial bulk volume. Cooperative rearrangement, 1000 spheres of carbonaceous material, carbonaceous material and silt/clay both ductile grains with rigid ratio=0.9R

Table 4.7: Cluster frequency distribution for D=0.001R at different levels of compaction of two component packing with 10 percent of carbonaceous material in the initial bulk volume. Cooperative rearrangement, 1000 spheres of carbonaceous material, carbonaceous material and silt/clay both ductile grains with rigid ratio =0.9R

Compaction stage	**Porosity**	**Max cluster size**	**Normalized max cluster size**	**Frequency of clusters by size**				
				0	2 to 5	5 to 10	10 to 50	50 to 500
Initial	0.6978	22	0.0218	395	151	30	3	0
0.9	0.6646	21	0.0209	359	147	30	6	0
0.7	0.5691	45	0.0447	255	95	48	10	0
0.5	0.3927	557	0.5531	124	39	12	10	1
0.44	0.3116	798	0.7925	68	20	7	2	1

Table 4.8: Number of spheres distribution for D=0.001R at different levels of compaction of two component packing with 10 percent of carbonaceous material in the initial bulk volume. Cooperative rearrangement, 1000 spheres of carbonaceous material, carbonaceous material and silt/clay both ductile grains with rigid ratio =0.9R

Compaction stage	**Porosity**	**Max cluster size**	**Normalized max cluster size**	**Total number of spheres in clusters of different size ranges**				
				0	2 to 5	5 to 10	10 to 50	50 to 500
Initial	0.6978	22	0.0218	395	382	186	44	0
0.9	0.6646	21	0.0209	359	380	181	87	0
0.7	0.5691	45	0.0447	255	251	312	189	0
0.52	0.3927	557	0.5531	124	100	71	155	557
0.44	0.3116	798	0.7925	68	50	42	49	798

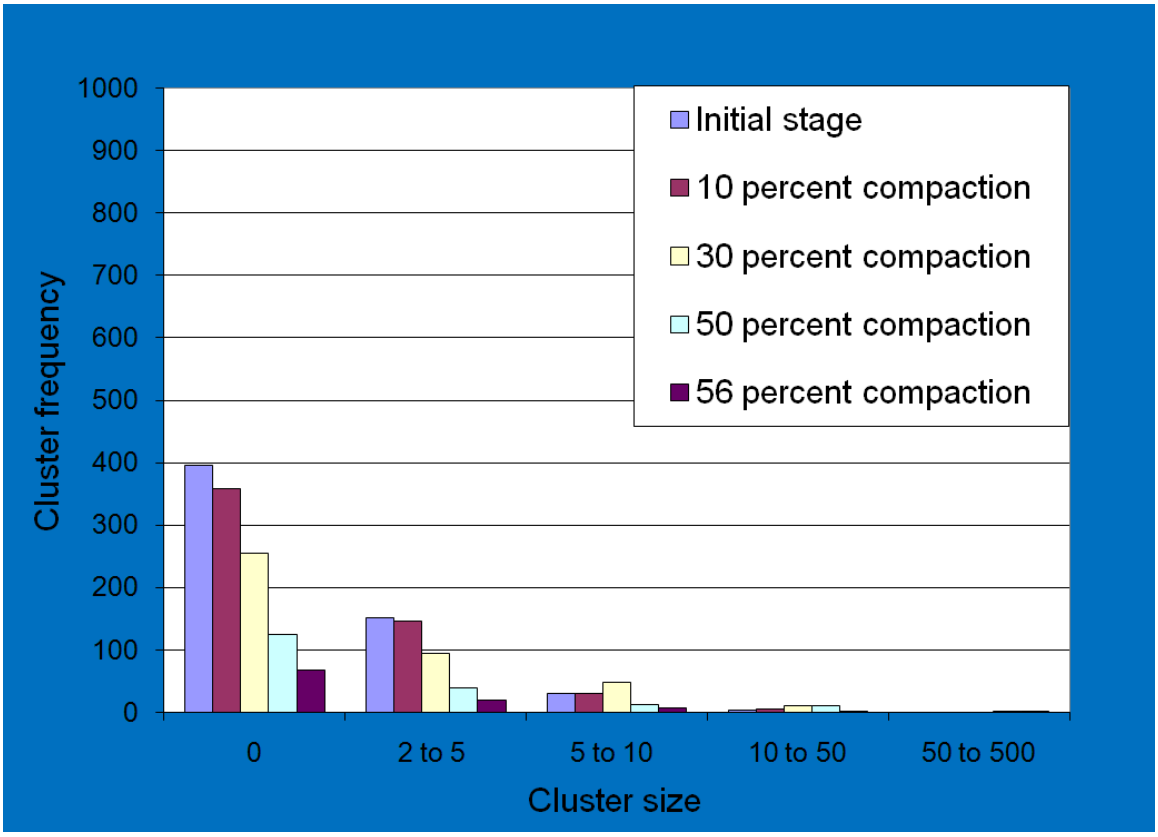

Figure 4.16: Cluster frequency distribution for D=0.001R at different levels of compaction of two component packing with 10 percent of carbonaceous material in the initial bulk volume. Cooperative rearrangement, 1000 spheres of carbonaceous material, carbonaceous material and silt/clay both ductile grains with rigid radius ratio =0.9R

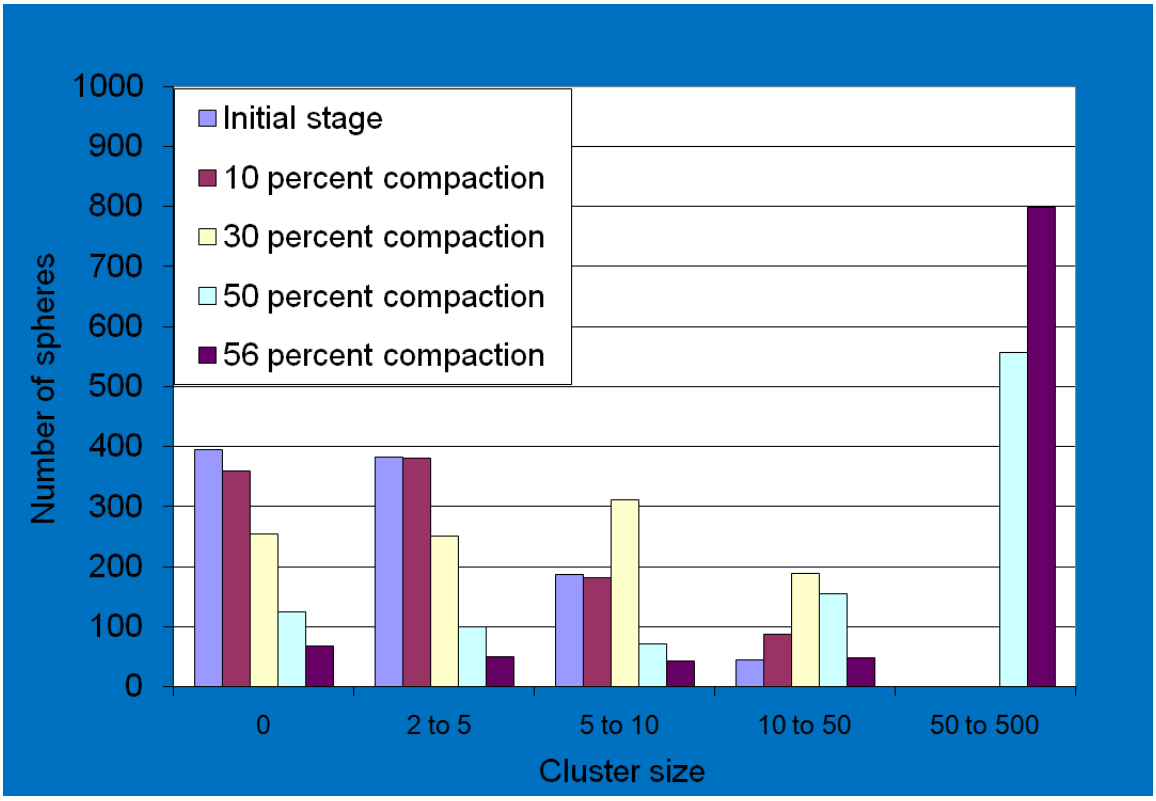

Figure 4.17: Number of spheres distribution for D=0.001R at different levels of compaction of two component packing with 10 percent of carbonaceous material in the initial bulk volume. Cooperative rearrangement, 1000 spheres of carbonaceous material, carbonaceous material and silt/clay both ductile grains with rigid ratio=0.9R

Table 4.9: Cluster frequency distribution for D=0.001R at different levels of compaction of two component packing with 5 percent of carbonaceous material in the initial bulk volume. Cooperative rearrangement, 1000 spheres of carbonaceous material, carbonaceous material and silt/clay both ductile grains with rigid ratio =0.8R

Compaction stage	**Porosity**	**Max cluster size**	**Normalized max cluster size**	**Frequency of clusters by size**				
				0	2 to 5	5 to 10	10 to 50	50 to 500
Initial	0.7032	5	0.0050	633	153	3	0	0
0.9	0.6702	6	0.0060	602	160	5	0	0
0.7	0.5759	10	0.0101	541	162	10	1	0
0.5	0.4115	15	0.0151	375	175	24	3	0
0.38	0.2300	33	0.0333	241	118	48	8	0

Table 4.10: Number of spheres distribution for D=0.001R at different levels of compaction of two component packing with 5 percent of carbonaceous material in the initial bulk volume. Cooperative rearrangement, 1000 spheres of carbonaceous material, carbonaceous material and silt/clay both ductile grains with rigid ratio =0.8R

Compaction stage	**Porosity**	**Max cluster size**	**Normalized max cluster size**	**Total number of spheres in clusters of different size ranges**				
				0	2 to 5	5 to 10	10 to 50	50 to 500
Initial	0.7032	5	0.0050	633	344	15	0	0
0.9	0.6702	6	0.0060	602	364	26	0	0
0.7	0.5759	10	0.0101	541	386	55	1	0
0.5	0.4115	15	0.0151	375	447	134	3	0
0.38	0.2300	33	0.0333	241	315	306	8	0

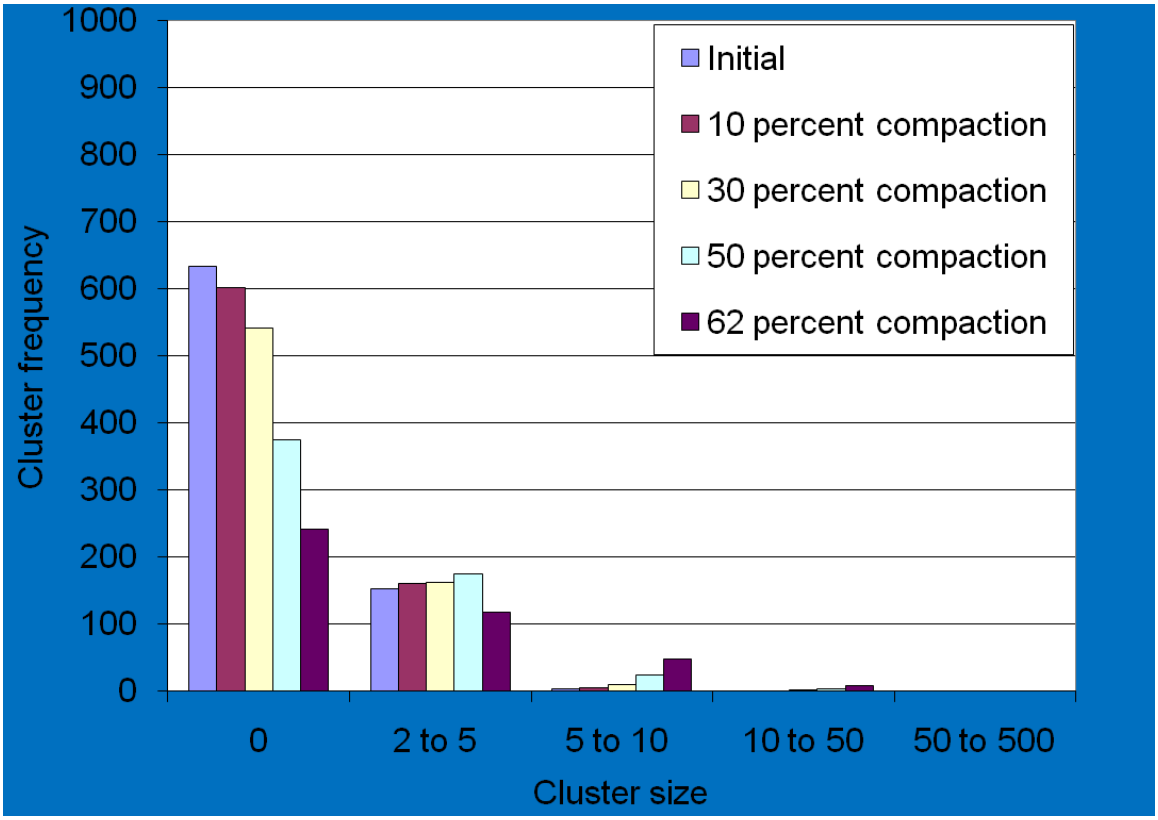

Figure 4.18: Cluster frequency distribution for D=0.001R at different levels of compaction of two component packing with 5 percent of carbonaceous material in the initial bulk volume. Cooperative rearrangement, 1000 spheres of carbonaceous material, carbonaceous material and silt/clay both ductile grains with rigid radius ratio =0.8R

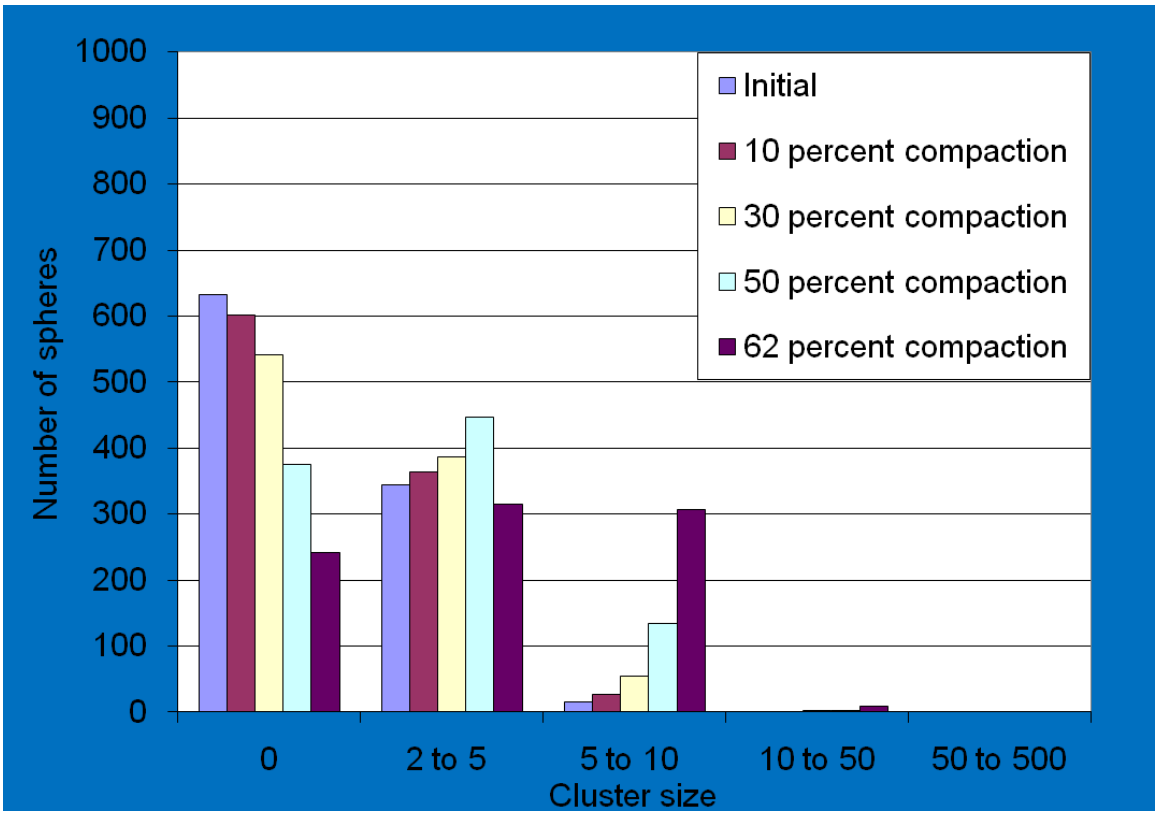

Figure 4.19: Number of spheres distribution for D=0.001R at different levels of compaction of two component packing with 5 percent of carbonaceous material in the initial bulk volume. Cooperative rearrangement, 1000 spheres of carbonaceous material, carbonaceous material and silt/clay both ductile grains with rigid ratio=0.8R

Table 4.11: Cluster frequency distribution for D=0.001R at different levels of compaction of two component packing with 10 percent of carbonaceous material in the initial bulk volume. Cooperative rearrangement, 1000 spheres of carbonaceous material, carbonaceous material and silt/clay both ductile grains with rigid ratio =0.8R

Compaction stage	**Porosity**	**Max cluster size**	**Normalized max cluster size**	**Frequency of clusters by size**				
				0	2 to 5	5 to 10	10 to 50	50 to 500
Initial	0.7056	14	0.0144	380	162	26	2	0
0.9	0.6714	14	0.0144	352	156	30	3	0
0.7	0.5744	30	0.0309	237	123	43	10	0
0.5	0.4120	97	0.0999	125	62	22	15	3
0.38	0.2329	846	0.8713	38	19	5	1	1

Table 4.12: Number of spheres distribution for D=0.001R at different levels of compaction of two component packing with 10 percent of carbonaceous material in the initial bulk volume. Cooperative rearrangement, 1000 spheres of carbonaceous material, carbonaceous material and silt/clay both ductile grains with rigid ratio =0.8R

Compaction stage	**Porosity**	**Max cluster size**	**Normalized max cluster size**	**Total number of spheres in clusters of different size ranges**				
				0	2 to 5	5 to 10	10 to 50	50 to 500
Initial	0.7056	14	0.0144	380	407	160	24	0
0.9	0.6714	14	0.0144	352	396	186	37	0
0.7	0.5744	30	0.0309	237	317	272	145	0
0.5	0.4120	97	0.0999	125	166	143	288	249
0.38	0.2329	846	0.8713	38	48	29	10	846

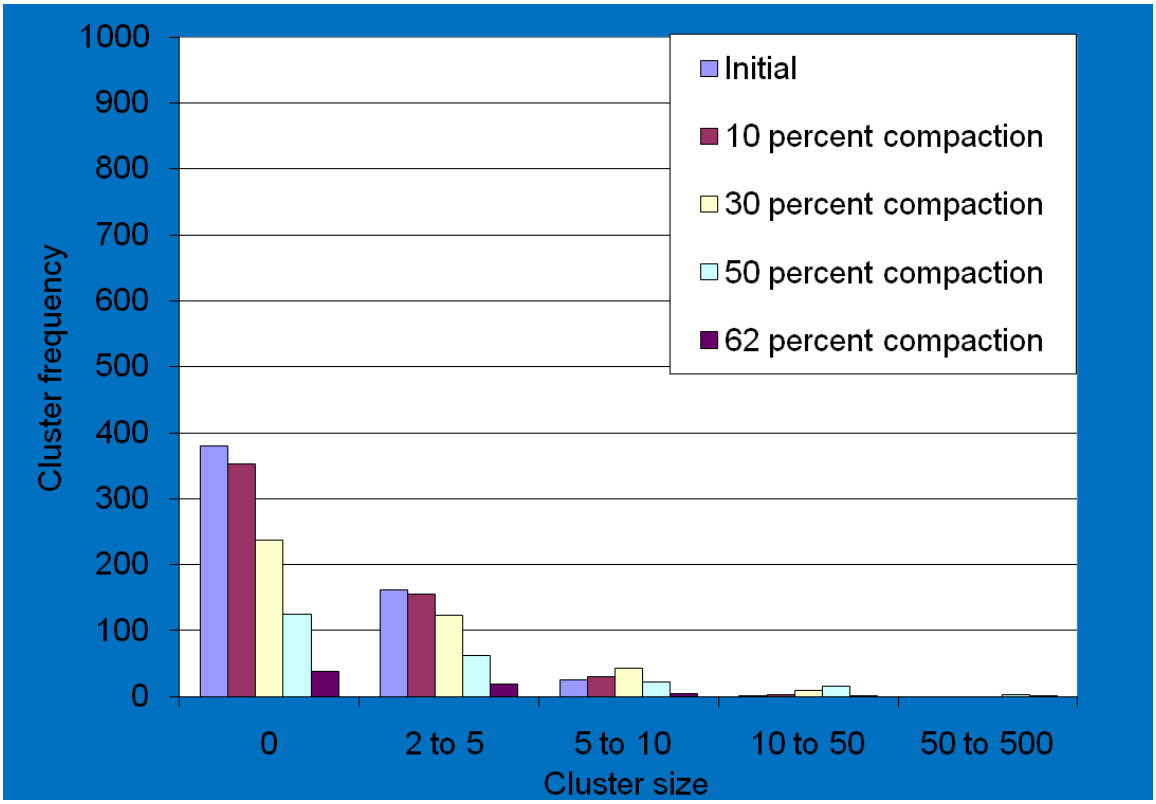

Figure 4.20: Cluster frequency distribution for D=0.001R at different levels of compaction of two component packing with 10 percent of carbonaceous material in the initial bulk volume. Cooperative rearrangement, 1000 spheres of carbonaceous material, carbonaceous material and silt/clay both ductile grains with rigid radius ratio =0.8R

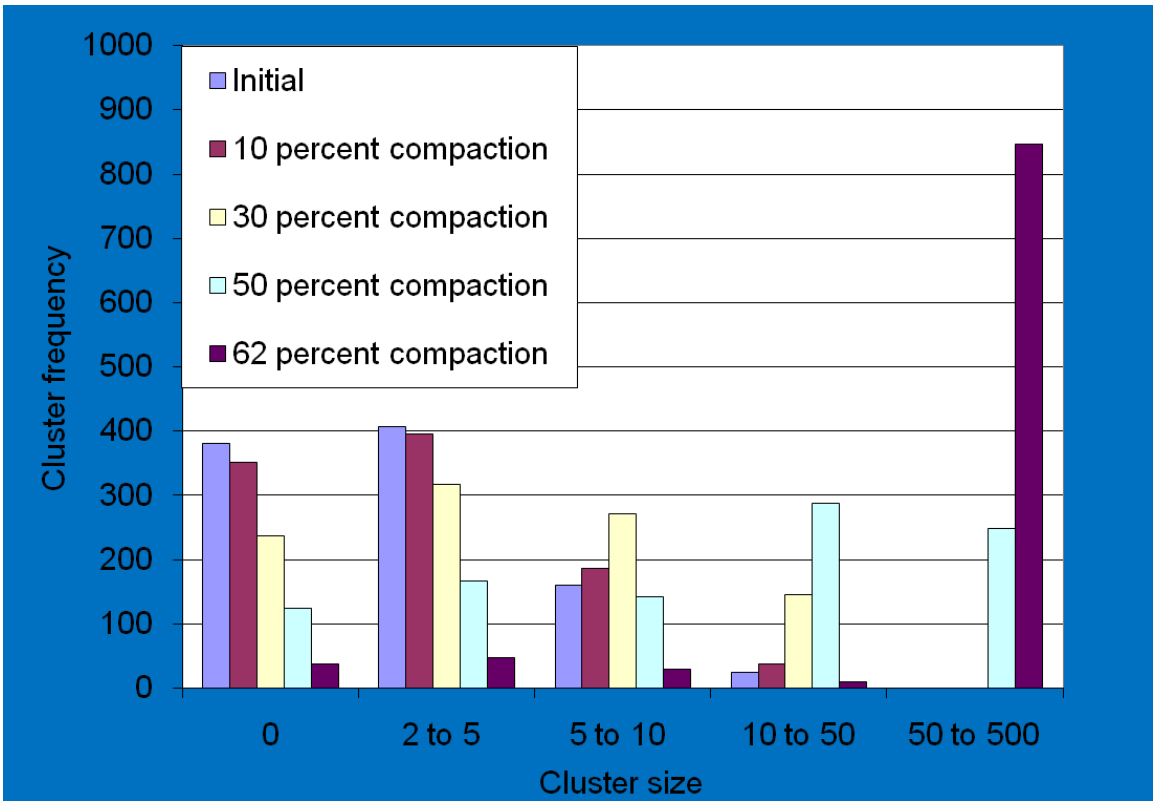

Figure 4.21: Number of spheres distribution for D=0.001R at different levels of compaction of two component packing with 10 percent of carbonaceous material in the initial bulk volume. Cooperative rearrangement, 1000 spheres of carbonaceous material, carbonaceous material and silt/clay both ductile grains with rigid ratio=0.8R

Table 4.13: Cluster frequency distribution for D=0.001R at different levels of compaction of two component packing with 5 percent of carbonaceous material in the initial bulk volume. Cooperative rearrangement, 1000 spheres of carbonaceous material, carbonaceous material and silt/clay both ductile grains with rigid ratio =0.7R

Compaction stage	**Porosity**	**Max cluster size**	**Normalized max cluster size**	**Frequency of clusters by size**				
				0	2 to 5	5 to 10	10 to 50	50 to 500
Initial	0.6974	9	0.0091	627	147	5	0	0
0.9	0.6725	9	0.0091	608	150	7	0	0
0.7	0.5814	11	0.0112	543	161	8	1	0
0.5	0.4134	15	0.0152	414	171	16	4	0
0.32	0.1315	27	0.0274	190	119	32	18	0

Table 4.14: Number of spheres distribution for D=0.001R at different levels of compaction of two component packing with 5 percent of carbonaceous material in the initial bulk volume. Cooperative rearrangement, 1000 spheres of carbonaceous material, carbonaceous material and silt/clay both ductile grains with rigid ratio =0.7R

Compaction stage	**Porosity**	**Max cluster size**	**Normalized max cluster size**	**Total number of spheres in clusters of different size ranges**				
				0	2 to 5	5 to 10	10 to 50	50 to 500
Initial	0.6974	9	0.0091	627	327	30	0	0
0.9	0.6725	9	0.0091	608	334	42	0	0
0.7	0.5814	11	0.0112	543	381	49	11	0
0.5	0.4134	15	0.0152	414	428	93	49	0
0.32	0.1315	27	0.0274	190	316	211	267	0

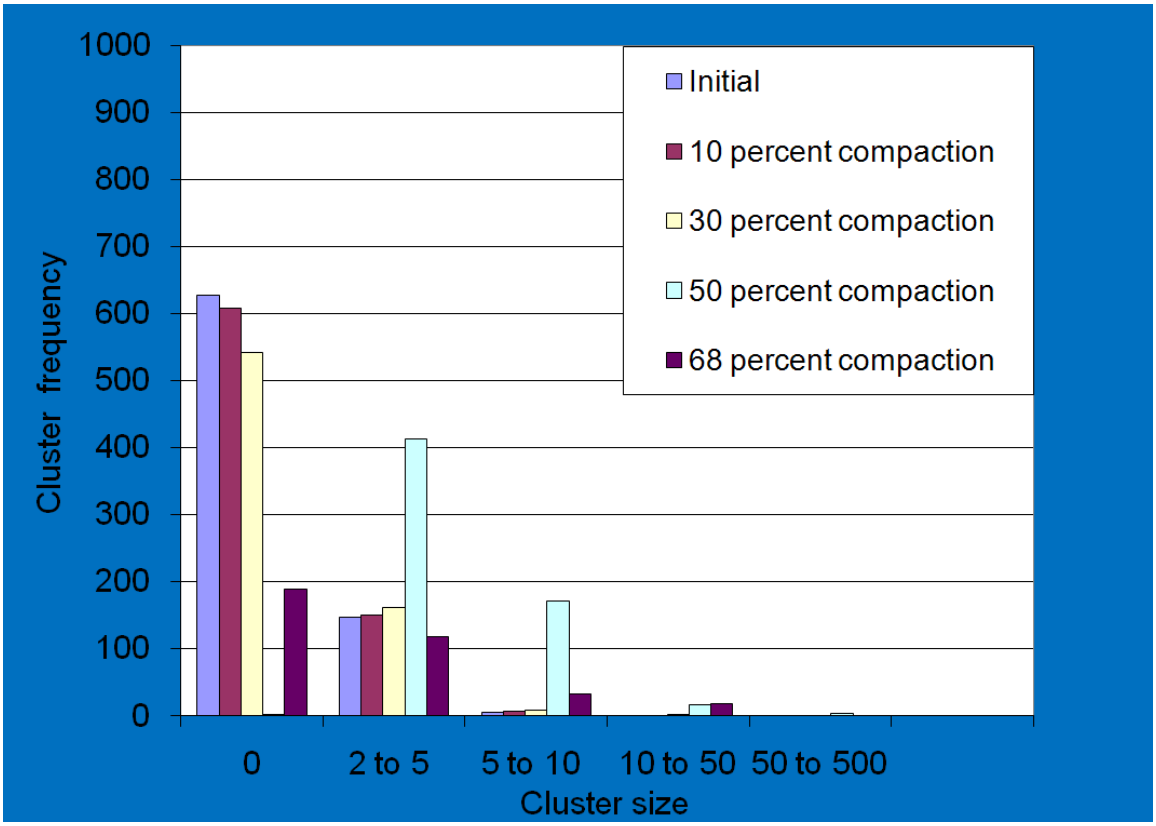

Figure 4.22: Cluster frequency distribution for D=0.001R at different levels of compaction of two component packing with 5 percent of carbonaceous material in the initial bulk volume. Cooperative rearrangement, 1000 spheres of carbonaceous material, carbonaceous material and silt/clay both ductile grains with rigid radius ratio =0.7R

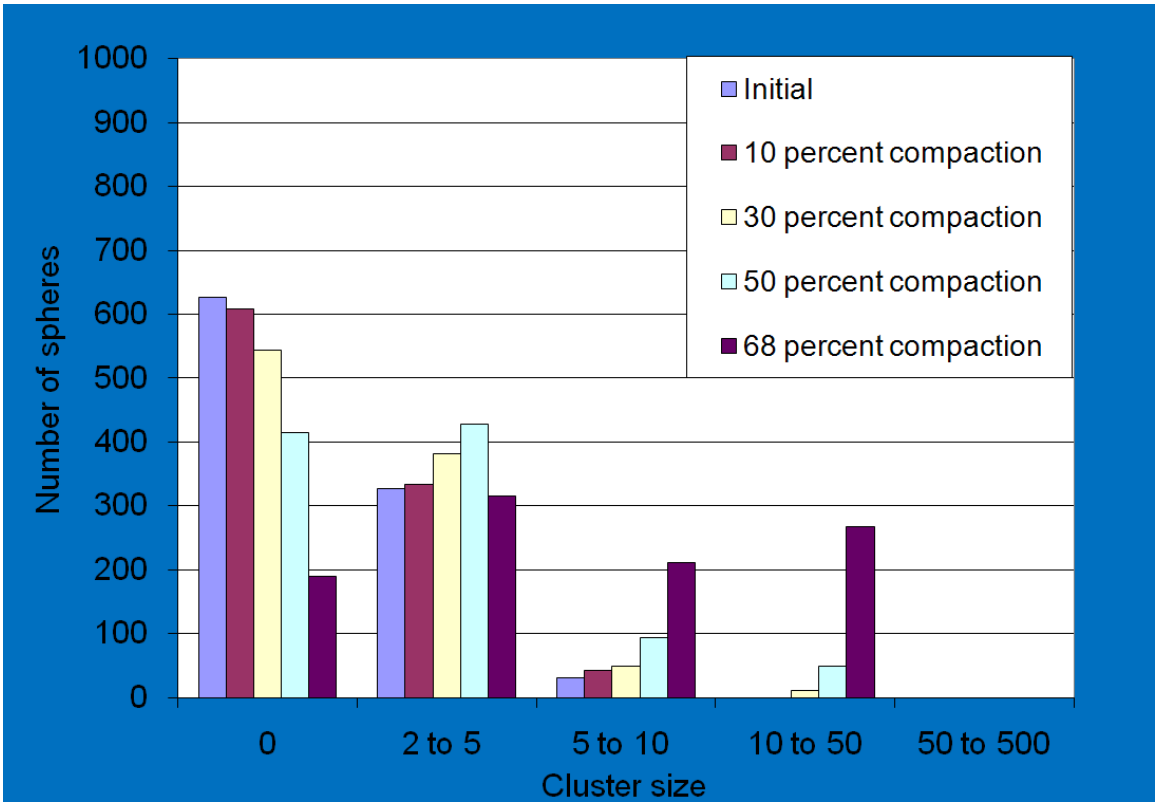

Figure 4.23: Number of spheres distribution for D=0.001R at different levels of compaction of two component packing with 5 percent of carbonaceous material in the initial bulk volume. Cooperative rearrangement, 1000 spheres of carbonaceous material, carbonaceous material and silt/clay both ductile grains with rigid ratio=0.7R

Table 4.15: Cluster frequency distribution for D=0.001R at different levels of compaction of two component packing with 10 percent of carbonaceous material in the initial bulk volume. Cooperative rearrangement, 1000 spheres of carbonaceous material, carbonaceous material and silt/clay both ductile grains with rigid ratio =0.7R

Compaction stage	**Porosity**	**Max cluster size**	**Normalized max cluster size**	**Frequency of clusters by size**				
				0	2 to 5	5 to 10	10 to 50	50 to 500
Initial	0.7011	19	0.0190	394	163	24	6	0
0.9	0.6678	19	0.0190	352	157	31	6	0
0.7	0.5796	22	0.0220	261	134	39	11	0
0.5	0.4178	53	0.0531	137	82	29	14	3
0.32	0.1318	916	0.9178	31	12	3	0	1

Table 4.16: Number of spheres distribution for D=0.001R at different levels of compaction of two component packing with 10 percent of carbonaceous material in the initial bulk volume. Cooperative rearrangement, 1000 spheres of carbonaceous material, carbonaceous material and silt/clay both ductile grains with rigid ratio =0.7R

Compaction stage	**Porosity**	**Max cluster size**	**Normalized max cluster size**	**Total number of spheres in clusters of different size ranges**				
				0	2 to 5	5 to 10	10 to 50	50 to 500
Initial	0.7011	19	0.0190	394	403	131	70	0
0.9	0.6678	19	0.0190	352	391	180	75	0
0.7	0.5796	22	0.0220	261	348	230	159	0
0.5	0.4178	53	0.0531	137	216	197	292	156
0.32	0.1318	916	0.9178	31	31	20	0	916

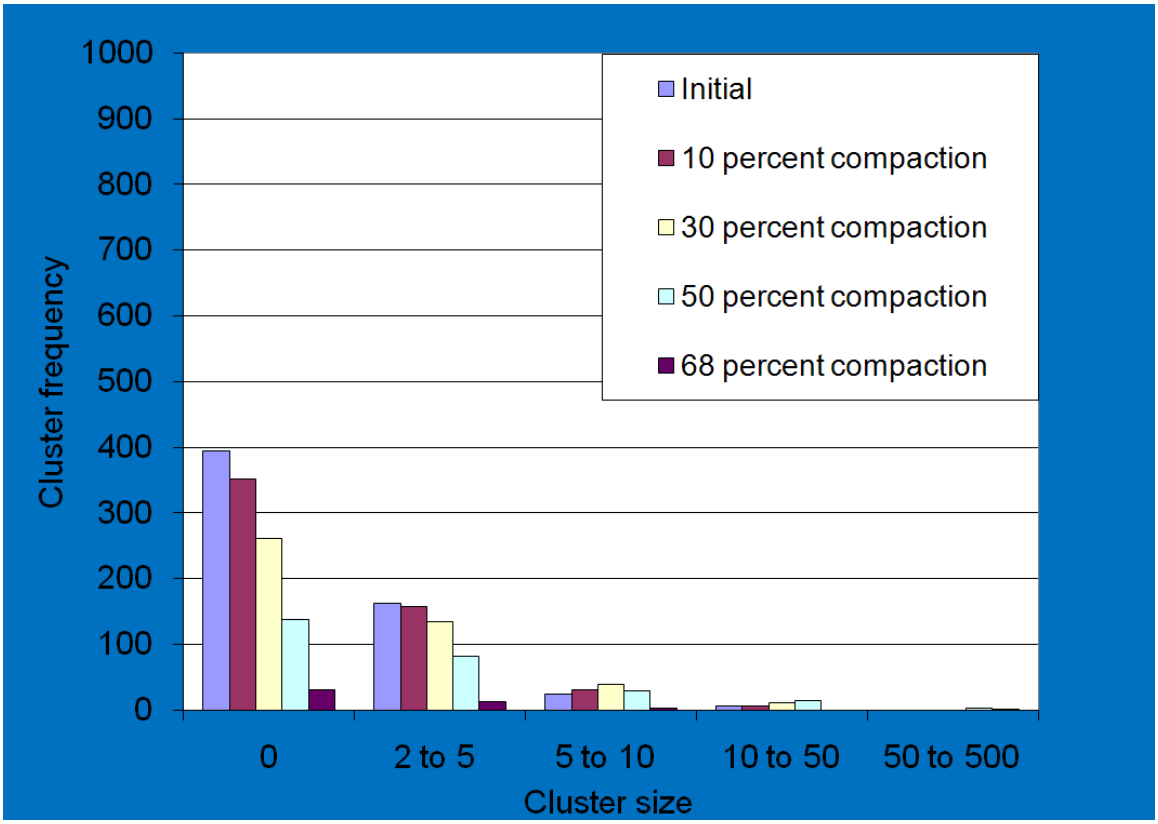

Figure 4.24: Cluster frequency distribution for D=0.001R at different levels of compaction of two component packing with 10 percent of carbonaceous material in the initial bulk volume. Cooperative rearrangement, 1000 spheres of carbonaceous material, carbonaceous material and silt/clay both ductile grains with rigid radius ratio =0.7R

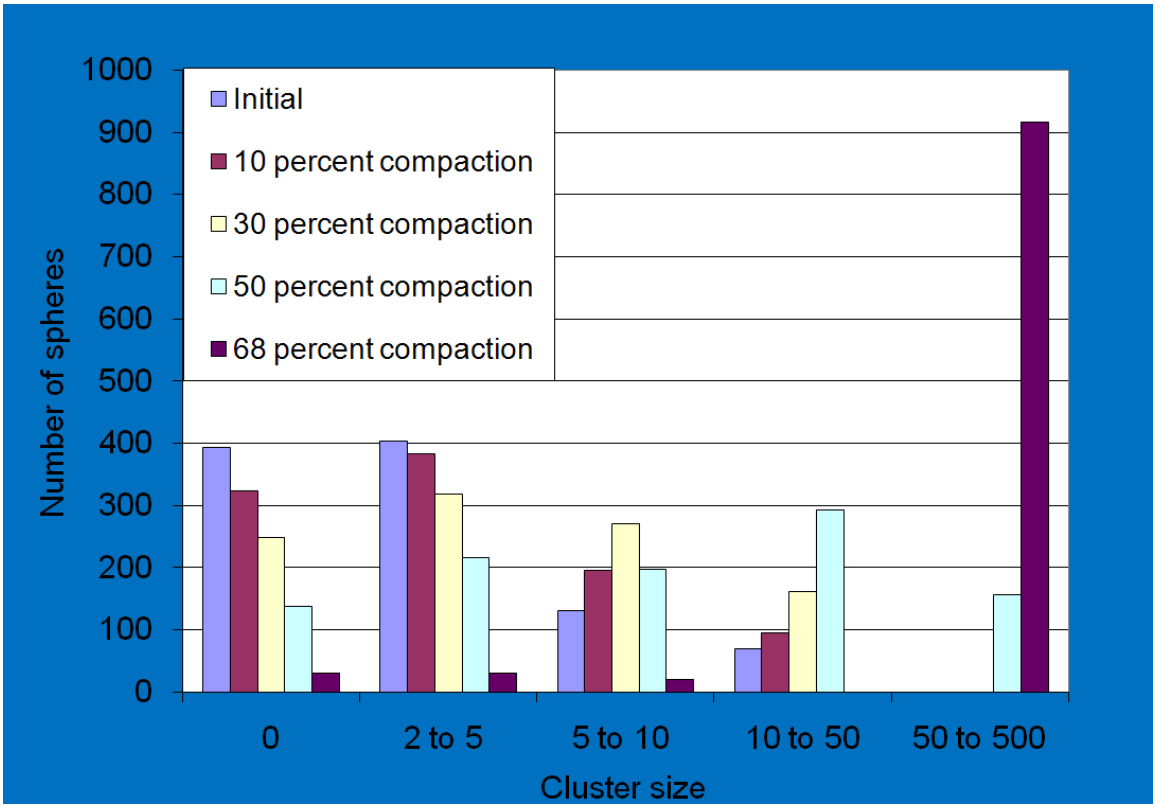

Figure 4.25: Number of spheres distribution for D=0.001R at different levels of compaction of two component packing with 10 percent of carbonaceous material in the initial bulk volume. Cooperative rearrangement, 1000 spheres of carbonaceous material, carbonaceous material and silt/clay both ductile grains with rigid ratio=0.7R

4.3.3 CARBONACEOUS MATERIAL IS DUCTILE AND SILT/CLAY GRAINS ARE RIGID

Under this scenario, only carbonaceous material is assumed to be ductile. The grain packing used for the scenario of all the spheres to be rigid was considered for this analysis which ensured that there was no overlap of spheres in the initial sediment setting. The grain packing is subjected to compaction and both cluster frequency vs. cluster size and number of spheres vs. cluster size are plotted in Figure 4.26-4.37 and summarized in Table 4.17-4.28. It is observed that the grain packing of prescribed

porosity 70% is compacted to 50% (c= 0.50) for all the cases (0.9 rigid radius, 0.8 rigid radius and 0.7 rigid radius) giving a final porosity of approximately 40%. The final volume fractions of carbonaceous material for initial 5% and 10% volume fraction of carbonaceous material is 10% and 20% respectively.

The results (Figure 4.26-4.37) shows that as the compaction increases, number of large cluster increases. However, the effect of compaction on connectivity of carbonaceous material is less pronounced than the case of both carbonaceous material and silt/clay grains as ductile grains (Figure 4.13-4.25). There is a minor effect of ductility of carbonaceous material on connectivity observed in 0.05 and 0.10 volume fraction of carbonaceous material grain packing (Figure 4.26-4.37).

Table 4.17: Cluster frequency distribution for D=0.001R at different levels of compaction of two component packing with 5 percent of carbonaceous material in the initial bulk volume. Cooperative rearrangement, 1000 spheres of carbonaceous material, carbonaceous material being ductile with rigid radius ratio =0.9R and silt/clay being rigid

Compaction stage	**Porosity**	**Max cluster size**	**Normalized max cluster size**	**Frequency of clusters by size**				
				0	2 to 5	5 to 10	10 to 50	50 to 500
Initial	0.702984	7	0.0070	744	107	3	0	0
0.9	0.667	5	0.0050	637	144	1	0	0
0.7	0.5664	10	0.0101	492	173	15	1	0
0.5	0.4007	11	0.0111	278	146	43	10	0

Table 4.18: Number of spheres distribution for D=0.001R at different levels of compaction of two component packing with 5 percent of carbonaceous material in the initial bulk volume. Cooperative rearrangement, 1000 spheres of carbonaceous material, carbonaceous material being ductile with rigid radius ratio=0.9R and silt/clay being rigid

Compaction stage	**Porosity**	**Max cluster size**	**Normalized max cluster size**	**Total number of spheres in clusters of different size ranges**				
				0	2 to 5	5 to 10	10 to 50	50 to 500
Initial	0.7030	7	0.0070	744	233	18	0	0
0.9	0.6670	5	0.0050	637	333	25	0	0
0.7	0.5664	10	0.0101	492	410	83	10	0
0.5	0.4007	11	0.0111	278	382	264	71	0

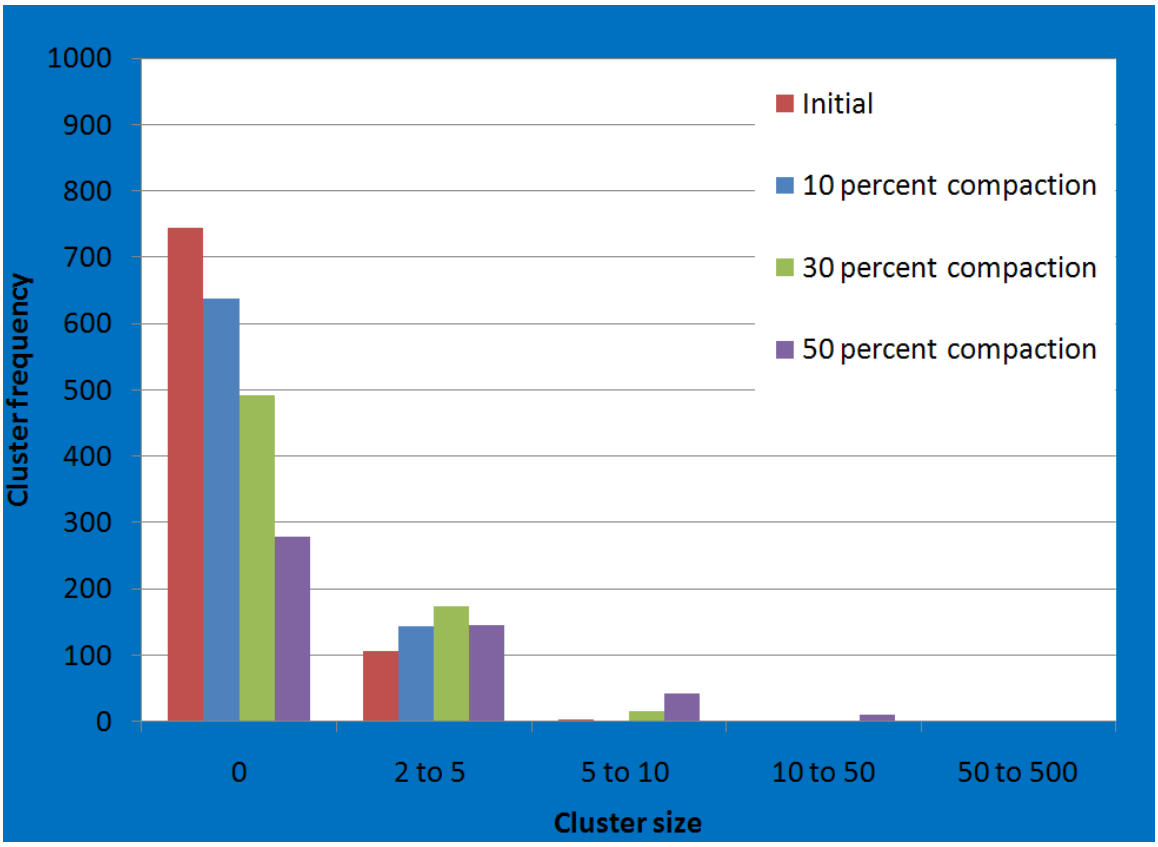

Figure 4.26: Cluster frequency distribution for D=0.001R at different levels of compaction of two component packing with 5 percent of carbonaceous material in the initial bulk volume. Cooperative rearrangement, 1000 spheres of carbonaceous material, carbonaceous material being ductile with rigid radius ratio=0.9R and silt/clay being rigid

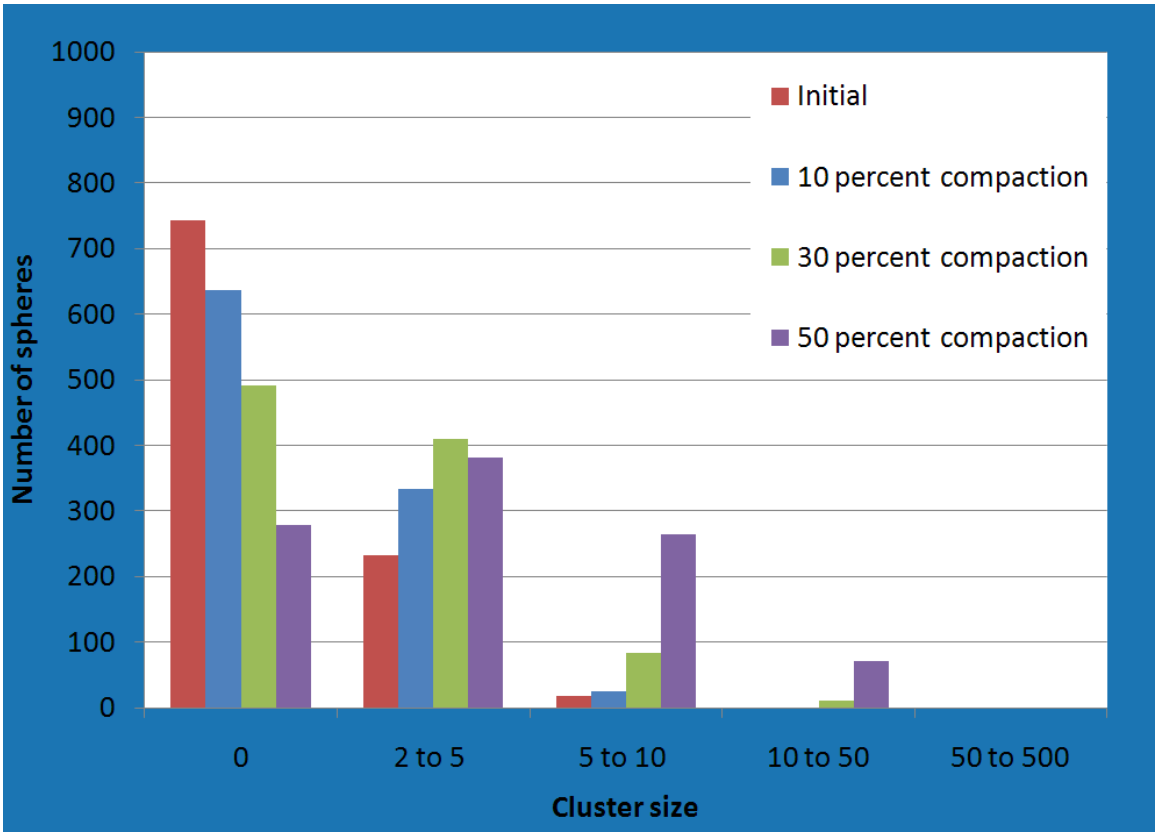

Figure 4.27: Number of spheres distribution for D=0.001R at different levels of compaction of two component packing with 5 percent of carbonaceous material in the initial bulk volume. Cooperative rearrangement, 1000 spheres of carbonaceous material, carbonaceous material being ductile with rigid radius ratio =0.9R and silt/clay being rigid

Table4.19: Cluster frequency distribution for D=0.001R at different levels of compaction of two component packing with 10 percent of carbonaceous material in the initial bulk volume. Cooperative rearrangement, 1000 spheres of carbonaceous material, carbonaceous material being ductile with rigid radius ratio =0.9R and silt/clay being rigid

Compaction stage	**Porosity**	**Max cluster size**	**Normalized max cluster size**	**Frequency of clusters by size**				
				0	2 to 5	5 to 10	10 to 50	50 to 500
Initial	0.6975	17	0.0178	432	149	20	2	0
0.9	0.6665	16	0.0167	371	150	26	4	0
0.7	0.5662	43	0.0450	252	127	37	9	0
0.5	0.4021	550	0.5753	83	43	10	9	0

Table 4.20: Number of spheres distribution for D=0.001R at different levels of compaction of two component packing with 10 percent of carbonaceous material in the initial bulk volume. Cooperative rearrangement, 1000 spheres of carbonaceous material, carbonaceous material being ductile with rigid radius ratio=0.9R and silt/clay being rigid

Compaction stage	**Porosity**	**Max cluster size**	**Normalized max cluster size**	**Total number of spheres in clusters of different size ranges**				
				0	2 to 5	5 to 10	10 to 50	50 to 500
Initial	0.6975	17	0.0178	432	369	133	22	0
0.9	0.6665	16	0.0167	371	367	170	48	0
0.7	0.5662	43	0.0450	252	320	234	150	0
0.5	0.4021	550	0.5753	83	114	60	149	550

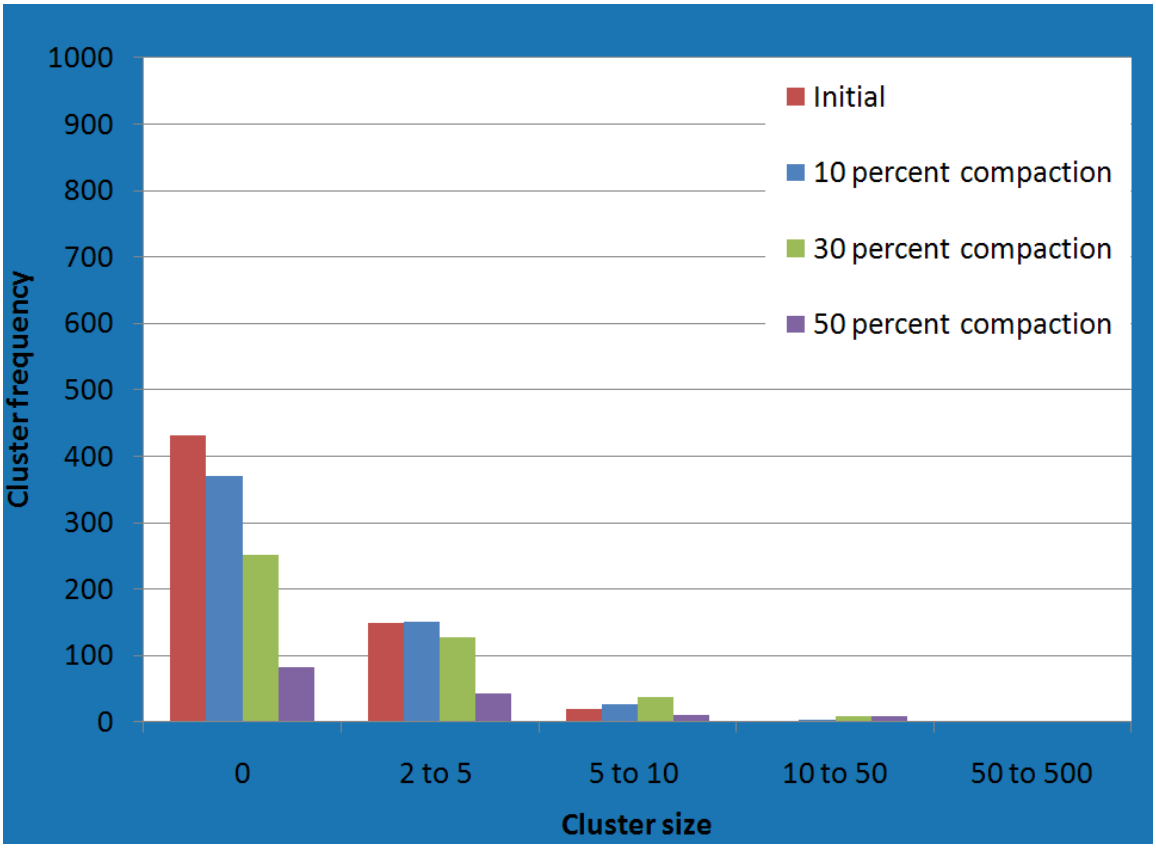

Figure 4.28: Cluster frequency distribution for D=0.001R at different levels of compaction of two component packing with 10 percent of carbonaceous material in the initial bulk volume. Cooperative rearrangement, 1000 spheres of carbonaceous material, carbonaceous material being ductile with rigid radius ratio=0.9R and silt/clay being rigid

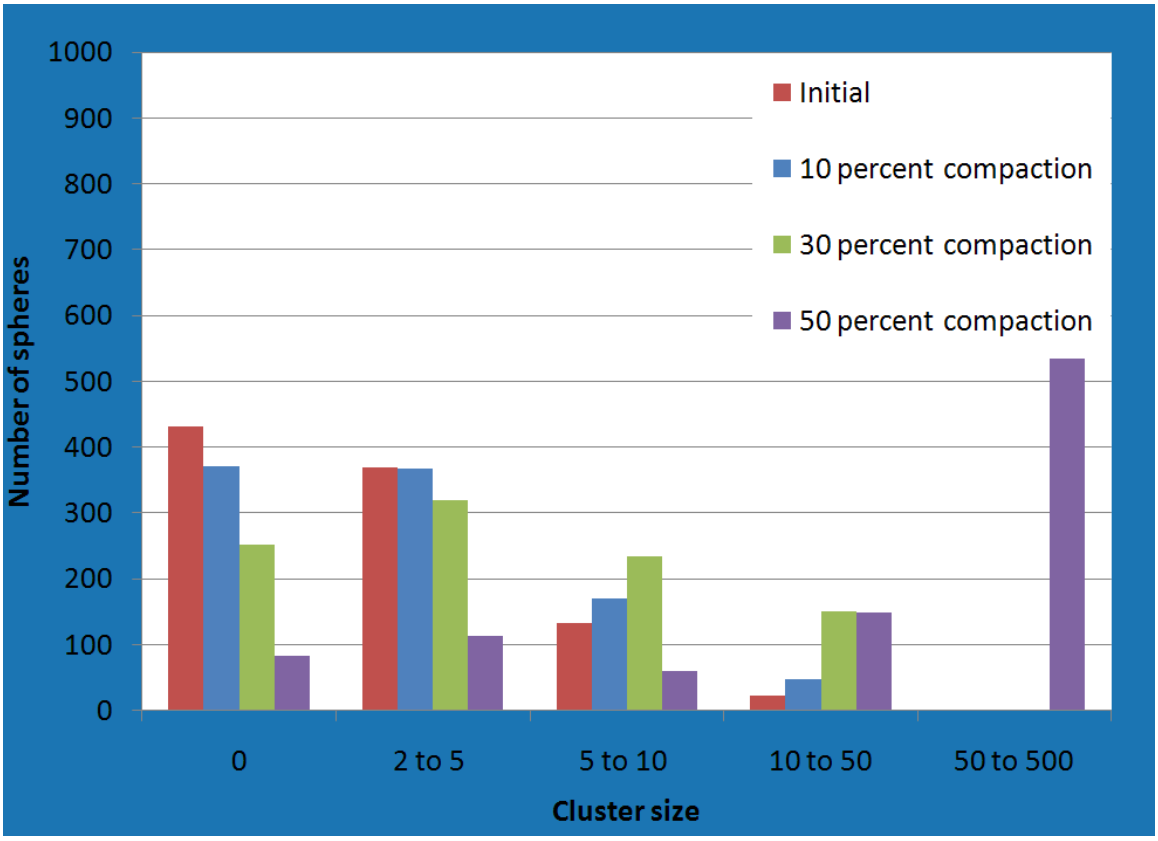

Figure 4.29: Number of spheres distribution for D=0.001R at different levels of compaction of two component packing with 10 percent of carbonaceous material in the initial bulk volume. Cooperative rearrangement, 1000 spheres of carbonaceous material, carbonaceous material being ductile with rigid radius ratio =0.9R and silt/clay being rigid

Table 4.21: Cluster frequency distribution for D=0.001R at different levels of compaction of two component packing with 5 percent of carbonaceous material in the initial bulk volume. Cooperative rearrangement, 1000 spheres of carbonaceous material, carbonaceous material being ductile with rigid radius ratio =0.8 R and silt/clay being rigid

Compaction stage	**Porosity**	**Max cluster size**	**Normalized max cluster size**	**Frequency of clusters by size**				
				0	2 to 5	5 to 10	10 to 50	50 to 500
Initial	0.7030	7	0.0070	744	107	3	0	0
0.9	0.6661	5	0.0050	636	149	4	0	0
0.7	0.5676	10	0.0101	498	173	14	1	0
0.5	0.3955	15	0.0151	261	145	48	5	0

Table 4.22: Number of spheres distribution for D=0.001R at different levels of compaction of two component packing with 5 percent of carbonaceous material in the initial bulk volume. Cooperative rearrangement, 1000 spheres of carbonaceous material, carbonaceous material being ductile with rigid radius ratio=0.8R and silt/clay being rigid

Compaction stage	**Porosity**	**Max cluster size**	**Normalized max cluster size**	**Total number of spheres in clusters of different size ranges**				
				0	2 to 5	5 to 10	10 to 50	50 to 500
Initial	0.7030	7	0.0070	744	233	18	0	0
0.9	0.6661	5	0.0050	636	339	20	0	0
0.7	0.5676	10	0.0101	498	410	77	10	0
0.5	0.3955	15	0.0151	261	377	298	59	0

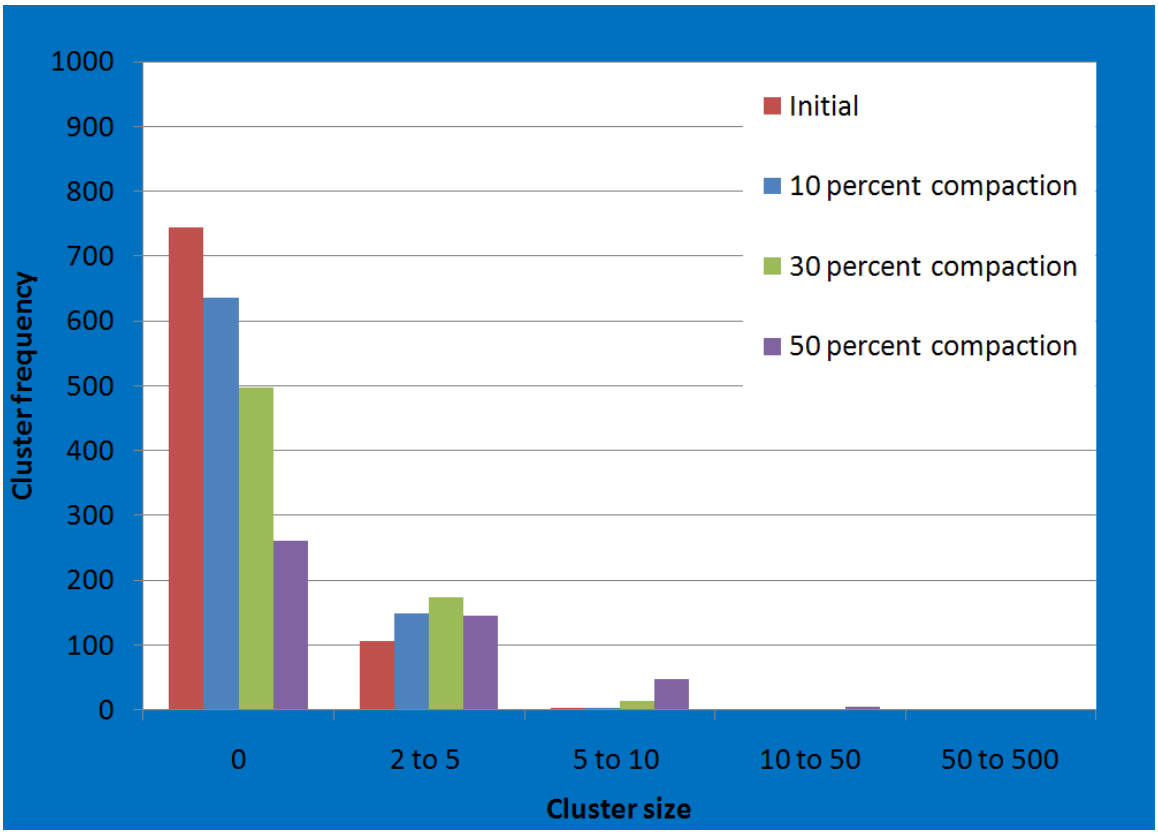

Figure 4.30: Cluster frequency distribution for D=0.001R at different levels of compaction of two component packing with 5 percent of carbonaceous material in the initial bulk volume. Cooperative rearrangement, 1000 spheres of carbonaceous material, carbonaceous material being ductile with rigid radius ratio=0.8R and silt/clay being rigid

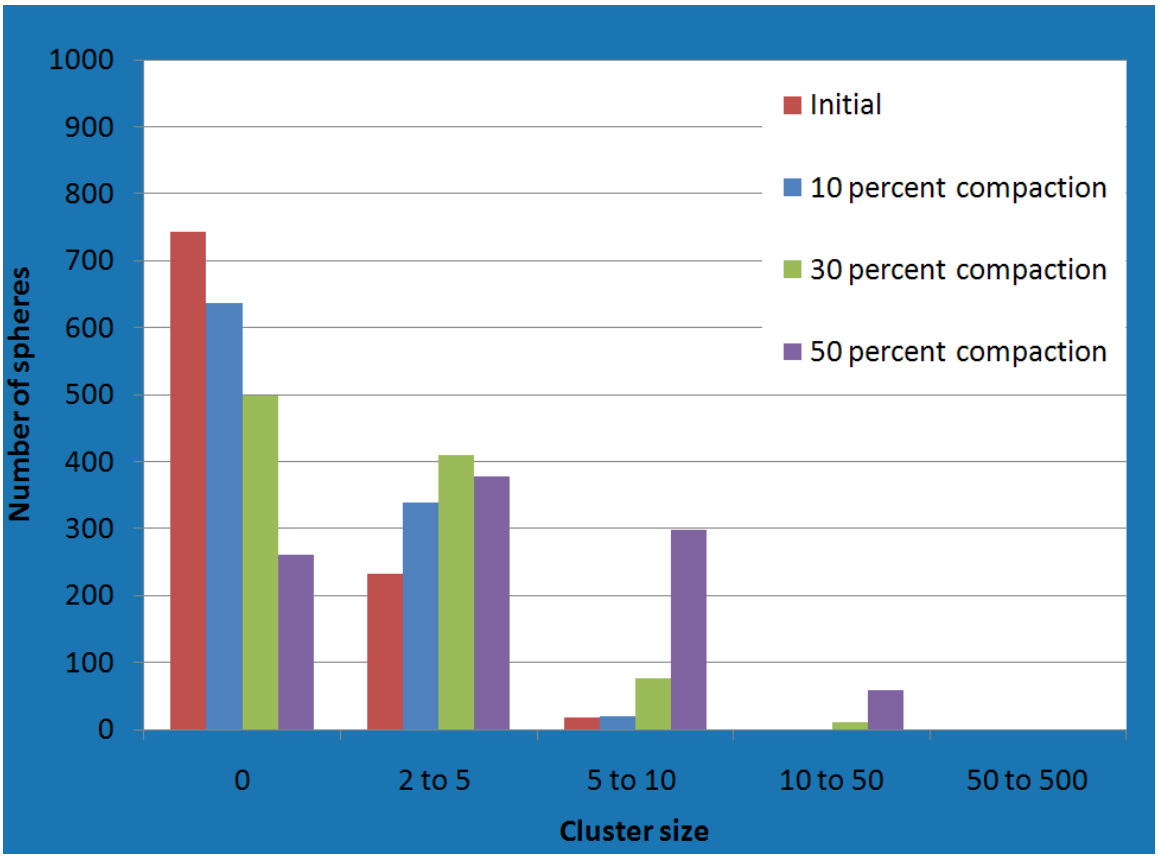

Figure 4.31: Number of spheres distribution for D=0.001R at different levels of compaction of two component packing with 5 percent of carbonaceous material in the initial bulk volume. Cooperative rearrangement, 1000 spheres of carbonaceous material, carbonaceous material being ductile with rigid radius ratio =0.8R and silt/clay being rigid

Table 4.23: Cluster frequency distribution for D=0.001R at different levels of compaction of two component packing with 10 percent of carbonaceous material in the initial bulk volume. Cooperative rearrangement, 1000 spheres of carbonaceous material, carbonaceous material being ductile with rigid radius ratio =0.8 R and silt/clay being rigid

Compaction stage	**Porosity**	**Max cluster size**	**Normalized max cluster size**	**Frequency of clusters by size**				
				0	2 to 5	5 to 10	10 to 50	50 to 500
Initial	0.6975	21	0.0220	369	139	26	5	0
0.9	0.6661	14	0.0146	338	147	33	3	0
0.7	0.5636	43	0.0450	211	136	32	12	0
0.5	0.3974	325	0.3400	60	41	15	7	2

Table 4.24: Number of spheres distribution for D=0.001R at different levels of compaction of two component packing with 10 percent of carbonaceous material in the initial bulk volume. Cooperative rearrangement, 1000 spheres of carbonaceous material, carbonaceous material being ductile with rigid radius ratio=0.8R and silt/clay being rigid

Compaction stage	**Porosity**	**Max cluster size**	**Normalized max cluster size**	**Total number of spheres in clusters of different size ranges**				
				0	2 to 5	5 to 10	10 to 50	50 to 500
Initial	0.6975	21	0.0220	369	347	171	69	0
0.9	0.6661	14	0.0146	338	358	224	36	0
0.7	0.5636	43	0.0450	211	351	204	190	0
0.5	0.3974	325	0.3400	60	111	92	154	539

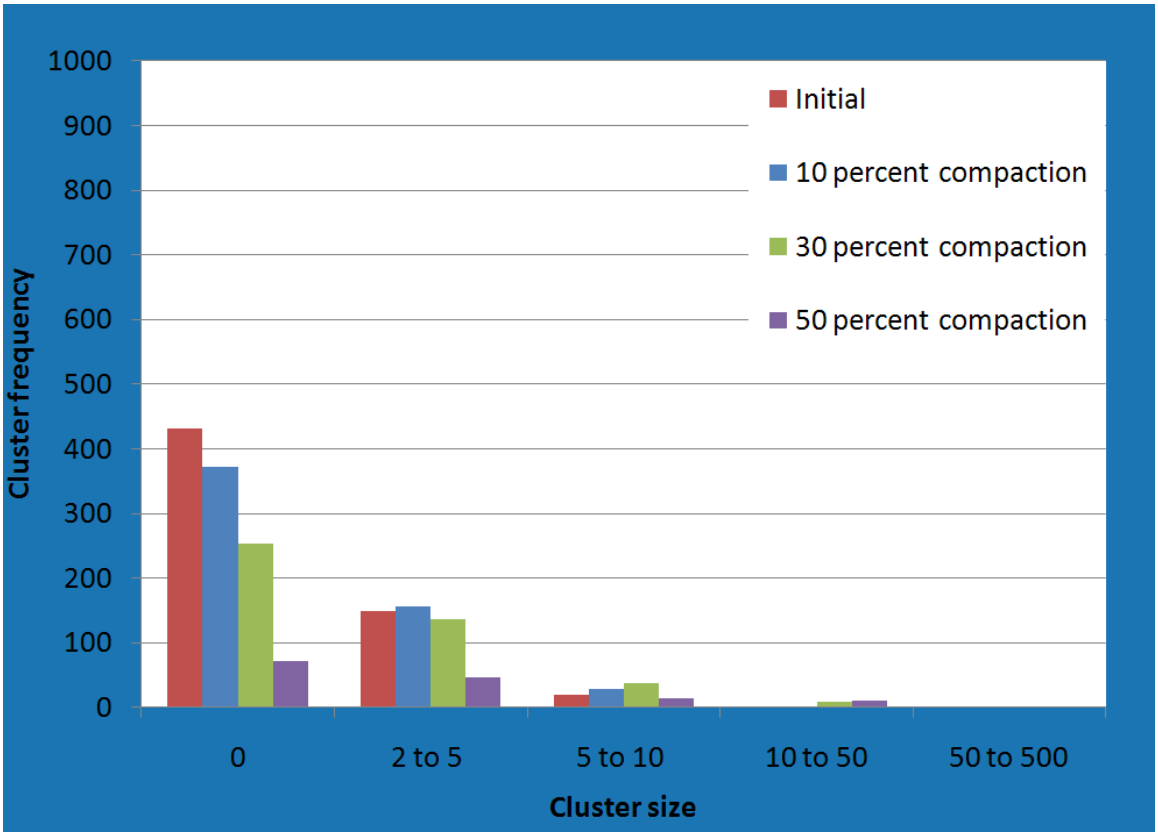

Figure 4.32: Cluster frequency distribution for D=0.001R at different levels of compaction of two component packing with 10 percent of carbonaceous material in the initial bulk volume. Cooperative rearrangement, 1000 spheres of carbonaceous material, carbonaceous material being ductile with rigid radius ratio=0.8R and silt/clay being rigid

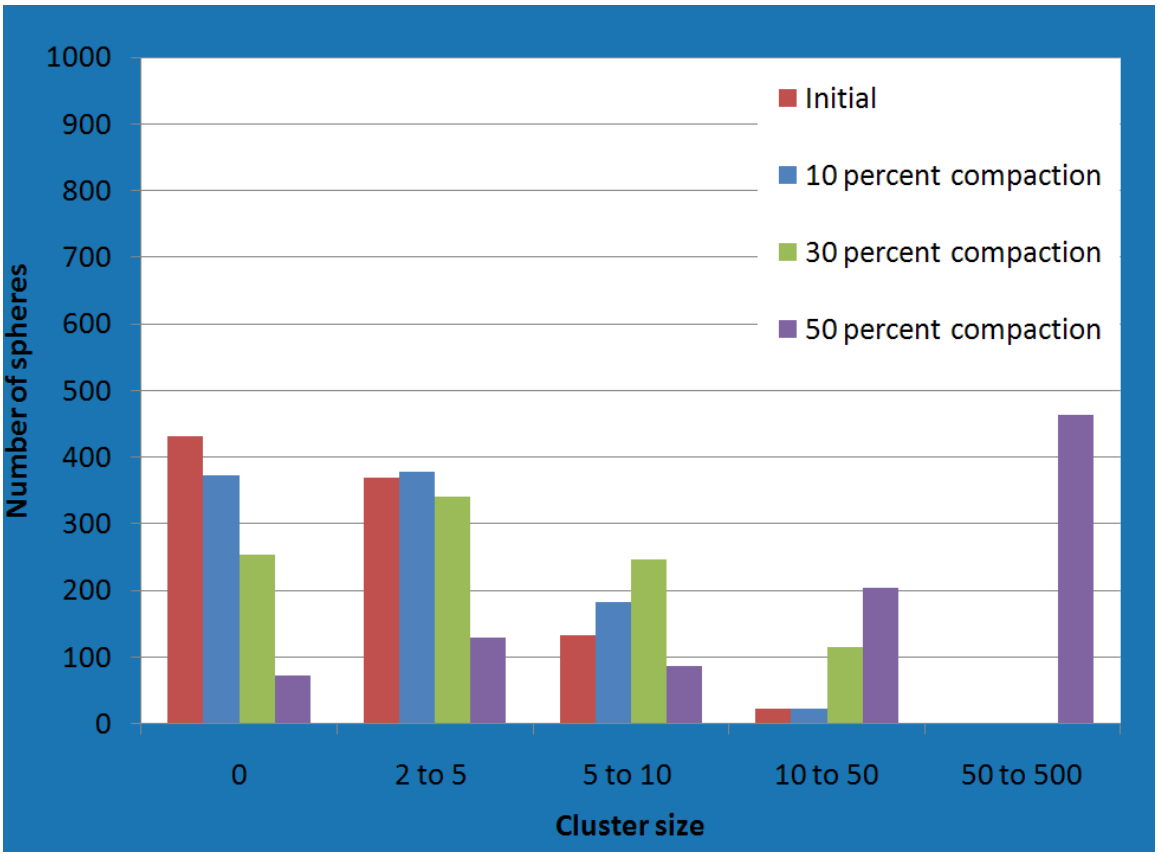

Figure 4.33: Number of spheres distribution for D=0.001R at different levels of compaction of two component packing with 10 percent of carbonaceous material in the initial bulk volume. Cooperative rearrangement, 1000 spheres of carbonaceous material, carbonaceous material being ductile with rigid radius ratio =0.8R and silt/clay being rigid

Table 4.25: Cluster frequency distribution for D=0.001R at different levels of compaction of two component packing with 5 percent of carbonaceous material in the initial bulk volume. Cooperative rearrangement, 1000 spheres of carbonaceous material, carbonaceous material being ductile with rigid radius ratio =0.7 R and silt/clay being rigid

Compaction stage	**Porosity**	**Max cluster size**	**Normalized max cluster size**	**Frequency of clusters by size**				
				0	2 to 5	5 to 10	10 to 50	50 to 500
Initial	0.7030	7	0.0070	744	107	3	0	0
0.9	0.6659	5	0.0050	635	149	4	0	0
0.7	0.5690	10	0.0101	498	174	15	1	0
0.5	0.3982	17	0.0171	262	162	40	5	0

Table 4.26: Number of spheres distribution for D=0.001R at different levels of compaction of two component packing with 5 percent of carbonaceous material in the initial bulk volume. Cooperative rearrangement, 1000 spheres of carbonaceous material, carbonaceous material being ductile with rigid radius ratio=0.7R and silt/clay being rigid

Compaction stage	**Porosity**	**Max cluster size**	**Normalized max cluster size**	**Total number of spheres in clusters of different size ranges**				
				0	2 to 5	5 to 10	10 to 50	50 to 500
Initial	0.7030	7	0.0070	744	233	18	0	0
0.9	0.6659	5	0.0050	635	340	20	0	0
0.7	0.5690	10	0.0101	498	406	81	10	0
0.5	0.3982	17	0.0171	262	420	249	64	0

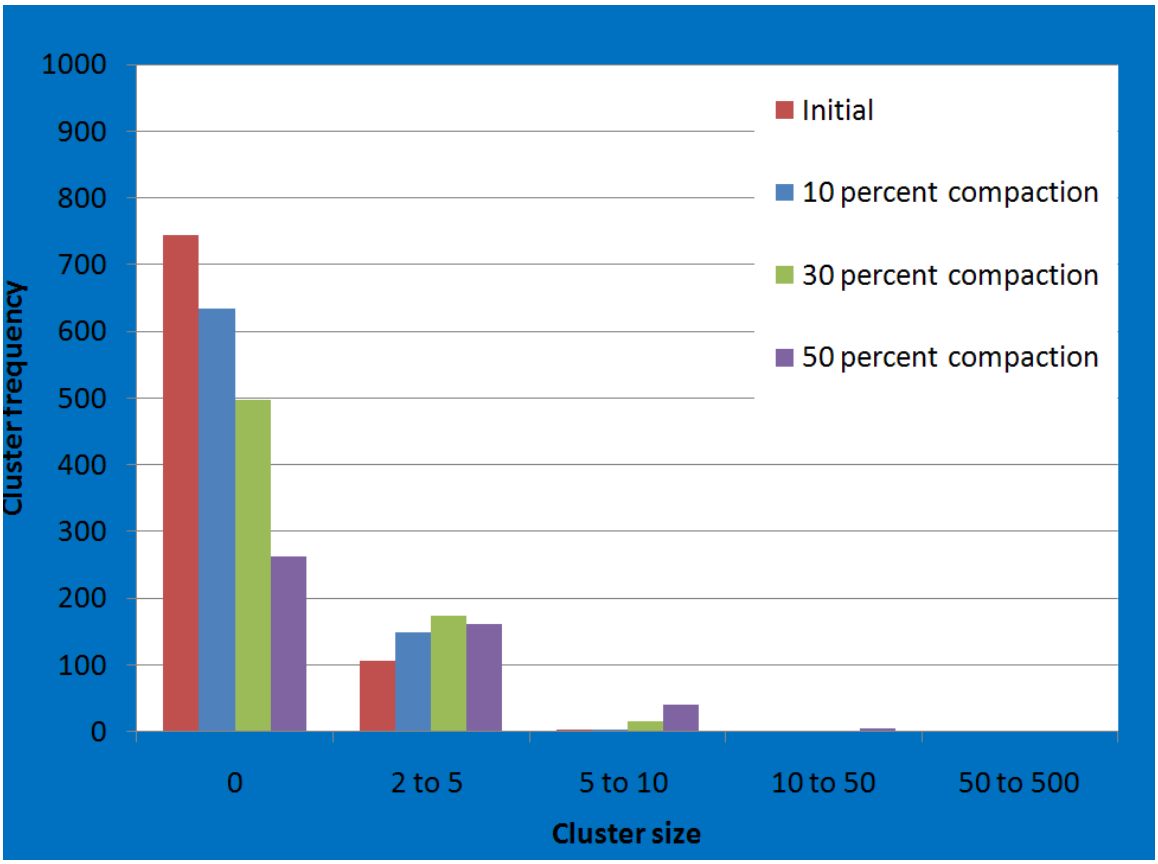

Figure 4.34: Cluster frequency distribution for D=0.001R at different levels of compaction of two component packing with 5 percent of carbonaceous material in the initial bulk volume. Cooperative rearrangement, 1000 spheres of carbonaceous material, carbonaceous material being ductile with rigid radius ratio=0.7R and silt/clay being rigid

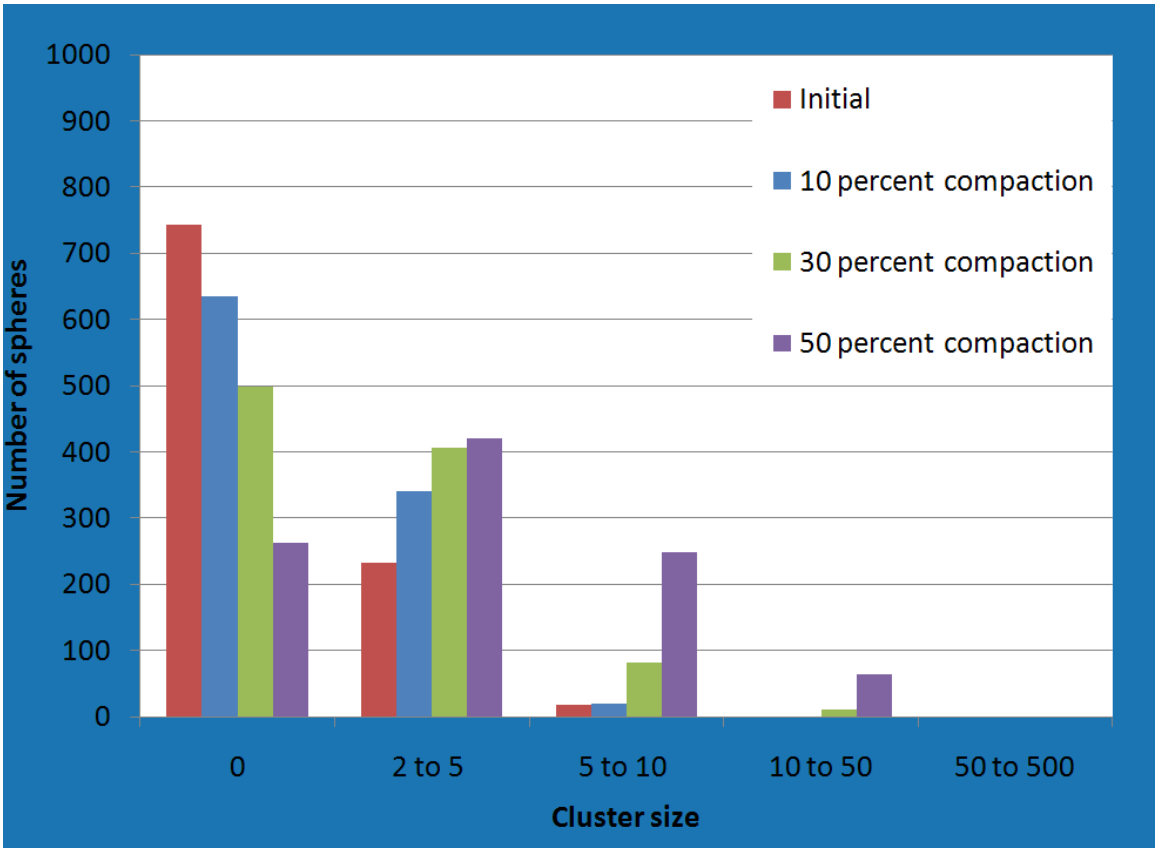

Figure 4.35: Number of spheres distribution for D=0.001R at different levels of compaction of two component packing with 5 percent of carbonaceous material in the initial bulk volume. Cooperative rearrangement, 1000 spheres of carbonaceous material, carbonaceous material being ductile with rigid radius ratio =0.7R and silt/clay being rigid

Table 4.27: Cluster frequency distribution for D=0.001R at different levels of compaction of two component packing with 10 percent of carbonaceous material in the initial bulk volume. Cooperative rearrangement, 1000 spheres of carbonaceous material, carbonaceous material being ductile with rigid radius ratio =0.7 R and silt/clay being rigid

Compaction stage	**Porosity**	**Max cluster size**	**Normalized max cluster size**	**Frequency of clusters by size**				
				0	2 to 5	5 to 10	10 to 50	50 to 500
Initial	0.6975	17	0.0178	432	149	20	2	0
0.9	0.6661	12	0.0126	373	157	28	2	0
0.7	0.5636	21	0.0220	250	142	38	7	0
0.5	0.3974	161	0.1684	78	48	12	14	5

Table 4.28: Number of spheres distribution for D=0.001R at different levels of compaction of two component packing with 10 percent of carbonaceous material in the initial bulk volume. Cooperative rearrangement, 1000 spheres of carbonaceous material, carbonaceous material being ductile with rigid radius ratio=0.7R and silt/clay being rigid

Compaction stage	**Porosity**	**Max cluster size**	**Normalized max cluster size**	**Total number of spheres in clusters of different size ranges**				
				0	2 to 5	5 to 10	10 to 50	50 to 500
Initial	0.6975	17	0.0178	432	369	133	22	0
0.9	0.6661	12	0.0126	373	381	180	22	0
0.7	0.5636	21	0.0220	250	359	244	103	0
0.5	0.3974	161	0.1684	78	130	79	232	437

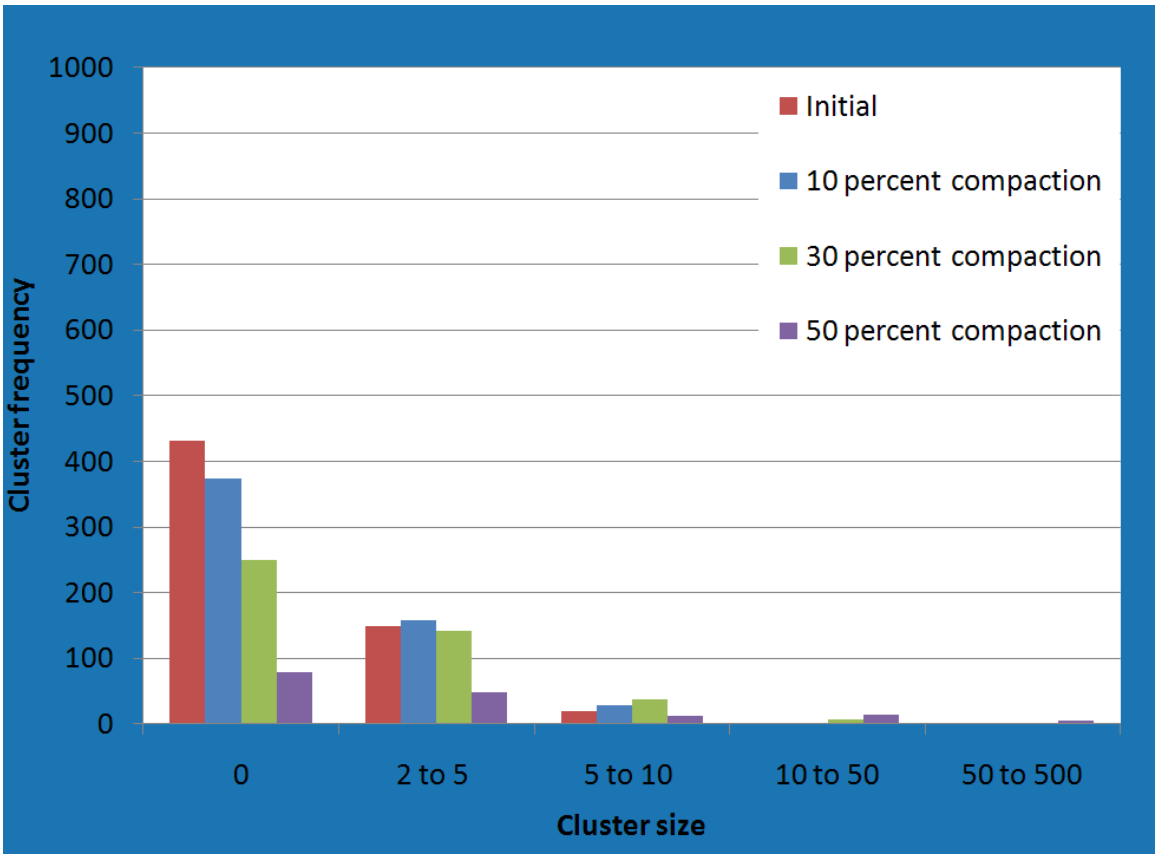

Figure 4.36: Cluster frequency distribution for D=0.001R at different levels of compaction of two component packing with 10 percent of carbonaceous material in the initial bulk volume. Cooperative rearrangement, 1000 spheres of carbonaceous material, carbonaceous material being ductile with rigid radius ratio=0.7R and silt/clay being rigid

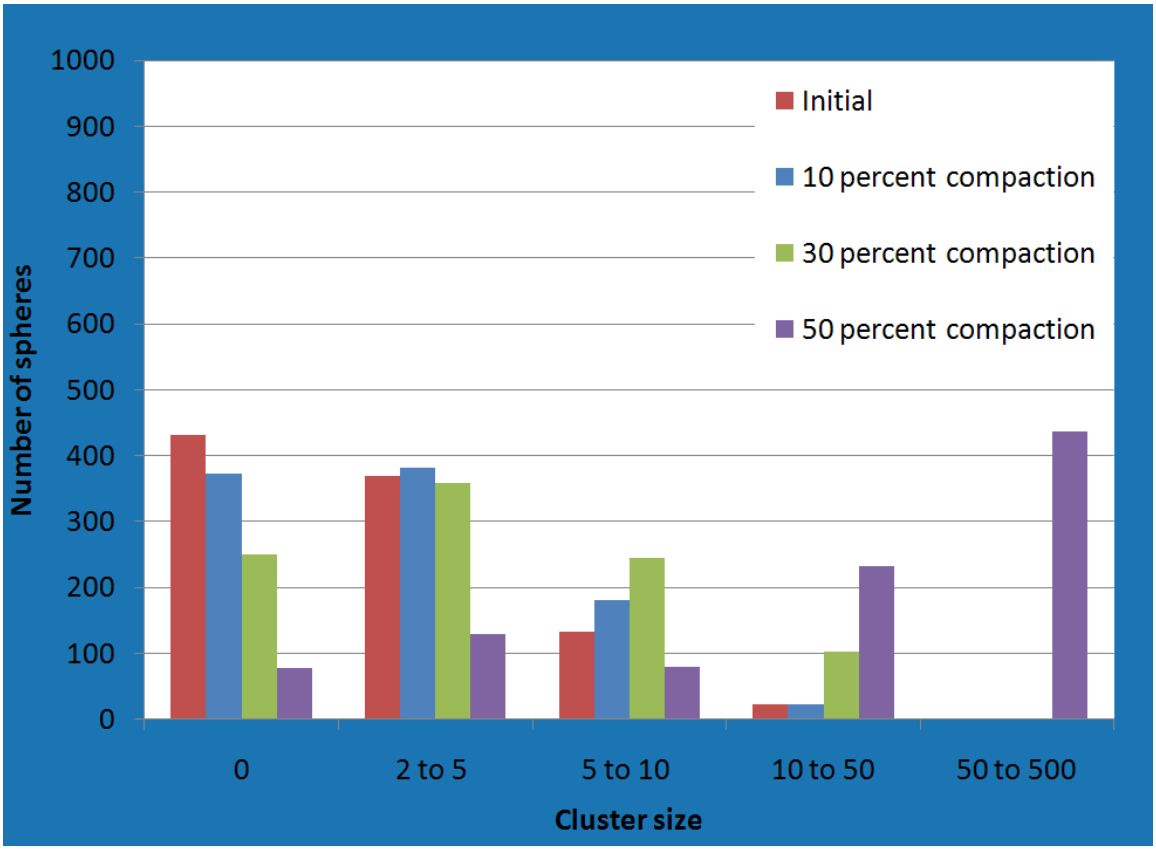

Figure 4.37: Number of spheres distribution for D=0.001R at different levels of compaction of two component packing with 10 percent of carbonaceous material in the initial bulk volume. Cooperative rearrangement, 1000 spheres of carbonaceous material, carbonaceous material being ductile with rigid radius ratio =0.7R and silt/clay being rigid

4.4 RELATIONSHIP OF CLUSTER STATISTICS TO POROSITY

Cluster statistics generated in the previous section for all the three scenarios were analyzed and related to the porosity values of the grain packing for 5 and 10 percent of carbonaceous material, considering all grains rigid, all grains ductile with rigid radius ratios of 0.9, 0.8 and 0.7 and only carbonaceous material ductile with rigid ratios of 0.9, 0.8 and 0.7 with target porosity of 70% as shown in plots in Figure 4.38-4.41. A relationship between porosity and number of clusters and porosity and number of spheres in different cluster sizes is observed. Isolated grains and small cluster sizes 2 to 5

decreased with decrease in porosity while large cluster size 5 to 10 and 10 to 50 increased with decrease in porosity for 5 percent and 10 percent of carbonaceous material by bulk volume grain packing of the scenarios discussed in the previous section. A porosity of 0.40 was observed as a critical point for clustering for the packing having 10 percent of carbonaceous for the above scenarios which corresponded to 50% of compaction.

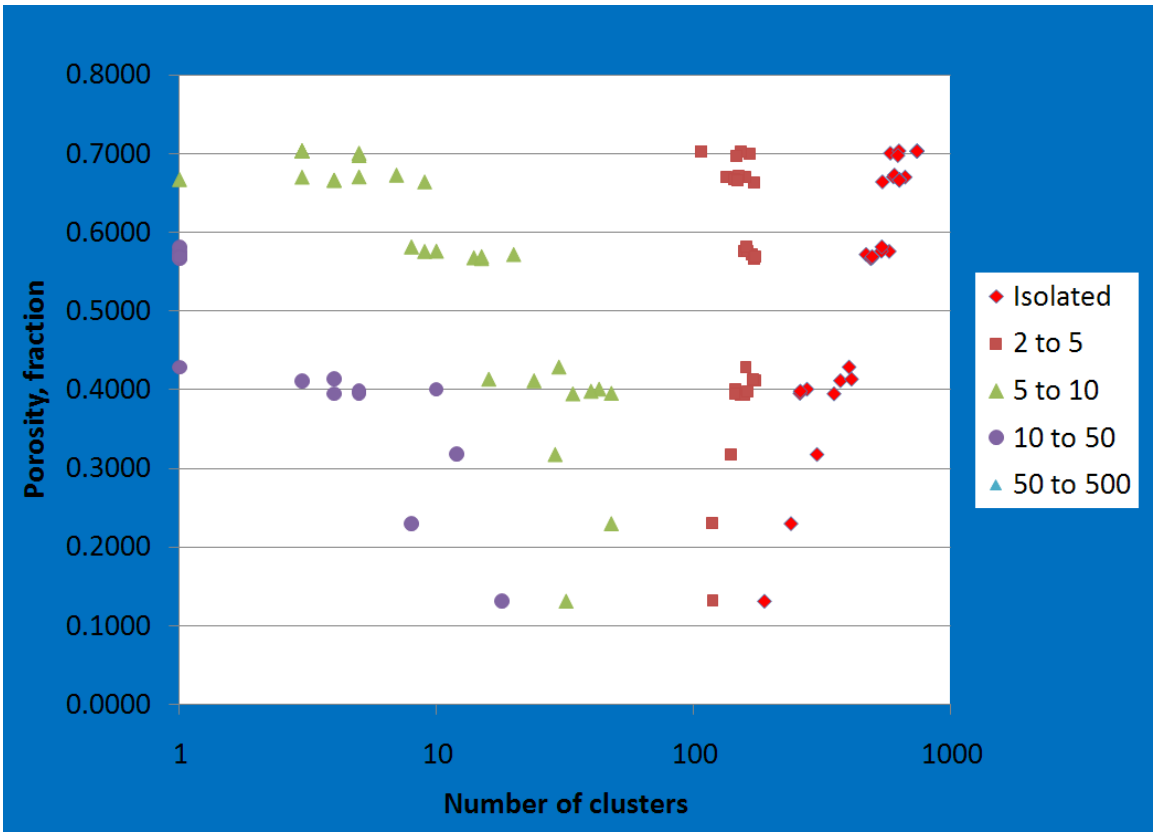

Figure 4.38: Relationship between number of clusters and sediment porosity with 5 percent of carbonaceous material in the initial bulk volume for initial sediment porosity of 70%. Values taken from Table 4.1, Table 4.5, Table 4.9, Table 4.13, Table 4.17, Table 4.21, Table 4.25

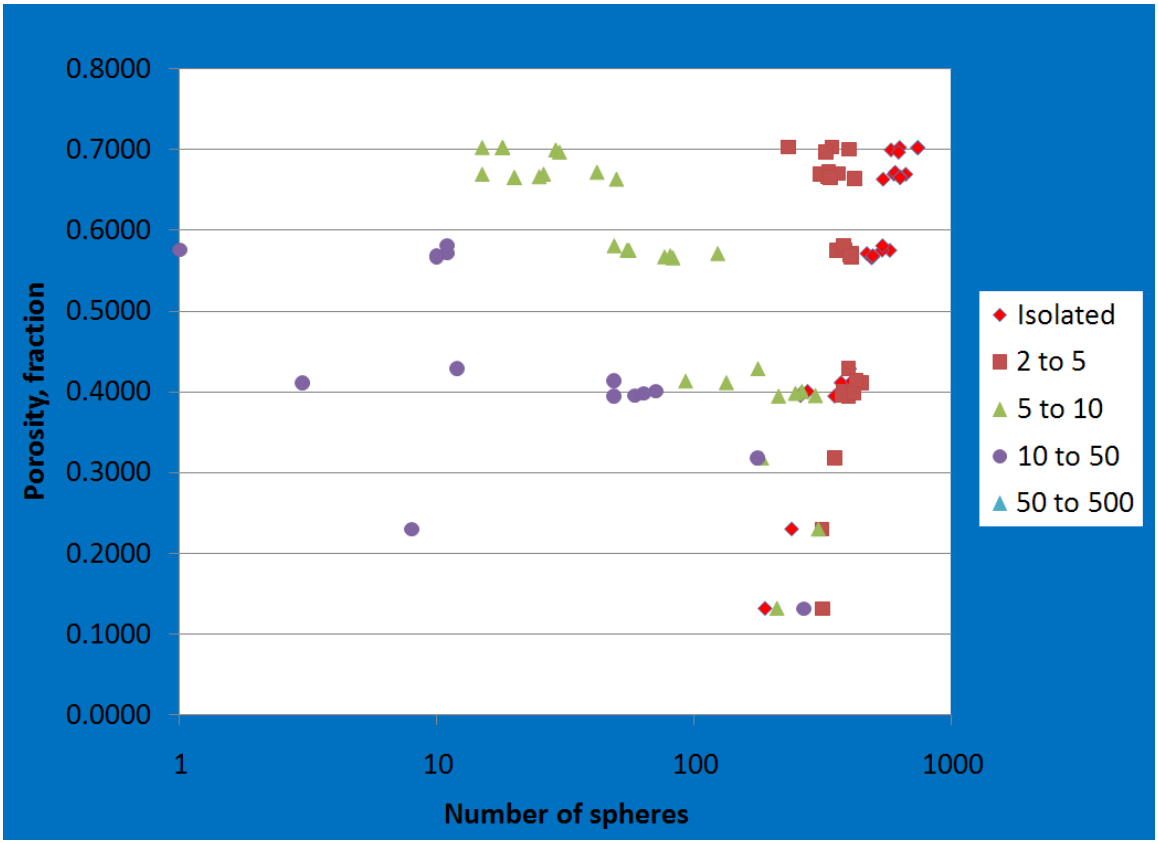

Figure 4.39: Relationship between number of spheres in cluster size and sediment porosity with 5 percent of carbonaceous material in the initial bulk volume for initial porosity 70%.Values taken from Table 4.2, Table 4.6, Table 4.10, Table 4.14, Table 4.18, Table 4.22, Table 4.26

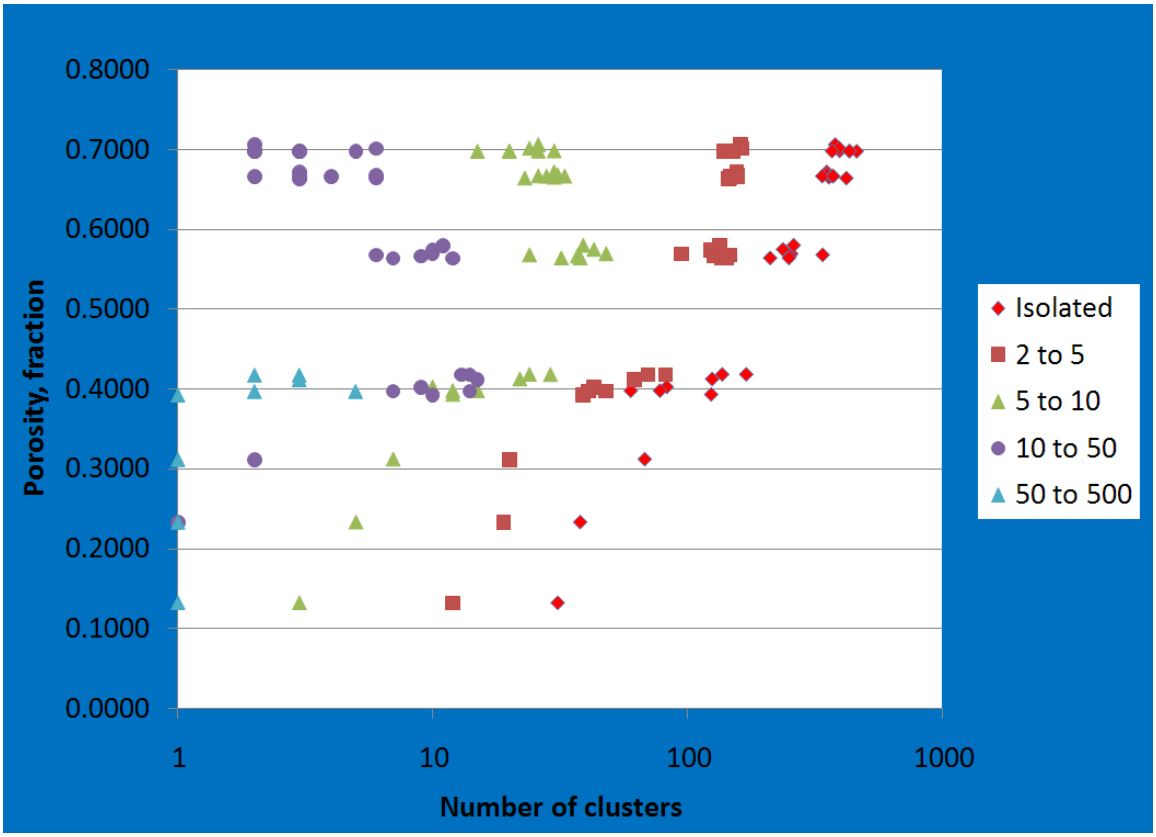

Figure 4.40: Relationship between number of clusters and sediment porosity with 10 percent of carbonaceous material in the initial bulk volume for initial porosity of 70%.Values taken from Table 4.3, Table 4.7, Table 4.11, Table 4.15, Table 4.19, Table 4.23, Table 4.27

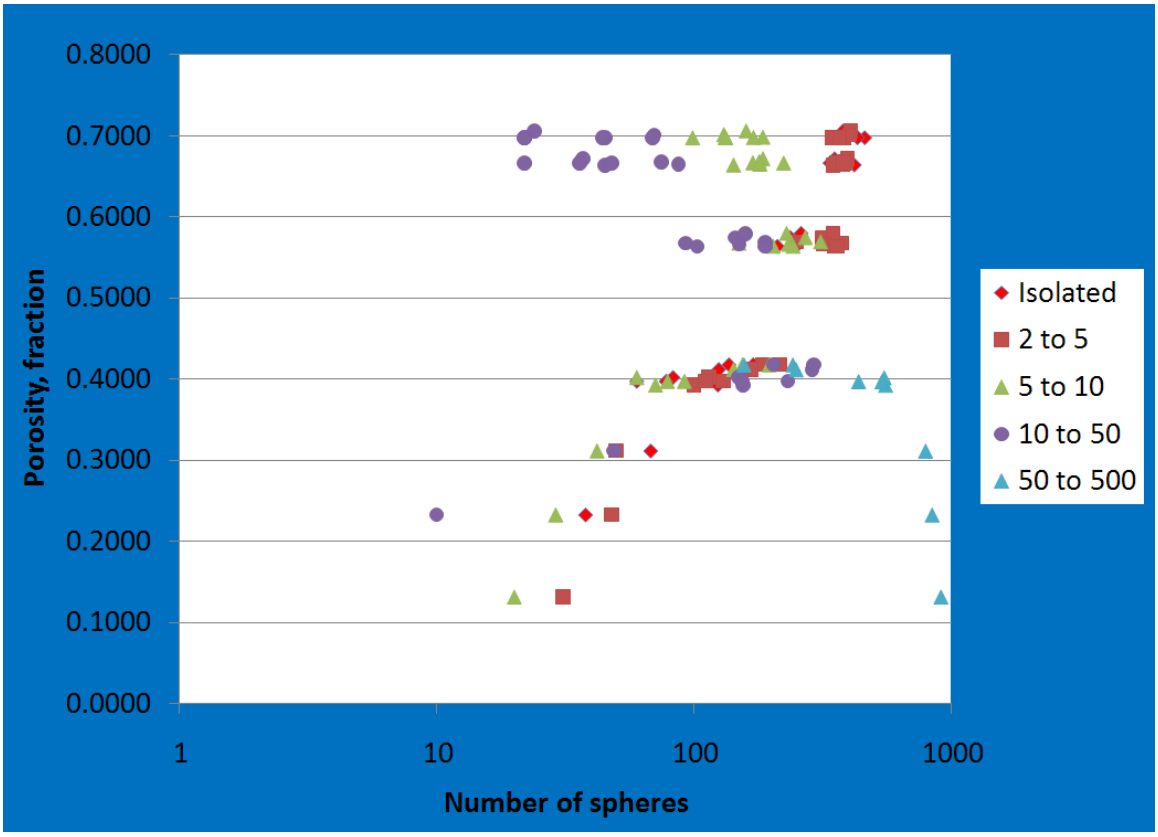

Figure 4.41: Relationship between number of spheres in cluster size and sediment porosity with 10 percent of carbonaceous material in the initial bulk volume for initial porosity of 70%.Values taken from Table 4.4, Table 4.8, Table 4.12, Table 4.16, Table 4.20, Table 4.24, Table 4.28

4.5 DISCUSSION OF CLUSTERING TRENDS

The results discussed in the previous section 4.3 have significant implications for the mudrock system. In the scenario of all the spheres to be rigid (section 4.3.1), for 5 percent of carbonaceous material by bulk volume and for 48 percent compaction, the cluster frequency distribution plot show only 31 big clusters in cluster size 5-10 and 10 to 50 as shown in Figure 4.10. However the number of spheres associated with these classes is 190 which is 20 percent of all the spheres of carbonaceous material as shown

in Figure 4.11. Similarly, for 10 percent of carbonaceous material as shown in Figure 4.13, the number of spheres associated with cluster size 5-10, 10-50 and 50-500 collectively are around 601 which is 60 percent of all the spheres of carbonaceous material.

Ductility of grains plays an important role in the connectivity of organic material in mudrocks which was studied in section 4.3.2 and 4.3.3. For 5 percent of carbonaceous material by bulk volume at last compaction stage, the total number of spheres associated with cluster sizes 5-10 and 10-50 is 361 with ductility of rigid radius ratio 0.9 R, 314 with ductility of rigid radius ratio 0.8R and 478 with ductility of rigid radius ratio 0.7R which is in a range of 30-50 % of the total carbonaceous material. For 10 percent of carbonaceous material by bulk volume at last compaction stage, the number of spheres associated with cluster size 5-10, 10-50 and 50-500 is 889 with ductility of rigid radius ratio 0.9 R, 885 with ductility of rigid radius ratio 0.8R and 936 with ductility of rigid radius ratio 0.7R which is in a range of 80-95 % of the total carbonaceous material.

Thus these results show the significant effect of burial and compaction on clustering of organic material in mudrocks which is important for evaluating the resource quality.

Chapter 5: Conclusions and Future directions

5.1 CONCLUSIONS

This study suggests a mechanism whereby small amounts of carbonaceous material can occur not as just isolated grains but as connected clusters of grains within a mudrock. This supports the hypothesis that gas production from mudrock is along the connected paths within the carbonaceous material. The study focuses on the dependence of the statistics of the clusters upon volume fraction of carbonaceous material and degree of compaction. The dependence can be useful for estimating the resource quality.

Volume fraction of carbonaceous material has a significant effect on the clustering statistics. In the model sediment, the number and size of carbonaceous clusters are small, but they increase with increase in volume fraction of carbonaceous material (Figure 3.5-3.8). The grain packing reaches to a maximum number of clusters after which two or more distinct small clusters merge to form a big cluster. This phenomenon happens at 0.20 volume fraction of carbonaceous material which only happens with cooperative rearrangement algorithm which induces clustering. The big cluster continues to grow and eventually all the spheres of the packing touch each other to form one cluster.

Degree of compaction is identified as one more important factor controlling the cluster statistics. The numbers of clusters start increasing in number and size with increase in degree of compaction (c) and at a 50% compaction stage a significantly large cluster is formed which may lead to percolation (Figure 4.1-4.12). However, there is less clustering of spheres if in initial sediment carbonaceous material is forced apart.

Ductility of grains is another important aspect of this study. With the same volume fraction of carbonaceous material, ductility enhances the connectivity of carbonaceous material in mudrocks. The connectivity of carbonaceous material with compaction increases more in scenario of both carbonaceous material and silt/clay ductile than of only carbonaceous material being ductile (Figure 4.13-4.36).

5.2 FUTURE DIRECTIONS

In general a reevaluation of the assumptions is needed in order to gain insight into the clustering mechanism. If after the revision the model succeeds, then it motivates further testing and validation through experiments.

Even if the grain packing of almost same size spheres captures the random spatial arrangements of grains in sediments, they are an oversimplification of grains naturally occurring in sediments. Therefore, these packings are not always representative of a physical system. A next step would be to study the cluster distribution of carbonaceous material with aspect ratios between the sizes of carbonaceous material and silt/clay.

In this study, grains are assumed to be spherical. It would be instructive to study the connectivity of carbonaceous material if these were angular or some random shape. This study may bring out any effect of shape on the connectivity of sediments.

A further extension of the current work can be taking the grain packing forward to commercial simulator for studying the multiphase effect on the gas permeability in mudrocks.

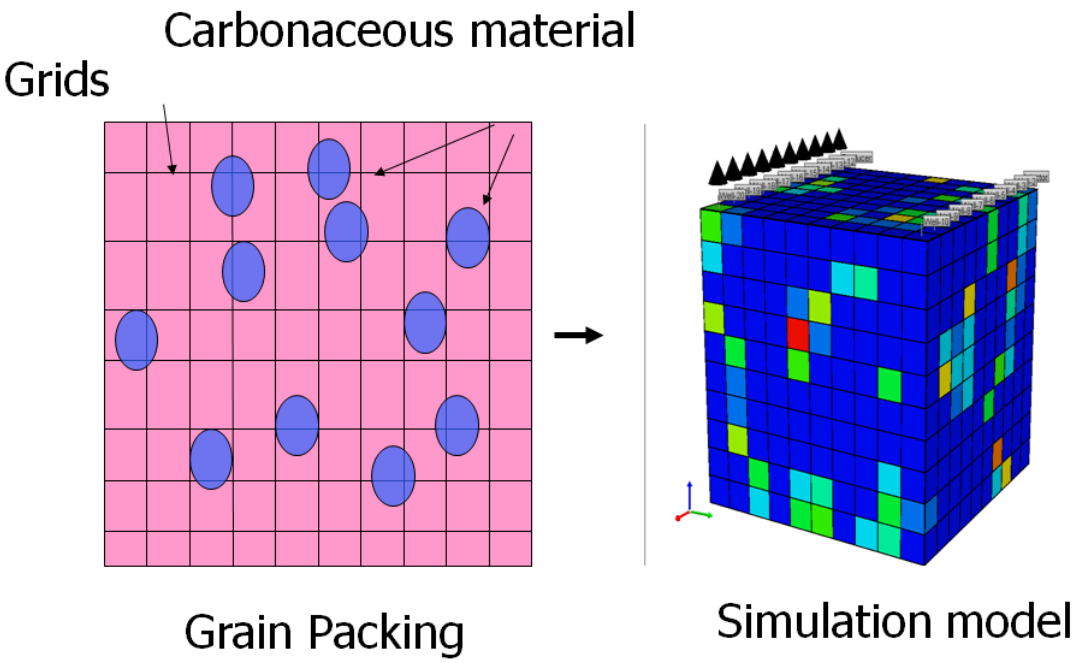

Figure 5.1: Schematic diagram showing the roadmap of taking grain packing forward to commercial simulator for studying multiphase effect on gas phase permeability in mudrocks.

Appendix

CODES

Some of the codes used in this thesis are showed in this appendix. Many of these codes refer to specific data files. Contact the author at email abhishek.kumar@mail.utexas.edu for more information.

Code for compaction with cooperative rearrangement

```
parameter (MAX =30000)
real array1(MAX,5)
real  array(MAX,5),cm(MAX),cv(MAX), newarray(MAX,5)
        real  compaction, step, grainvolume,porosity,ff,gg
integer  counter, iteration,ak,bk,sd,pin(MAX),ii,pinflag(MAX)
logical qq, ww, ee
real    xx,yy,zz,mincomp,maxrad
        integer p
real rb, rs
write(*,*)' Number of Spheres'
read(*,*)p
write(*,*)' Radius of big spheres'
read(*,*)rb
        write(*,*)' Radius of small spheres'
read(*,*)rs
        write(*,*) ' Compaction Step'
step =0.02
maxrad = 0
ductility = 0.35
open(5, file='new.txt' , status ='UNKNOWN')
        !$$$$$$ reading the input file
do i = 1,p
        read(5,*) array1(i,1:5)
if(maxrad.lt.array1(i,5)) maxrad = array1(i,5)
end do
close(5)
open(2, file='results.txt' , status ='UNKNOWN')
compaction = 1
array =0
```

```
 do i = 1,p
 array(i,1) =array1(i,1)
 array(i,2)= array1(i,2)
 array(i,3)=array1(i,3)
 array(i,4)=array1(i,4)
 array(i,5)=array1(i,5)
 enddo
 !Compaction loop
          mincomp = (2*maxrad/70)+0.01
77   compaction = compaction -step
          if (compaction.lt.mincomp) compaction = mincomp


! Initialization of the array containing spheres
  do ii = 1,p
 array(ii,2)= array(ii,2)*compaction/(compaction+step)
 enddo
          !-------------Making of Conjugates-----------------------------------------------
array(p+1:MAX,:) =0
call conjugate(p,array,mp,pin,compaction,pinflag)
          write(1,*) mp
counter = 1
iteration=0
do while(counter.gt.0 .and. iteration.lt.250)
iteration = iteration +1
write(1,*) 'Overlaps', counter
          counter =0
          write(2,*) 'Iteration', iteration
write(1,*) 'Iteration', iteration
 do  ak= 1,mp
 do bk = 1,mp
  if(ak.ne.bk)then
  d  =     ((array(ak,2)-  array(bk,2))**2  +  (array(ak,3)-  array(bk,3))**2+(array(ak,4)-
array(bk,4))**2)**0.5
  if( array(ak,5).eq.rb .and. array(bk,5) .eq. rb)then
  overlap = array(ak,5)+array(bk,5)- d
  overlap = overlap - ductility *((array(ak,5)+array(bk,5))/2)

     else
    overlap = array(ak,5)+array(bk,5)- d
     endif
             if (overlap.gt. 0.01) then
!---------------------------Removal of  overlap-----------------------------------------------
```

```
   counter = counter
   dx= abs(array(ak,2)- array(bk,2))
   dy=abs(array(ak,3)- array(bk,3))
   dz= abs(array(ak,4)- array(bk,4))
 !-----   X direction ------------------------------------------------------------------
    xx =  overlap*dx/(2*d)
    yy =  overlap*dy/(2*d)
    zz =  overlap*dz/(2*d)
    if (array(ak,2).gt.array(bk,2) )then
    array(ak,2)= array(ak,2) + xx
    array(bk,2)= array(bk,2) - xx
    else
    array(ak,2)= array(ak,2) - xx
    array(bk,2)= array(bk,2) + xx
    xx= -xx
    endif
!------  Y direction-------------------------------------------------------------------
     if (array(ak,3).gt.array(bk,3))then
     array(ak,3)= array(ak,3) + yy
     array(bk,3)= array(bk,3) - yy
       else
       array(ak,3)= array(ak,3) - yy
       array(bk,3)= array(bk,3) + yy
      yy = -yy
      endif
!--------- Z direction-------------------------------------------------------------------
       if (array(ak,4).gt.array(bk,4))then
       array(ak,4)= array(ak,4) + zz
       array(bk,4)= array(bk,4) - zz
       else
       array(ak,4)=  array(ak,4) - zz
       array(bk,4)= array(bk,4) +  zz
       zz = -zz
       endif
!-------------MOVE CONJUGATES-----------------------------------------------------------

      if ( pinflag(ak).eq.1 )   then
      array(pin(ak),2) = array(pin(ak),2)+xx ; array(pin(ak),3)=array(pin(ak),3)+yy
      array(pin(ak),4) = array(pin(ak),4) +zz
      endif
     if ( pinflag(bk).eq.1 )   then
     array(pin(bk),2) = array(pin(bk),2)-xx ; array(pin(bk),3)=array(pin(bk),3)-yy
     array(pin(bk),4) = array(pin(bk),4) -zz
```

```
endif

if ( pinflag(ak).eq.2 )   then
if(ak.le.p) then
do i = 0,2
array(pin(ak)+i,2)=array(pin(ak)+i,2)+xx
array(pin(ak)+i,3)=array(pin(ak)+i,3)+yy
array(pin(ak)+i,4) = array(pin(ak)+i,4) +zz
end do
else
array(pin(ak),2) = array(pin(ak),2)+xx ; array(pin(ak),3)=array(pin(ak),3)+yy
array(pin(ak),4) = array(pin(ak),4) +zz
do i = -2,2
if( (i.ne.0).and.(pin(ak+i).eq.pin(ak)) ) then
array(ak+i,2) = array(ak+i,2)+xx ; array(ak+i,3)=array(ak+i,3)+yy
array(ak+i,4) = array(ak+i,4) +zz
end if
end do
end if
end if
if ( pinflag(bk).eq.2 )   then
if(bk.le.p) then
do i = 0,2
array(pin(bk)+i,2)=array(pin(bk)+i,2)-xx
array(pin(bk)+i,3)=array(pin(bk)+i,3)-yy
array(pin(bk)+i,4) = array(pin(bk)+i,4) - zz
end do
 else
 array(pin(bk),2) = array(pin(bk),2)- xx ; array(pin(bk),3)=array(pin(bk),3)- yy
 array(pin(bk),4) = array(pin(bk),4) -zz
 do i = -2,2
 if( (i.ne.0).and.(pin(bk+i).eq.pin(bk)) ) then
 array(bk+i,2) = array(bk+i,2)- xx ; array(bk+i,3)=array(bk+i,3)- yy
 array(bk+i,4) = array(bk+i,4) - zz
 end if
 end do
 end if
 end if
 if ( pinflag(ak).eq.3 )   then
 if(ak.le.p) then
 do i = 0,6
 array(pin(ak)+i,2)=array(pin(ak)+i,2)+xx
 array(pin(ak)+i,3)=array(pin(ak)+i,3)+yy
```

```
array(pin(ak)+i,4) = array(pin(ak)+i,4) +zz
end do
else
array(pin(ak),2) = array(pin(ak),2)+xx ; array(pin(ak),3)=array(pin(ak),3)+yy
array(pin(ak),4) = array(pin(ak),4) +zz
do i = -6,6
if( (i.ne.0).and.(pin(ak+i).eq.pin(ak)) ) then
array(ak+i,2) = array(ak+i,2)+xx ; array(ak+i,3)=array(ak+i,3)+yy
array(ak+i,4) = array(ak+i,4) +zz
 end if
 end do
 end if
 end if
          if ( pinflag(bk).eq.3 )   then
 if(bk.le.p) then
 do i = 0,6
 array(pin(bk)+i,2)=array(pin(bk)+i,2)-xx
 array(pin(bk)+i,3)=array(pin(bk)+i,3)-yy
 array(pin(bk)+i,4) = array(pin(bk)+i,4) - zz
 end do
 else
 array(pin(bk),2) = array(pin(bk),2)- xx
 array(pin(bk),3)=array(pin(bk),3)- yy
 array(pin(bk),4) = array(pin(bk),4) -zz
  do i = -6,6
  if( (i.ne.0).and.(pin(bk+i).eq.pin(bk)) ) then
  array(bk+i,2) = array(bk+i,2)- xx ; array(bk+i,3)=array(bk+i,3)- yy
  array(bk+i,4) = array(bk+i,4) - zz
  end if
  end do
  end if
  end if


!-------------Making of Conjugates Again before finding next overlap----------------
  newarray =0
  do ii = 1,p
  qq = (array(ii,2).gt.0).and.(array(ii,2).lt.70*compaction)
  ww =  (array(ii,3).gt.0).and.(array(ii,3).lt.70)
  ee =  (array(ii,4).gt.0).and.(array(ii,4).lt.70)
  if ( (.not.qq).and.(.not.ww).and.(.not.ee) ) then
  newarray(ii,1:5) = array(pin(ii),1:5)
 else
```

```
      newarray(ii,:) = array(ii,:)
      endif
      end do
      array = newarray
      call conjugate(p,array,mp,pin,compaction,pinflag)
     endif
     endif
     end do
     end do
     write(1,*)'Number of spheres including conjugates', mp
     write(2,*) counter
     end do
!-------------------------------------------calculation for volume of overlap----------
            if (iteration .lt.250.or.counter.lt.mp*0.01) then
   write(2,*) ' Compaction Step',compaction
   do i = 1,mp
  write(2,'(2i8,5F15.4)')pinflag(i),
 pin(i),array(i,1),array(i,2),array(i,3),array(i,4),array(i,5)
 end do
 if(compaction.gt.mincomp) go to  77
 endif
 write(2,*)"Compaction not possible at the stage", compaction
 end program
!------------------------------ Subroutine of calculation of Conjugates ----------------
         subroutine conjugate(p,array,mp,pin,compaction,pinflag)
 real  array(30000,5),compaction
 integer p, mp,tk,pin(30000),pinflag(30000)
 logical  aax, aay, aaz, bbx,bby,bbz,check
 real xx,yy,zz
 pinflag =0
 mp = p
 pin =0
 do tk = 1,p
 aax=  (array(tk,2)-array(tk,5)).lt.0
 aay = (array(tk,3)-array(tk,5)).lt.0
 aaz=  (array(tk,4)-array(tk,5)).lt.0
 bbx = (array(tk,2)+array(tk,5)).gt.70*compaction
 bby = (array(tk,3)+array(tk,5)).gt.70
 bbz=  (array(tk,4)+array(tk,5)).gt.70


! Xdirection LHS
```

```
 if (aax  .and. (.not.aay).and.(.not.bby).and.(.not.bbz).and.( .not.aaz) )then
 mp = mp+1
 array(mp,1)= mp
 array(mp,2) = array(tk,2)+ 70*compaction
 array(mp,3) = array(tk,3)
 array(mp,4)=array(tk,4)
 array(mp,5)=array(tk,5)
 pin(tk)= mp
 pin(mp) = tk
 pinflag(tk)=1;pinflag(mp)=1
 endif
! Xdirection RHS
 if (bbx .and.(.not.aay).and.(.not.bby).and.(.not.aaz).and. (.not. bbz) )then
 mp = mp+1
  array(mp,1) = mp
  array(mp,2) = array(tk,2)- 70*compaction
  array(mp,3) = array(tk,3)
  array(mp,4)=array(tk,4)
  array(mp,5)=array(tk,5)
  pin(tk)=mp
  pin(mp) =tk
  pinflag(tk)=1;pinflag(mp)=1
  endif
! Y direction LHS
if (aay  .and. (.not.aax) .and.(.not.bbx).and.(.not.bbz).and. (.not.aaz) )then
 mp = mp+1
 array(mp,1)= mp
 array(mp,2) = array(tk,2)
 array(mp,3) = array(tk,3)+ 70
 array(mp,4)=array(tk,4)
 array(mp,5)=array(tk,5)
 pin(tk)=mp
 pin(mp) =tk
 pinflag(tk)=1;pinflag(mp)=1
 endif
! Y direction RHS
if (bby  .and. (.not.aax).and.(.not.bbx) .and.(.not.aaz).and.(.not. bbz))then
 mp = mp+1
 array(mp,1)= mp
 array(mp,2) = array(tk,2)
 array(mp,3) = array(tk,3)- 70
  array(mp,4)=array(tk,4)
  array(mp,5)=array(tk,5)
```

```
 pin(tk)= mp
 pin(mp)=tk
 pinflag(tk)=1;pinflag(mp)=1
 endif

! Z direction LHS
            if (aaz  .and. (.not.aax) .and.(.not.bbx).and. (.not.bby).and. (.not.aay) )then
  mp = mp+1
  array(mp,1) = mp
  array(mp,2) = array(tk,2)
  array(mp,3) = array(tk,3)
  array(mp,4)=array(tk,4)+ 70
  array(mp,5)=array(tk,5)
  pin(tk)=mp
  pin(mp)=tk
  pinflag(tk)=1;pinflag(mp)=1
  endif
! Z direction RHS
  if (bbz  .and. (.not.bbx) .and. (.not.aax).and. (.not.aay).and.(.not. bby) )then
   mp = mp+1
   array(mp,1)= mp
   array(mp,2) = array(tk,2)
   array(mp,3) = array(tk,3)
   array(mp,4)=array(tk,4)- 70
   array(mp,5)=array(tk,5)
   pin(tk)=mp
   pin(mp)=tk
   pinflag(tk)=1;pinflag(mp)=1
   endif

!-------------------------MAKING CONJUGATES FOR EDGES----------------------
          ! X direction edge1
 if (aax  .and. aay .and.(.not.bbz).and. (.not.aaz) )then
 mp = mp+1
 array(mp,:) = array(tk,:); array(mp,1) = mp
 array(mp,2) = array(mp,2)+ 70*compaction ;array(mp,3) = array(mp,3)+70
 pin(tk)= mp; pin(mp) = tk
 pinflag(tk) = 2;pinflag(mp)=2
 mp = mp +1
 array(mp,:) = array(tk,:)
 array(mp,1) = mp; array(mp,2) = array(mp,2)+ 70*compaction
 pin(mp) = tk ; pinflag(mp)=2
           mp = mp +1
```

```
array(mp,:) = array(tk,:); array(mp,1) = mp;array(mp,3) = array(mp,3)+70
pin(mp) = tk
pinflag(mp)=2
          endif
! X direction edge2
if (aax  .and. (.not.bby).and.(.not.aay) .and. aaz)then
 mp = mp+1
 array(mp,:) = array(tk,:); array(mp,1) = mp
 array(mp,2) = array(tk,2)+ 70*compaction ;array(mp,4)=array(tk,4)+70
 pin(tk)= mp ;pin(mp) = tk; pinflag(tk) = 2;pinflag(mp)=2
           mp = mp +1
array(mp,:) =array(tk,:)
array(mp,1) = mp; array(mp,2) = array(mp,2)+ 70*compaction
pin(mp) = tk ; pinflag(mp)=2
          mp = mp +1
array(mp,:) = array(tk,:); array(mp,1) = mp; array(mp,4)=array(mp,4)+70
pin(mp) = tk ; pinflag(mp)=2
endif
! Xdirection edge3
if (aax  .and. bby .and.(.not.bbz).and. (.not.aaz) )then
          mp = mp+1
array(mp,:) = array(tk,:); array(mp,1) = mp
array(mp,2) = array(tk,2)+ 70*compaction ;array(mp,3) = array(mp,3)-70
pin(tk)= mp ;pin(mp) = tk; pinflag(tk) = 2;pinflag(mp)=2
mp = mp+1
array(mp,:) = array(tk,:)
array(mp,1) = mp; array(mp,2) = array(mp,2)+ 70*compaction
pin(mp) = tk ; pinflag(mp)=2
          mp = mp+1
array(mp,:) = array(tk,:); array(mp,1) = mp; array(mp,3) = array(mp,3)-70
pin(mp) = tk ; pinflag(mp)=2
endif
! X direction edge4
          if (aax  .and. (.not.bby) .and.(.not.aay).and. bbz)then
          mp = mp+1
array(mp,:) = array(tk,:); array(mp,1) = mp
array(mp,2) = array(tk,2)+ 70*compaction; array(mp,4)=array(mp,4)-70
  pin(tk)= mp ;pin(mp) = tk; pinflag(tk) = 2;pinflag(mp)=2
  mp = mp+1
  array(mp,:) = array(tk,:)
  array(mp,1) = mp; array(mp,2) = array(mp,2)+ 70*compaction
  pin(mp) = tk ; pinflag(mp)=2
           mp = mp+1
```

```
array(mp,:) = array(tk,:); array(mp,1) = mp; array(mp,4)=array(mp,4)-70
pin(mp) = tk ; pinflag(mp)=2
endif
! X direction edge5
          if (bbx  .and. aay .and.(.not.bbz).and.(.not.aaz))then
          mp = mp+1
 array(mp,:) = array(tk,:); array(mp,1) = mp
 array(mp,2) = array(tk,2)- 70*compaction ; array(mp,3) = array(tk,3)+70
 pin(tk)= mp ;pin(mp) = tk; pinflag(tk) = 2;pinflag(mp)=2
          mp = mp+1
 array(mp,:) = array(tk,:)
 array(mp,1) = mp
 array(mp,2) = array(tk,2)- 70*compaction
 pin(mp) = tk ; pinflag(mp)=2
          mp = mp+1
 array(mp,:) = array(tk,:); array(mp,1) = mp; array(mp,3) = array(tk,3)+70
 pin(mp) = tk ; pinflag(mp)=2
 endif

     ! X direction edge6
     if (bbx  .and. (.not.aay) .and.(.not.bby).and. aaz)then
     mp = mp+1
     array(mp,:) = array(tk,:); array(mp,1) = mp
     array(mp,2) = array(tk,2)- 70*compaction ;array(mp,4)=array(tk,4)+70
     pin(tk)= mp ;pin(mp) = tk; pinflag(tk) = 2;pinflag(mp)=2
     mp = mp+1
     array(mp,:) = array(tk,:)
     array(mp,1) = mp
    array(mp,2) = array(tk,2)- 70*compaction
     pin(mp) = tk
     pinflag(mp)=2
     mp = mp+1
     array(mp,:) = array(tk,:); array(mp,1) = mp; array(mp,4)=array(tk,4)+70
     pin(mp) = tk ; pinflag(mp)=2
     endif
     ! X direction edge 7
     if (bbx  .and. bby .and. (.not.bbz).and. (.not.aaz) ) then
     mp = mp+1
     array(mp,:) = array(tk,:)
     array(mp,1) = mp
     array(mp,2) = array(tk,2)- 70*compaction
     array(mp,3) = array(tk,3)-70
     pin(tk)= mp ;pin(mp) = tk; pinflag(tk) = 2;pinflag(mp)=2
```

```
 mp = mp+1
 array(mp,:) = array(tk,:)
 array(mp,1) = mp;array(mp,2) = array(tk,2)- 70*compaction
 pin(mp) = tk ; pinflag(mp)=2
           mp = mp+1
 array(mp,:) = array(tk,:); array(mp,1) = mp;array(mp,3) = array(tk,3)-70
 pin(mp) = tk ; pinflag(mp)=2
 endif
! X direction edge8
   if (bbx  .and. (.not.aay) .and. (.not.bby).and. bbz)then

     mp = mp+1
     array(mp,:) = array(tk,:); array(mp,1) = mp
     array(mp,2) = array(tk,2)- 70*compaction ; array(mp,4)=array(tk,4)-70
     pin(tk)= mp ;pin(mp) = tk; pinflag(tk) = 2;pinflag(mp)=2

     mp = mp+1
     array(mp,:) = array(tk,:); array(mp,1) = mp;array(mp,2) = array(tk,2)- 70*compaction
     pin(mp) = tk ; pinflag(mp)=2

     mp = mp+1
     array(mp,:) = array(tk,:); array(mp,1) = mp;array(mp,4)=array(tk,4)-70
     pin(mp) = tk ; pinflag(mp)=2
     !write(1,*) '14'
   endif


! X direction edge9
   if ((.not.aax).and.(.not.bbx)  .and. aay .and.aaz)then


     mp = mp+1
     array(mp,:) = array(tk,:); array(mp,1) = mp
     array(mp,3) = array(mp,3) +70; array(mp,4) = array(mp,4)+70
     pin(tk)= mp ;pin(mp) = tk; pinflag(tk) = 2;pinflag(mp)=2

     mp = mp+1
     array(mp,:) = array(tk,:); array(mp,1) = mp; array(mp,3) = array(mp,3) +70
     pin(mp) = tk ; pinflag(mp)=2

     mp = mp+1
     array(mp,:) = array(tk,:); array(mp,1) = mp;array(mp,4) = array(mp,4)+70
```

```
    pin(mp) = tk ; pinflag(mp)=2

    !write(1,*) '15'
   endif


! X direction edge 10
   if ((.not.aax).and.(.not.bbx).and.aay .and. bbz)then

    mp = mp+1
    array(mp,:) = array(tk,:); array(mp,1) = mp
    array(mp,3) = array(mp,3) +70; array(mp,4) = array(mp,4)-70
    pin(tk)= mp ;pin(mp) = tk; pinflag(tk) = 2;pinflag(mp)=2

    mp = mp+1
    array(mp,:) = array(tk,:); array(mp,1) = mp; array(mp,3) = array(mp,3) +70
    pin(mp) = tk ; pinflag(mp)=2

    mp = mp+1
    array(mp,:) = array(tk,:); array(mp,1) = mp;array(mp,4) = array(mp,4)-70
    pin(mp) = tk ; pinflag(mp)=2
    !write(1,*) '16'
   endif


! X direction edge 11
   if ((.not.aax).and.(.not.bbx).and. bby .and.aaz)then
    mp = mp+1
    array(mp,:) = array(tk,:); array(mp,1) = mp
    array(mp,3) = array(mp,3) -70; array(mp,4) = array(mp,4)+70
    pin(tk)= mp ;pin(mp) = tk; pinflag(tk) = 2;pinflag(mp)=2

    mp = mp+1
    array(mp,:) = array(tk,:); array(mp,1) = mp; array(mp,3) = array(mp,3) -70
    pin(mp) = tk ; pinflag(mp)=2

    mp = mp+1
    array(mp,:) = array(tk,:); array(mp,1) = mp;array(mp,4) = array(mp,4)+70
    pin(mp) = tk ; pinflag(mp)=2
    !write(1,*) '17'
   endif
```

```
! X direction edge 12
  if ((.not.aax).and.(.not.bbx)  .and. bby.and.bbz)then
    mp = mp+1
    array(mp,:) = array(tk,:); array(mp,1) = mp
    array(mp,3) = array(mp,3) -70; array(mp,4) = array(mp,4)-70
    pin(tk)= mp ;pin(mp) = tk; pinflag(tk) = 2;pinflag(mp)=2

    mp = mp+1
    array(mp,:) = array(tk,:); array(mp,1) = mp; array(mp,3) = array(mp,3) -70
    pin(mp) = tk ; pinflag(mp)=2

    mp = mp+1
    array(mp,:) = array(tk,:); array(mp,1) = mp;array(mp,4) = array(mp,4)-70
    pin(mp) = tk ; pinflag(mp)=2
    !write(1,*) '18'
  endif

!--------------------------------MAKING CONGUGATES FOR CORNER SPHERES--------
--------------
   if (aax  .and. aay .and. aaz) then
     xx = 70*compaction; yy = 70 ; zz = 70
   endif

   if (aax  .and. aay .and. bbz)then
    xx = 70*compaction; yy = 70 ; zz = -70
   endif

   if (aax  .and. bby .and. aaz)then
   xx = 70*compaction; yy = -70 ; zz = 70
   endif

   if (aax  .and. bby .and. bbz)then
    xx = 70*compaction; yy = -70 ; zz = -70
   endif

   if (bbx  .and. aay .and. aaz)then
    xx = -70*compaction; yy = 70 ; zz = 70
   endif

   if (bbx  .and. aay .and. bbz)then
    xx = -70*compaction; yy = 70 ; zz = -70
   endif
```

```
 if (bbx  .and. bby .and. aaz)then
 xx = -70*compaction; yy = -70 ; zz = 70
 endif

 if (bbx  .and. bby .and. bbz)then
 xx = -70*compaction; yy = -70 ; zz =- 70
 endif

check =  (aax  .and. aay .and. aaz).or.(aax  .and. aay .and. bbz).or.  &
(aax  .and. bby .and. aaz).or.(aax  .and. bby .and. bbz).or.  &
(bbx  .and. aay .and. aaz).or.(bbx  .and. aay .and. bbz).or.  &
(bbx  .and. bby .and. aaz).or.(bbx  .and. bby .and. bbz)

if(check) then
mp = mp+1
array(mp,:) = array(tk,:)
array(mp,1) = mp
array(mp,2) = array(mp,2)+xx
array(mp,3)= array(mp,3)+yy
array(mp,4)= array(mp,4)+zz
pin(tk)= mp ;pin(mp) = tk
pinflag(tk) = 3
pinflag(mp)=3

mp = mp+1
array(mp,:) = array(tk,:); array(mp,1) = mp
array(mp,2) = array(mp,2)+xx
array(mp,3)= array(mp,3)
array(mp,4)= array(mp,4)
pin(mp) = tk
pinflag(mp)=3

mp = mp+1
array(mp,:) = array(tk,:); array(mp,1) = mp
array(mp,2) = array(mp,2)+xx
array(mp,3)= array(mp,3)+yy
array(mp,4)= array(mp,4)
pin(mp) = tk; pinflag(mp)=3

mp = mp+1
array(mp,:) = array(tk,:)
array(mp,1) = mp
array(mp,2) = array(mp,2)+xx
```

```
 array(mp,3)= array(mp,3)
 array(mp,4)= array(mp,4)+zz
 pin(mp) = tk; pinflag(mp)=3

 mp = mp+1
 array(mp,:) = array(tk,:)
array(mp,1) = mp
array(mp,2) = array(mp,2)
array(mp,3)= array(mp,3)+yy
array(mp,4)= array(mp,4)
pin(mp) = tk; pinflag(mp)=3

mp = mp+1
array(mp,:) = array(tk,:)
array(mp,1) = mp
array(mp,2) = array(mp,2)
array(mp,3)= array(mp,3)+yy
array(mp,4)= array(mp,4)+zz
pin(mp) = tk; pinflag(mp)=3

mp = mp+1
array(mp,:) = array(tk,:); array(mp,1) = mp
array(mp,2) = array(mp,2)
array(mp,3)= array(mp,3)
array(mp,4)= array(mp,4)+zz
          pin(mp) = tk; pinflag(mp)=3
          endif


          end do
end
```

Code for volume conservation "spheregrowth.m"

```
new;
Vold=0;
disp('Total number of spheres')
P = input('prompt') ;
for i = 1:P
    for j = i+1:P

    x1 = M(i,4);
    y1= M(i,5);
    z1= M(i,6);
    r1 = M(i,7);

    x2 = M(j,4);
    y2= M(j,5);
    z2= M(j,6);
    r2 = M(j,7);

    if r1 >r2
        R=r1;
        r=r2;
    else
        R=r2;
        r=r1;
    end


    d = (( x2-x1)^2+ (y2-y1)^2+ (z2-z1)^2)^0.5;
    if d < R+r+0.1
    a = (( 4*d^2*R^2 -(d^2-r^2+R^2)^2)^0.5)/(2*d);
    V= 3.14*(R+r-d)^2*(d^2+2*d*r-3*r^2+2*d*R+6*r*R-3*R^2)/(12*d);
    r1new = (r1^3+(3*V/8*3.14))^0.33;
    r2new= (r2^3+(3*V/8*3.14))^0.33;
    %M(i,7)=r1new;
    %M(j,7)=r2new;
    Vold=Vold+V;
    end

    end
end
Vold

for i = 1:P
rnew = ( M(i,7)^3+(Vold*3)/(P*4*3.14))^0.3333;
N(i)= rnew;
end
NN= N';
```

Code for cluster ID for two component packing "connectivity_bidispersed.m"

```
new;
disp('Number of real spheres')
P = input('prompt') ;
for x = 1: size(M,1)
    ID(x) = 0;
end
tol =0.001*M(1,7);
m = 1;
for i = 1:size(M,1)
    tt(i,1)= M(i,2);
    tt(i,2) = M(i,3);
end
%for i = 1:P
 %   M(i,2)=i;

%end

for i = 1:size(M,1)
      M(i,3)=i;
end
for i = P+1:size(M,1)
    for j = 1:P
        %tt(i,1)

        %tt(j,1)

    if( tt(i,1) == tt(j,2))
        disp('abhi')
         M(i,2)=j;
    end
    end
end


for i = 1:P
    M(i,2)= i;
end




for i = 1:size(M,1)
    for j = i+1:size(M,1)
```

```
        if ((M(i,4)-M(j,4))^2+(M(i,5)-M(j,5))^2+(M(i,6)-
M(j,6))^2)^0.5<= (M(i,7)+M(j,7)+tol)

            if ((ID(i) ==0) && (ID(j)==0))

                ID(i) = m;
                m = m+1;


            end



            if ((ID(i)~=0)&&(ID(j)==0))

                ID(j) = ID(i);

            elseif ((ID(j)~=0) && (ID(i)==0))

                ID(i) = ID(j);

            elseif ((ID(i)~=0) && (ID(j)~=0))

                count_merged = 0;

                merging_cluster_id = ID(j);

                for k = 1:size(M,1)

                    if ID(k) == merging_cluster_id

                        ID(k) = ID(i);
                        count_merged = count_merged + 1;

                    end

                end

            end


        end

    end

end
```

```
%loop to identify the conjugate sphere and assign it in the group the
same ID

for i = P+1:size(M,1)
    if ID(i)==0

        continue
    else

        if ID(i)~=ID(M(i,2))

            if ID(M(i,2))==0

                ID(M(i,2)) = ID(i);

            else

                check = ID(i);
                for j = 1: size(M,1)
                    if ID(j)==check
                        ID(j) = ID(M(i,2));
                    else
                        continue
                    end
                end

            end

        else

            continue

        end

    end

end
for i = 1:P
    final(i,1) = ID(i);
    final(i,2)=  M(i,1);
    final(i,3) = M(i,2);
    final(i,4)=  M(i,3);
    final(i,5)=  M(i,4);
    final(i,6)=  M(i,5);
    final(i,7)=  M(i,6);
    final(i,8)=  M(i,7);


end
```

```
for i = 1:size(M,1)
    finalt(i,1) = ID(i);
    finalt(i,2)=  M(i,1);
    finalt(i,3) = M(i,2);
    finalt(i,4)=  M(i,3);
    finalt(i,5)=  M(i,4);
    finalt(i,6)=  M(i,5);
    finalt(i,7)=  M(i,6);
    finalt(i,8)=  M(i,7);
end
 AK = unique(final(:,1));
 kk = transpose(ID);
```

Code for geometrical transformation of cluster length “think4rev.m”

```
new;

P = size(M,1);

r = M(1,5);

tol = 0.001*M(1,5);

for i = 1: P

 %the first 9

   x(i)= M(i,2)- 70;
   y(i)= M(i,3)-70;
   z(i)= M(i,4)-70;


   x(i+P)= M(i,2)- 70;
   y(i+P)= M(i,3)-70;
   z(i+P)= M(i,4);

   x(i+(2*P))= M(i,2)- 70;
   y(i+(2*P))= M(i,3)-70;
   z(i+(2*P))= M(i,4)+70;


   x(i+(3*P))= M(i,2)- 70;
   y(i+(3*P))= M(i,3);
   z(i+(3*P))= M(i,4)-70;

   x(i+(4*P))= M(i,2)- 70;
   y(i+(4*P))= M(i,3);
   z(i+(4*P))= M(i,4);

   x(i+(5*P))= M(i,2)- 70;
   y(i+(5*P))= M(i,3);
   z(i+(5*P))= M(i,4)+70;

   x(i+(6*P))= M(i,2)- 70;
   y(i+(6*P))= M(i,3)+70;
   z(i+(6*P))= M(i,4)-70;


   x(i+(7*P))= M(i,2)- 70;
   y(i+(7*P))= M(i,3)+70;
```

```
    z(i+(7*P))= M(i,4);



    x(i+(8*P))= M(i,2)- 70;
    y(i+(8*P))= M(i,3)+70;
    z(i+(8*P))= M(i,4)+70;


    %%%The second 9

     x(i+(9*P))=M(i,2);
     y(i+(9*P))=M(i,3)-70;
     z(i+(9*P))=M(i,4)-70;

     x(i+(10*P))=M(i,2);
     y(i+(10*P))=M(i,3)-70;
     z(i+(10*P))=M(i,4);

     x(i+(11*P))=M(i,2);
     y(i+(11*P))=M(i,3)-70;
     z(i+(11*P))=M(i,4)+70;

     x(i+(12*P))=M(i,2);
     y(i+(12*P))=M(i,3);
     z(i+(12*P))=M(i,4)-70;

     x(i+(13*P))=M(i,2);
     y(i+(13*P))=M(i,3);
     z(i+(13*P))=M(i,4);

     x(i+(14*P))=M(i,2);
     y(i+(14*P))=M(i,3);
     z(i+(14*P))=M(i,4)+70;

     x(i+(15*P))=M(i,2);
     y(i+(15*P))=M(i,3)+70;
     z(i+(15*P))=M(i,4)-70;

     x(i+(16*P))=M(i,2);
     y(i+(16*P))=M(i,3)+70;
     z(i+(16*P))=M(i,4);

     x(i+(17*P))=M(i,2);
     y(i+(17*P))=M(i,3)+70;
     z(i+(17*P))=M(i,4)+70;


%The third 9
```

```
    x(i+(18*P))=M(i,2)+70;
    y(i+(18*P))=M(i,3)-70;
    z(i+(18*P))=M(i,4)-70;

    x(i+(19*P))=M(i,2)+70;
    y(i+(19*P))=M(i,3)-70;
    z(i+(19*P))=M(i,4);

    x(i+(20*P))=M(i,2)+70;
    y(i+(20*P))=M(i,3)-70;
    z(i+(20*P))=M(i,4)+70;

    x(i+(21*P))=M(i,2)+70;
    y(i+(21*P))=M(i,3);
    z(i+(21*P))=M(i,4)-70;

    x(i+(22*P))=M(i,2)+70;
    y(i+(22*P))=M(i,3);
    z(i+(22*P))=M(i,4);

    x(i+(23*P))=M(i,2)+70;
    y(i+(23*P))=M(i,3);
    z(i+(23*P))=M(i,4)+70;

    x(i+(24*P))=M(i,2)+70;
    y(i+(24*P))=M(i,3)+70;
    z(i+(24*P))=M(i,4)-70;

    x(i+(25*P))=M(i,2)+70;
    y(i+(25*P))=M(i,3)+70;
    z(i+(25*P))=M(i,4);

    x(i+(26*P))=M(i,2)+70;
    y(i+(26*P))=M(i,3)+70;
    z(i+(26*P))=M(i,4)+70;

end


   for i=1:27*P
       r(i)=M(1,5);
   end


   for i = 1:27*P
    if(mod(i,P)==0)
        PIN(i)=P;
    else
    PIN(i)=mod(i,P);
```

```
    end
   end

  for i = 1:27*P
       info(i,1)= i;
       info(i,2)= PIN(i);
       info(i,3)=x(i);
       info(i,4)=y(i);
       info(i,5)=z(i);
       info(i,6)= r(i);

end


   for x = 1:27*P
    IDNP(x) = 0;
end

m = 1;

for i = 1:27*P
    for j = i+1:27*P

        if ((info(i,3)-info(j,3))^2+(info(i,4)-info(j,4))^2+(info(i,5)-
info(j,5))^2)^0.5<= (2*(r+tol))

            if ((IDNP(i) ==0) & (IDNP(j)==0))

                IDNP(i) = m;
                m = m+1;


            end



            if ((IDNP(i)~=0)&(IDNP(j)==0))

                IDNP(j) = IDNP(i);

            elseif ((IDNP(j)~=0) & (IDNP(i)==0))

                IDNP(i) = IDNP(j);

            elseif ((IDNP(i)~=0) & (IDNP(j)~=0))

                count_merged = 0;

                merging_cluster_id = IDNP(j);
```

```
                for k = 1:27*P

                    if IDNP(k) == merging_cluster_id

                        IDNP(k) = IDNP(i);
                        count_merged = count_merged + 1;

                    end

                end

            end


        end

    end

end

for i = 1:P
    data(i,1)= info(13*P+i,1);
    data(i,2)= info(13*P+i,2);
    data(i,3)=info(13*P+i,3);
    data(i,4)=info(13*P+i,4);
    data(i,5)= info(13*P+i,5);
    data(i,6)= IDNP(13*P+i);
end

for i = 1:P
    ID14(i)= IDNP(13*P+i);
end

AB = unique(ID14);
BC = size(unique(ID14));
CD = BC(2);
m1 = 1;

for i = 2:CD
    for j = 1:27*P
    if AB(i) == IDNP(j)
        set(m1,1) = info(j,2);
        set(m1,2)= info(j,3);
        set(m1,3)= info(j,4);
        set(m1,4)= info(j,5);
        set(m1,5)= IDNP(j);
        m1 = m1+1;
    else
```

```
    end
    end
end

IID =[];
no = 1;

    az1 = set(:,5);
    bz1 = unique(az1);
    cz1 = size(bz1);
    dz1 = cz1(1);

    ez1 = size(set);
    fz1 = ez1(1);

    for i = 1:dz1
        m = 1;
        for j = 1:fz1
            if set(j,5)==bz1(i)

               Pc(m)= set(j,2);
               m=m+1;
            else
                continue
            end
        end

        ay= size(Pc);
        by= ay(1);
        cy = unique(Pc);
        dy = size(cy);
        ey = dy(1);
        if by ~= ey
            IID(no)= bz1(i);
            no = no+1;
        else
        end
    end

    at = size(IID);
    bt=  at(1);
    ct = size(set);
    dt = ct(1);

    if IID ~= []
        for i = 1:bt
            for j = 1:dt
                if IID(i)==set(j,5)
                    set(j:2)=[];
                end
            end
```

```
        end
    end

        KA  = size(set);
   AK = KA(1);



sset(1,:)=set(1,:);
l=1; check=0;
for i =2:1:AK
    for k= 1:1:l
    if set(i,1)== sset(k,1)
        check=1;
    end
    end
    if check==0
        l=l+1;
        sset(l,:)=set(i,:);
    end
    check=0;
end



    az = sset(:,5);
    bz = unique(az);
    cz = size(bz);
    dz = cz(1);

    ez = size(sset);
    fz = ez(1);

    for i = 1:dz
        m = 1;
        for j = 1:fz
            if sset(j,5)==bz(i)
                xc(m) = sset(j,2);
                yc(m) = sset(j,3);
                zc(m) = sset(j,4);
                m = m+1;

            else
                continue
            end
        end
        lc(i,1) = bz(i);
        lc(i,2) = max(xc)-min(xc);
        lc(i,3) = max(yc)-min(yc);
        lc(i,4) = max(zc)-min(zc);
        xc = [];
```

```
        yc = [];
        zc = [];
    end


  for i = 1:dz
        m= 1;
        for j = 1:fz



            if  sset(j,5)== bz(i)
                a_x(m)= sset(j,2);
                a_y(m)= sset(j,3);
                a_z(m)=sset(j,4);
                m=m+1;
            else
                continue
            end
        end



             dmax = 0 ;
             for k = 1:m-1
                 for j = k+1:m-1


                     d = ( (a_x(k) - a_x(j))^2 + (a_y(k)- a_y(j))^2 +
(a_z(k)-a_z(j))^2)^0.5;
                     if d >dmax
                         dmax= d;
                         x1 = a_x(k);
                         y1 = a_y(k);
                         z1 = a_z(k);
                         x2 = a_x(j);
                         y2 = a_y(j);
                         z2 = a_z(j);
                         a_p = x2-x1;
                         b_p = y2-y1;
                         c_p = z2-z1;

                     end
                 end
             end


            for c = 1:m-1
                x_1 = a_x(c)- x1;
                y_1 = a_y(c)- y1;
```

```
                z_1 = a_z(c)- z1;
                theta = atan(a_p/b_p);

                x_2 = x_1*cos(theta)-y_1*sin(theta);
                    y_2 = x_1*sin(theta)+y_1*cos(theta);
                    z_2 = z_1;

                    b_p2 = a_p*sin(theta)+b_p*cos(theta);
                    c_p2 = c_p;

                    beta = atan(b_p2/c_p2);



                x_3 = x_2;
                y_3 = y_2 *cos(beta)-z_2*sin(beta);
                z_3 = y_2 *sin(beta)+ z_2*cos(beta);


                akx(c)= x_3;
                aky(c)= y_3;
                akz(c)= z_3;

            end
            ang(1) = 0;

            for lj = 2:18
                ang(lj)= ang(lj-1)+10;
            end

            for lk = 1:18
                for kk = 1:m-1




                    x_4(kk) = akx(kk)*cos(ang(lk)*pi()/180) -
aky(kk)*sin(ang(lk)*pi()/180);
                    y_4(kk) = akx(kk)*sin(ang(lk)*pi()/180) +
aky(kk)*cos(ang(lk)*pi()/180);
                    z_4(kk) = akz(kk);

                end

                lx(lk,i)= max(x_4)- min(x_4);
                ly(lk,i)= max(y_4)- min(y_4);
                lz(lk,i) = max(z_4)- min(z_4);
                %disp( lx(lk));
```

```
        end


            lx_mx(i) = max(lx(:,i));
            lx_mn(i) = min(lx(:,i));
            ly_mx(i)=  max(ly(:,i));
            ly_mn(i)=  min(ly(:,i));
            lz_mx(i)=  dmax  ;
            lz_mn(i)=  dmax ;

           %  lx =[]; use it as protection whenever i want.
            % ly= [];
            % lz =[];
            akx= [];
            aky= [];
            akz = [];
            a_x = [];
            a_y = [];
            a_z= [];
            x_4 = [];
            y_4 = [];
            z_4 = [];

end

lengthxmax = transpose(lx_mx);
lengthxmin = transpose(lx_mn);
lengthymax = transpose(ly_mx);
lengthymin = transpose(ly_mn);
lengthzmax = transpose(lz_mx);
lengthzmin = transpose(lz_mn);
```

Example1

ALL GRAINS ARE RIGID – ONE COMPONENT SPHERE PACKING

Example One component packing 100 spheres, initial solid volume fraction 0.10

Step-1

Input as 'new.txt' in the format

1	64.3152	61.1154	16.5717	4.42066
2	5.12127	65.5449	6.56328	4.42066
3	41.7998	14.2885	54.3993	4.42066
4	42.9682	46.3281	62.8295	4.42066
5	68.1881	18.9823	45.9197	4.42066
6	27.4172	15.1841	21.8533	4.42066
7	5.39529	43.063	33.9452	4.42066
8	66.4971	28.8453	48.3717	4.42066
9	20.8603	63.5977	17.9447	4.42066
10	61.1153	23.6796	32.4177	4.42066
11	38.4182	18.307	12.8857	4.42066
12	63.3086	4.953	43.5418	4.42066
13	24.3458	17.7904	64.8494	4.42066
14	32.9137	16.1907	63.3661	4.42066
15	58.8082	27.1795	40.2021	4.42066
16	55.3443	17.0602	46.5662	4.42066
17	12.0036	63.7222	28.135	4.42066
18	18.0623	62.0612	34.7786	4.42066
19	8.90147	47.1308	67.3395	4.42066
20	53.6698	40.3002	68.0009	4.42066
21	58.0985	63.0142	60.349	4.42066
22	9.65243	53.5514	59.2295	4.42066
23	9.5111	28.3269	54.5062	4.42066
24	45.7866	30.2432	0.77409	4.42066
25	23.679	26.3789	60.1616	4.42066
26	20.9009	24.7888	29.765	4.42066
27	2.69366	28.1429	36.3308	4.42066
28	68.5528	34.3397	63.817	4.42066
29	27.4188	54.7597	7.63641	4.42066
30	38.3611	66.822	36.1583	4.42066
31	24.3677	22.6555	43.4505	4.42066
32	52.0507	44.5058	56.6997	4.42066
33	3.89714	45.7972	51.1726	4.42066

34	1.14048	9.80115	55.5389	4.42066
35	38.2726	22.2805	59.8495	4.42066
36	57.1312	55.0728	22.9506	4.42066
37	42.3264	32.3924	49.846	4.42066
38	27.3877	17.4786	56.1209	4.42066
39	35.3696	27.7489	52.7113	4.42066
40	4.33824	38.1008	26.7045	4.42066
41	14.8969	7.38921	32.0145	4.42066
42	17.1904	17.5534	19.8834	4.42066
43	39.4456	9.96123	21.4988	4.42066
44	64.3893	44.3794	39.9179	4.42066
45	5.37651	21.393	41.3717	4.42066
46	38.7906	27.6783	14.5531	4.42066
47	57.2995	67.894	26.7476	4.42066
48	34.7183	53.9304	67.5735	4.42066
49	60.6679	31.1901	66.2822	4.42066
50	49.3796	15.7616	64.4784	4.42066
51	26.095	14.1431	45.1012	4.42066
52	60.4493	14.7371	54.0706	4.42066
53	36.049	25.6279	27.9126	4.42066
54	53.7238	42.472	12.6156	4.42066
55	38.8643	39.3716	32.9501	4.42066
56	23.147	32.3416	52.3507	4.42066
57	64.5879	49.5271	25.7237	4.42066
58	65.2887	20.2022	62.7928	4.42066
59	36.049	37.4574	41.1759	4.42066
60	52.2754	25.3047	22.1158	4.42066
61	50.2761	49.4942	23.1866	4.42066
62	20.7255	34.0634	2.81624	4.42066
63	5.90911	38.9795	65.4063	4.42066
64	0.41612	49.4626	43.9189	4.42066
65	28.3427	0.70533	39.418	4.42066
66	20.6719	32.1862	43.8644	4.42066
67	69.749	15.8771	13.7157	4.42066
68	41.0172	37.7721	0.39839	4.42066
69	16.3468	23.08	56.484	4.42066
70	58.9129	60.0086	30.4063	4.42066
71	29.6047	24.879	21.7047	4.42066
72	3.69457	66.6863	25.9177	4.42066
73	67.3916	65.3356	55.6687	4.42066
74	28.1137	29.9743	5.57866	4.42066
75	46.4193	19.1253	9.214	4.42066
76	54.9332	9.66853	39.4852	4.42066

77	33.1813	25.8385	39.1472	4.42066
78	16.4429	0.20532	14.0724	4.42066
79	24.9399	37.9338	9.55629	4.42066
80	35.3873	32.0887	60.4142	4.42066
81	28.6679	45.1392	48.9426	4.42066
82	5.45088	54.3286	13.5096	4.42066
83	3.4303	22.8294	69.0104	4.42066
84	33.1901	40.718	59	4.42066
85	64.3341	28.3039	17.4674	4.42066
86	26.868	34.6253	60.0389	4.42066
87	66.6422	66.2169	8.97621	4.42066
88	29.3707	67.8059	62.7894	4.42066
89	43.0755	41.8129	44.3109	4.42066
90	26.0606	57.7624	30.0357	4.42066
91	10.5918	29.0461	17.8544	4.42066
92	68.8917	7.66753	37.2466	4.42066
93	35.7184	57.1503	5.74664	4.42066
94	18.4495	62.2288	43.6099	4.42066
95	58.2147	51.716 4	9.6046	4.42066
96	48.9608	42.4549	5.16691	4.42066
97	15.6215	50.6625	1.87134	4.42066
98	36.9951	29.9441	69.5535	4.42066
99	59.9446	17.5321	21.3205	4.42066
100	24.6784	60.0419	49.4909	4.42066

Step-2
Enter number of spheres 100
Enter compaction step 0.02
Enter ductility 0

Step-3
Output file with successful compaction stage will be displayed like

Iteration 1
38
Iteration 2
14
Iteration 3
4
Iteration 4
3
Iteration 5
0

Compaction Step 0.980000

0	0	1.0000	63.0289	61.1154	16.5717	4.4207
0	0	2.0000	5.0966	65.5386	6.5407	4.4207
0	0	3.0000	40.9638	14.2885	54.3993	4.4207
0	0	4.0000	42.1088	46.3281	62.8295	4.4207
1	101	5.0000	66.7764	18.9659	45.9506	4.4207
0	0	6.0000	26.8689	15.1841	21.8533	4.4207
0	0	7.0000	5.2874	43.0630	33.9452	4.4207
1	102	8.0000	65.1672	28.8453	48.3717	4.4207
0	0	9.0000	20.4539	63.5812	17.9543	4.4207
0	0	10.0000	59.8945	23.6772	32.4124	4.4207
0	0	11.0000	37.5847	18.3002	12.9162	4.4207
0	0	12.0000	62.0206	4.9422	43.5669	4.4207
0	0	13.0000	23.7653	17.8083	64.8659	4.4207
0	0	14.0000	32.3172	16.1353	63.3711	4.4207
0	0	15.0000	57.6305	27.1819	40.2074	4.4207
0	0	16.0000	54.2374	17.0602	46.5662	4.4207
0	0	17.0000	11.7635	63.7222	28.1350	4.4207
0	0	18.0000	17.7004	62.0609	34.7633	4.4207
1	103	19.0000	8.6902	47.1607	67.3163	4.4207
1	104	20.0000	52.6123	40.2928	67.9764	4.4207
0	0	21.0000	56.9365	63.0142	60.3490	4.4207
0	0	22.0000	9.4594	53.5514	59.2295	4.4207
0	0	23.0000	9.2622	28.3731	54.4889	4.4207
1	105	24.0000	44.9374	30.2455	0.7835	4.4207
0	0	25.0000	23.2625	26.3535	60.2039	4.4207
0	0	26.0000	20.4829	24.7888	29.7650	4.4207
1	106	27.0000	2.6350	28.1551	36.3217	4.4207
1	107	28.0000	67.1791	34.3105	63.7532	4.4207
0	0	29.0000	26.7976	54.7383	7.6533	4.4207
1	108	30.0000	37.5939	66.8220	36.1583	4.4207
0	0	31.0000	23.8803	22.6555	43.4505	4.4207
0	0	32.0000	51.0097	44.5058	56.6997	4.4207
1	109	33.0000	3.8277	45.7880	51.1908	4.4207
1	110	34.0000	1.1177	9.8012	55.5389	4.4207
0	0	35.0000	37.5389	22.3180	59.8280	4.4207
0	0	36.0000	56.0293	55.1066	22.9492	4.4207
0	0	37.0000	41.5224	32.4214	49.8281	4.4207
0	0	38.0000	26.8399	17.4786	56.1209	4.4207
0	0	39.0000	34.6196	27.7199	52.7292	4.4207
1	111	40.0000	4.2515	38.1008	26.7045	4.4207
0	0	41.0000	14.5990	7.3892	32.0145	4.4207
0	0	42.0000	16.8466	17.5534	19.8834	4.4207

0	0	43.0000	38.6567	9.9612	21.4988	4.4207
0	0	44.0000	63.0722	44.3541	39.8981	4.4207
0	0	45.0000	5.3217	21.3972	41.3499	4.4207
0	0	46.0000	38.0148	27.6783	14.5531	4.4207
1	112	47.0000	56.1535	67.8940	26.7476	4.4207
1	113	48.0000	34.0239	53.9304	67.5735	4.4207
1	114	49.0000	59.3391	31.1432	66.3194	4.4207
0	0	50.0000	48.3920	15.7616	64.4784	4.4207
0	0	51.0000	25.5731	14.1431	45.1012	4.4207
0	0	52.0000	59.2403	14.7371	54.0706	4.4207
0	0	53.0000	35.3280	25.6279	27.9126	4.4207
0	0	54.0000	52.6661	42.4721	12.6424	4.4207
0	0	55.0000	38.0870	39.3716	32.9501	4.4207
0	0	56.0000	22.6755	32.3327	52.3404	4.4207
0	0	57.0000	63.2961	49.5271	25.7237	4.4207
0	0	58.0000	63.9829	20.2022	62.7928	4.4207
0	0	59.0000	35.2842	37.4297	41.1559	4.4207
0	0	60.0000	51.2299	25.3047	22.1158	4.4207
0	0	61.0000	49.2299	49.4604	23.1880	4.4207
1	115	62.0000	20.2729	34.0768	2.7950	4.4207
0	0	63.0000	5.8887	38.9971	65.4193	4.4207
1	116	64.0000	0.4286	49.4971	43.9205	4.4207
1	117	65.0000	27.7758	0.7053	39.4180	4.4207
0	0	66.0000	20.2527	32.1858	43.8442	4.4207
1	118	67.0000	68.3540	15.8771	13.7157	4.4207
1	119	68.0000	40.1969	37.7721	0.3984	4.4207
0	0	69.0000	15.9984	22.9965	56.4602	4.4207
0	0	70.0000	57.7346	60.0086	30.4063	4.4207
0	0	71.0000	29.0126	24.8790	21.7047	4.4207
2	120	72.0000	3.6207	66.6863	25.9177	4.4207
1	123	73.0000	66.0438	65.3356	55.6687	4.4207
0	0	74.0000	27.5841	29.9558	5.5911	4.4207
0	0	75.0000	45.5561	19.1321	9.1835	4.4207
0	0	76.0000	53.8345	9.6685	39.4852	4.4207
0	0	77.0000	32.5177	25.8385	39.1472	4.4207
1	124	78.0000	16.1033	0.2218	14.0628	4.4207
0	0	79.0000	24.4465	37.9388	9.5651	4.4207
0	0	80.0000	34.7339	32.0719	60.4166	4.4207
0	0	81.0000	28.0945	45.1392	48.9426	4.4207
0	0	82.0000	5.3419	54.3286	13.5096	4.4207
2	125	83.0000	3.3617	22.8294	69.0104	4.4207
0	0	84.0000	32.5722	40.7624	58.9923	4.4207
0	0	85.0000	63.0474	28.3039	17.4674	4.4207

0	0	86.0000	26.2678	34.6696	60.0736	4.4207
2	128	87.0000	65.2315	66.2232	8.9988	4.4207
1	131	88.0000	28.7833	67.8059	62.7894	4.4207
0	0	89.0000	42.2578	41.8406	44.3309	4.4207
0	0	90.0000	25.5394	57.7624	30.0357	4.4207
0	0	91.0000	10.3800	29.0461	17.8544	4.4207
1	132	92.0000	67.5357	7.6784	37.2215	4.4207
0	0	93.0000	35.0769	57.1717	5.7297	4.4207
0	0	94.0000	18.0469	62.2414	43.5923	4.4207
0	0	95.0000	57.0504	51.7160	49.6046	4.4207
0	0	96.0000	47.9489	42.4622	5.1646	4.4207
1	133	97.0000	15.3627	50.6912	1.9082	4.4207
1	134	98.0000	36.1887	29.9418	69.5441	4.4207
0	0	99.0000	58.7457	17.5321	21.3205	4.4207
0	0	100.0000	24.2190	60.0297	49.5238	4.4207
1	5	101.0000	-1.8236	18.9659	45.9506	4.4207
1	8	102.0000	-3.4328	28.8453	48.3717	4.4207
1	19	103.0000	8.6902	47.1607	-2.6837	4.4207
1	20	104.0000	52.6123	40.2928	-2.0236	4.4207
1	24	105.0000	44.9374	30.2455	70.7835	4.4207
1	27	106.0000	71.2350	28.1551	36.3217	4.4207
1	28	107.0000	-1.4209	34.3105	63.7532	4.4207
1	30	108.0000	37.5939	-3.1780	36.1583	4.4207
1	33	109.0000	72.4277	45.7880	51.1908	4.4207
1	34	110.0000	69.7177	9.8012	55.5389	4.4207
1	40	111.0000	72.8515	38.1008	26.7045	4.4207
1	47	112.0000	56.1535	-2.1060	26.7476	4.4207
1	48	113.0000	34.0239	53.9304	-2.4265	4.4207
1	49	114.0000	59.3391	31.1432	-3.6806	4.4207
1	62	115.0000	20.2729	34.0768	72.7950	4.4207
1	64	116.0000	69.0286	49.4971	43.9205	4.4207
1	65	117.0000	27.7758	70.7053	39.4180	4.4207
1	67	118.0000	-0.2460	15.8771	13.7157	4.4207
1	68	119.0000	40.1969	37.7721	70.3984	4.4207
2	72	120.0000	72.2207	-3.3137	25.9177	4.4207
2	72	121.0000	72.2207	66.6863	25.9177	4.4207
2	72	122.0000	3.6207	-3.3137	25.9177	4.4207
1	73	123.0000	-2.5562	65.3356	55.6687	4.4207
1	78	124.0000	16.1033	70.2218	14.0628	4.4207
2	83	125.0000	71.9617	22.8294	-0.9896	4.4207
2	83	126.0000	71.9617	22.8294	69.0104	4.4207
2	83	127.0000	3.3617	22.8294	-0.9896	4.4207
2	87	128.0000	-3.3685	-3.7768	8.9988	4.4207

2	87	129.0000	-3.3685	66.2232	8.9988	4.4207
2	87	130.0000	65.2315	-3.7768	8.9988	4.4207
1	88	131.0000	28.7833	-2.1941	62.7894	4.4207
1	92	132.0000	-1.0643	7.6784	37.2215	4.4207
1	97	133.0000	15.3627	50.6912	71.9082	4.4207
1	98	134.0000	36.1887	29.9418	-0.4559	4.4207

and last stage at which compaction failed will be displayed in the end

Compaction not possible at the stage 0.160000

Step-4

Output file
1st column:
0 - Sphere is inside the domain
1 - Sphere is coming out of a face and will have one image
2 - Sphere is coming out of a edge and will have three images
3 - Sphere is coming out of corner and will have seven images

2nd column:
If the number is greater than number of spheres here 100 it means its a real sphere information and this sphere have image.
zero means that the sphere is inside the box and have no image
All the image information can be found out by tracking this number in the third column

3rd column:
Serial number of spheres, all the real sphere's information will be displayed for values from 1 to 100 in this column and rest of them corresponds to their images.

4th, 5th, 6th and 7th column:
x coordinate, y coordinate, z-coordinate and sphere radius

Step-5
Now take the data from the desired compaction stage and use "connectivity.m" for monodispersed and "conectivity_bidispersed.m" for bidispersed packing.
For bidispersed packing, extract the information of the desired component and count the real spheres in that component before using it.

Step-6
Enter number of spheres 100
Variable AK will give unique cluster ID
Variable kk will give the cluster ID of all the spheres
Prepare histogram of cluster frequency vs. cluster size

Example2

ALL GRAINS ARE DUCTILE- TWO COMPONENT SPHERE PACKING

Example Two component packing 300 spheres, initial porosity 70%, 109 spheres are carbonaceous, ductility is 0.8R rigid radius

Step-1

input as 'new.txt' in the format

1	38.614	65.3685	16.5275	4.38567
2	23.9096	33.1537	46.3459	4.38567
3	39.7042	36.9746	41.5909	4.34225
4	3.84725	68.6688	28.1609	4.34225
5	25.1577	47.779	0.95618	4.38567
6	40.1337	16.9463	60.5663	4.34225
7	5.12384	1.69274	60.6869	4.34225
……..				
……..				
291	13.8143	69.6904	37.3667	4.38567
292	36.1176	44.8832	41.6954	4.34225
293	64.3497	3.6026	27.9382	4.34225
294	16.3426	2.89365	24.4047	4.34225
295	35.9981	22.7161	6.00591	4.38567
296	36.5576	2.99496	66.9997	4.34225
297	57.0817	41.2418	15.0779	4.38567
298	27.3935	16.4844	36.6992	4.34225
299	15.0327	4.77338	63.7226	4.34225
300	51.5859	33.8824	53.2982	4.34225

Step-2
Enter number of spheres 300
Enter compaction step 0.02
Enter ductility 0.2

At compaction 0.38

Compaction Step 0.380000

0	0	1.0000	16.5506	62.4088	15.5390	4.3857
0	0	2.0000	9.8920	33.5356	43.8953	4.3857
0	0	3.0000	16.4590	38.5009	40.1152	4.3422
2	301	4.0000	-0.0661	69.2647	27.8571	4.3422
1	304	5.0000	6.9735	49.2056	1.7025	4.3857
0	0	6.0000	13.8577	18.5367	61.2797	4.3422
2	305	7.0000	1.5510	-1.5532	64.9363	4.3422
1	308	8.0000	25.3496	18.4692	62.5437	4.3422

……

……..

1	290	497.0000	9.8133	56.4653	74.2894	4.3422
2	291	498.0000	29.4994	-1.8938	37.0494	4.3857
2	291	499.0000	29.4994	68.1062	37.0494	4.3857
2	291	500.0000	2.8994	-1.8938	37.0494	4.3857
1	293	501.0000	-2.0178	7.2326	26.6382	4.3422
1	296	502.0000	14.4307	4.5441	-2.8444	4.3422
1	299	503.0000	7.1153	73.9151	64.4992	4.3422

Compaction not possible at the stage 0.360000

Step-4

Repeat step-4 of the above example

For compaction stage of 0.5 you will get:

Compaction Step 0.500000

0	0	1.0000	21.8518	63.5844	16.8294	4.3857
0	0	2.0000	11.3426	31.0490	45.0536	4.3857
0	0	3.0000	20.8884	37.0683	40.3816	4.3422
2	301	4.0000	0.8502	69.5569	27.5341	4.3422
1	304	5.0000	11.4112	49.0509	1.3858	4.3857
0	0	6.0000	19.6195	18.2272	59.6093	4.3422
2	305	7.0000	3.6512	0.6881	63.7288	4.3422

……..

……..

1	284	455.0000	38.9679	39.3175	8.1109	4.3857

1	287	456.0000	25.2231	35.1909	2.7098	4.3857
1	289	457.0000	36.6400	54.0036	43.8283	4.3422
1	290	458.0000	12.0297	58.1974	72.9164	4.3422
1	291	459.0000	7.1796	-0.0025	37.1526	4.3857
1	293	460.0000	-2.9060	6.3457	28.4041	4.3422
1	294	461.0000	7.0944	74.1773	26.5956	4.3422
2	296	462.0000	17.0766	73.6650	-3.0481	4.3422
2	296	463.0000	17.0766	73.6650	66.9519	4.3422
2	296	464.0000	17.0766	3.6650	-3.0481	4.3422

Step-5

Use the "spheregrowth.m" for the volume conservation and with the new radius of the carbonaceous spheres proceed ahead. The grain volume lost is distributed evenly on every sphere.
Variable NN gives you the new radius

0	0	1	21.8518	63.5844	16.8294	4.4192
0	0	2	11.3426	31.049 4	5.0536	4.4192
1	304	5	11.4112	49.0509	1.3858	4.4192
0	0	10	24.3555	18.3208	31.4154	4.4192
1	312	14	8.4468	30.2545	68.3682	4.4192
2	314	16	3.3838	65.2379	69.4089	4.4192
0	0	19	7.0784	62.2216	38.4587	4.4192
0	0	22	22.532	23.1209	54.2061	4.4192
……						
……						
2	283	452	0.0573	24.6659	-4.3476	4.4192
2	283	453	0.0573	24.6659	65.6524	4.4192
2	283	454	35.0573	24.6659	-4.3476	4.4192
1	284	455	38.9679	39.3175	8.1109	4.4192
1	287	456	25.2231	35.1909	2.7098	4.4192
1	291	459	7.1796	-0.0025	37.1526	4.4192

Step-6

Use "connectivity_bidispersed.m" and enter the number of real spheres as 109.

Variable AK will give unique cluster ID
0
4
12
13

20
23
26
27

Variable kk will give cluster ID of all the spheres

23
12
12
4
12
20
12
0
12
4
……
…….....
12
0
13
12
12
12
0
12
0

Step-7

Prepare histogram for cluster frequency

Cluster size	Cluster frequency	Number of spheres
0	12	12
3	1	3
4	1	4
5	1	5
6	1	6
7	1	7
11	1	11
61	1	61

Example 3

ONLY CARBONACEOUS GRAINS ARE DUCTILE- TWO COMPONENT SPHERE PACKING

Example Two component packing of 5percent carbonaceous material 600 spheres, initial porosity 70%, 114 spheres are carbonaceous, and ductility is 0.9R rigid radius for carbonaceous material

Step-1

Input as 'new.txt' in the format

1	43.3756	42.0647	5.64082	3.44644
2	9.45584	12.0812	44.73	3.44644
3	13.2906	67.8776	48.9911	3.44644
4	52.7517	16.8941	1.04113	3.44644
……				
……..				
594	41.6039	53.4568	69.0052	3.48091
595	52.9037	24.39	51.2843	3.44644
596	49.8183	46.931	44.9142	3.48091
597	5.3906	20.1967	12.3326	3.48091
598	30.9958	55.0525	12.495	3.44644
599	28.467	30.787	60.1761	3.44644
600	51.3148	25.2639	24.4413	3.44644

Step-2
Enter number of spheres 600
Enter compaction step 0.02
Enter ductility 0.1
Enter radius of big sphere 3.48091 (carbonaceous material)
Enter radius of small sphere 3.44644

Step-3
For compaction stage 0.54, Take the data to "ductilenonductile.m" for volume conservation and proceed ahead

Compaction Step 0.540000

0	0	1.0000	23.7941	42.5990	3.8480	3.4464
0	0	2.0000	5.7371	9.5439	45.0713	3.4464
1	601	3.0000	6.1036	68.5846	49.0296	3.4464
1	602	4.0000	30.8783	16.0726	1.2535	3.4464
0	0	5.0000	21.9006	51.4536	47.3278	3.4464
0	0	6.0000	4.6334	9.2399	6.5568	3.4464
…….						
…….						
2	588	852.0000	-0.8084	23.4064	-3.3180	3.4464
1	590	853.0000	36.9514	10.6119	43.2300	3.4809
1	591	854.0000	-3.1447	47.7646	17.7416	3.4464
1	592	855.0000	39.7801	25.6242	32.9461	3.4464
1	594	856.0000	21.1381	54.6249	1.8433	3.4809

Step-4
Use the "ductilenonductile.m" for the volume conservation and with the new radius of the carbonaceous spheres proceed ahead. The grain volume lost is distributed within carbonaceous material.
Variable NN gives you the new radius.

0	0	16	32.1451	35.0883	57.921	3.4824
0	0	19	22.2518	4.5388	6.2196	3.4824
0	0	22	21.6239	36.1552	8.5481	3.4824
2	614	41	2.7705	-0.1713	65.9801	3.4824
0	0	46	27.3269	37.046 5	3.846	3.4824
……..						
……..						
1	571	840	1.2495	20.4923	16.9735	3.4824
1	578	844	-0.3331	4.3273	31.7483	3.4824
1	583	848	4.3354	53.0745	70.8896	3.4824
1	590	853	36.9514	10.6119	43.23	3.4824
1	594	856	21.1381	54.6249	1.8433	3.4824

Step-5

Prepare histogram for cluster frequency

Cluster size	Cluster frequency	Number of spheres
0	36	36
2	2	4
3	4	12
4	6	24
5	1	5
6	2	12
7	1	7
14	1	14

Bibliography

Javadpour, F., Fisher. D, Unsworth, M., Nanoscale gas flow in shale sediments; Journal of Canadian petroleum technology, Vol. 46, No. 10, pp. 55-61, October 2007.

Jones, S.C., A technique for faster pulse –decay permeability measurements in tight rocks, SPE Formation Evaluation, March 1997, Oklahoma city, Oklahoma, SPE 28450.

Luffel, D., L., Guidry, F., K., ResTech Houston Inc., New core analysis methods for measuring reservoir rock properties of Devonian shale. JPT November 1992, page 1184-1190.

Maxwell, J., C., The scientific letters and papers of James Clerk Maxwell, Vol. II: 1862-1873: Harmon P., M., (et al.), Cambridge University press, Cambridge, UK 1995

Mousavi, M., A., Pore scale characterization and modeling of two –phase flow in tight gas sandstones, P.H.D Dissertation, The University of Texas at Austin, USA, 2010.

Rodríguez, E., Straining of Small Particles in Porous Media, M.S. Thesis, The University of Texas at Austin, USA, 2006.

Roy Subrata and Reni Raju, Modeling gas flow through micro channels and nanopores: Journal of applied physics, Vol.93, No.8, pp.4870-4879, 2003.

Thane, C., Geometry and topology of model sediments and their influence in sediment properties, M.S. Thesis, The University of Texas at Austin, USA, 2006.

Wang,F.,P. and Reed, R., M., Bureau of Economic Geology, John, A. and Katerine, G., Jackson School of Geosciences, The University of Texas at Austin, Pore networks and Fluid flow in shales, ATCE 2009, New Orleans, LA, SPE 124253

X.Cui, A., M., M., Bustin and R., M., Bustin, Measurements of gas permeability and diffusivity of tight reservoir rocks: different approaches and their applications, Earth and Ocean sciences, The University of British Columbia, Vancouver, Canada. Geofluids (2009)

Vita

Abhishek Kumar graduated with a bachelor's degree in Petroleum Engineering from the Indian School of Mines, Dhanbad, India in May 2005. He worked for three years as a reservoir engineer in Reliance Industries limited, Mumbai before enrolling as a Master student in Petroleum Engineering at The University of Texas at Austin in fall 2008. During the completion of his master's degree he worked as a Graduate Research Assistant under the supervision of Dr. Steven L. Bryant.

Email address: Abhishek_kumar@mail.utexas.edu

This thesis was typed by Abhishek Kumar.